

SYNDROMIC CRANIOSYNOSTOSIS

Joyce M.G. Florisson

Syndromic Craniosynostosis
Joyce Maria Gerardus Florisson

ISBN: 978-94-6416-321-6

Layout and design: Daniëlle Balk, persoonlijkproefschrift.nl
Printing: Ridderprint, www.ridderprint.nl

© Joyce Maria Gerardus Florisson, 2021

All rights reserved. No part of this thesis may be reproduced, stored or transmitted in any form or by any means without prior permission of the author.

Syndromic Craniosynostosis

Syndromale Craniosynostose

Proefschrift

Ter verkrijging van de graad van doctor aan de
Erasmus Universiteit Rotterdam
op gezag van de
rector magnificus

Prof. dr. R.C.M.E. Engels

en volgens besluit van het College voor Promoties.
De openbare verdediging zal plaatsvinden op

donderdag 7 januari 2021 om 13.30 uur

door

Joyce Maria Gerardus Florisson
geboren te Maastricht

PROMOTIECOMMISSIE

Promotor Prof. dr. I.M.J Mathijssen

Overige leden Prof. dr. P.J. van der Spek
Prof. dr. R.R.J.W. van der Hulst
Prof. dr. C.M.F Dirven

Copromotor Dr. M.H. Lequin

TABLE OF CONTENTS

1	Chapter 1 General Introduction	7
2	Chapter 2 Boston type craniosynostosis: report of a second mutation in <i>MSX2</i> .	25
3	Chapter 3 Complex craniosynostosis is associated with the 2p15p16.1 microdeletion syndrome.	41
4	Chapter 4 Venous hypertension in syndromic and complex craniosynostosis: the abnormal anatomy of the jugular foramen and collaterals.	59
5	Chapter 5 Assessment of white matter microstructural integrity in children with syndromic craniosynostosis: a diffusion-tensor imaging study	79
6	Chapter 6 Diffusion tensor imaging and fiber tractography in young and unoperated craniosynostosis patients	95
7	Chapter 7 Sleep apnoea in syndromic craniosynostosis occurs independent of hindbrain herniation	111
8	Chapter 8 General Discussion	127
9	Chapter 9 Summary Samenvatting	139 140 142
A	Appendices PhD Portfolio List of Publications Dankwoord Curriculum Vitae	145 146 148 149 151



CHAPTER 1

General Introduction

INTRODUCTION

Craniosynostosis, defined as premature fusion of one or more of the cranial sutures, most commonly occurs sporadically as an isolated defect. In contrast, syndromic craniosynostosis typically involves multiple sutures as part of a larger constellation of associated anomalies (1). Syndromic craniosynostosis is frequently associated with different genetic mutations. Common features of these conditions are, hypertelorism, midface hypoplasia, ptosis of the eyes, and hand or foot anomalies. Increased intracranial pressure (ICP) is a well-known problem in craniosynostosis patients and is the main reason to operate. Increased intracranial pressure may damage the optic nerve and lead to visual loss. Understanding the complex pathophysiology of elevated ICP in syndromic craniosynostosis patients will improve their treatment, and possibly their physical and mental outcome. Additional difficulties are developmental and behavioural problems,.

This thesis on syndromic craniosynostosis describes the genetic background, the causes and effects of intracranial hypertension, and the developmental and psychological consequences in these patients.

CRANIOSYNOSTOSIS

The skull is composed of bony plates separated by sutures which permit future growth of the brain. The main sutures which contribute to calvarial development are the metopic, coronal, sagittal, and lambdoid sutures (2). During the first two years after birth, the brain increases in size to 75 percent of its adult volume. The remaining 25 percent of growth occurs during the next 18 years. Fontanelle and suture closure occurs in a specific pattern. At two months of age, the posterior fontanelle closes, followed by the metopic suture which typically closes within the first year. Next is the anterior fontanelle, which closes at approximately two years of age. All remaining patent sutures close in adulthood following completion of craniofacial growth. Initially growth is mainly accomplished by the calvarian sutures, but from the age of six the skull grows by apposition of the bone at the outer site of the skull and resorption of the bone on the inner site of the skull. (3)

Premature fusion of the cranial sutures impedes normal growth of the skull, resulting in characteristic anatomic malformations of the skull. Craniosynostosis affects 1 in 2500 births and can be either isolated (nonsyndromic) or occur as part of a syndrome. (4)

Isolated craniosynostosis patients have no other abnormalities besides the premature closure of one cranial suture. The characteristic skull shape betrays which of the sutures is prematurely closed. Scaphocephaly is caused by sagittal suture craniosynostosis, trigonocephaly by metopic suture craniosynostosis, frontal plagiocephaly by unilateral coronal synostosis and posterior plagiocephaly by unilateral lambdoid suture synostosis.

Chapter 1

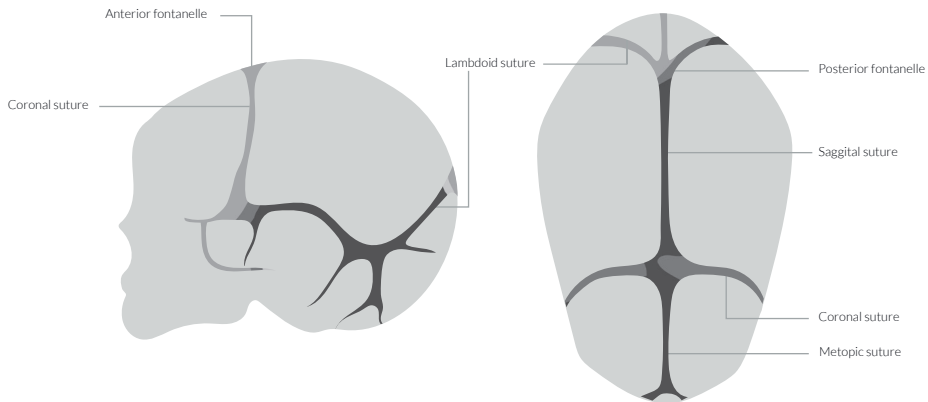


Figure 1: Open calvarian sutures, the normal anatomy.

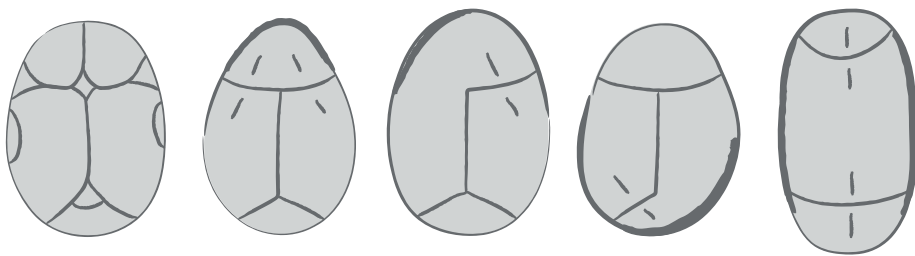


Figure 2: Isolated craniosynostosis, note the characteristic skull shapes

Craniosynostosis is in 24% of all cases a part of a syndrome and caused by mutations in various genes.⁽⁵⁾ Children with syndromic craniosynostosis usually have other birth defects present next to the craniosynostosis. The most common syndromes are Apert, Crouzon-Pfeiffer, Muenke and Saethre-Chotzen syndrome. Complex craniosynostosis is part of the syndromic craniosynostosis group: it includes patients where at least two sutures have been fused without known genetic mutation.

In 1993 the first genetic mutation causing craniosynostosis is described in a three generation family within the *MSX2* gene (6, 7). Nowadays, there are 57 human genes for which there is reasonable evidence to cause craniosynostosis (8).

Apert syndrome (acrocephalosyndactyly type I) is rare and occurs around one in 60.000 - 160.000 livebirths.^(4, 9-12) Although Apert syndrome is an autosomal dominant disorder most cases are sporadic. Mutations in the gene encoding fibroblast growth-factor receptor 2 (*FGFR2*), located on chromosome 10, account for almost all known cases. It is almost always caused by pathogenic mutations of Ser252Trp or Pro253Argin the *FGFR2*-gene

(13-15). It often originates from the father in whom spermatogonia are mutated during spermatogenesis, therefore it correlates with increasing paternal age (16, 17). Apert syndrome is first described by the French paediatrician Dr. Eugene Charles Apert in 1906. It manifests clinically by a bicoronal synostosis and maxillary hypoplasia, that causes a flat, recessed forehead and a flat midface. In addition, affected patients typically present with exorbitism and hypertelorism. Furthermore patients suffer from a class III malocclusion and a V-shaped maxillary dental arch.(18-20) Syndactyly is also a characteristic finding of the Apert syndrome. The Apert hand can be classified in three types, according to increased severity. All of them have a complex syndactyly of digits two through four and a short broad thumb. In the spade hand (Type I) the thumb is free and there is a simple syndactyly of the fourth webspace, the mitten hand (Type II) additionally has a simple syndactyly of the thumb while the rosebud hand (Type III) consists of a complex syndactyly of all the fingers. At the feet there is also a symmetrical syndactyly (20, 21). The intelligence varies, scores were found between 62 and 94 in previous literature.(22-24) A recent study from our unit finds a significantly lower result , a mean of 77, for Apert patients compared to the syndromic craniosynostosis subgroups. They argue that children who have Apert syndrome have the highest risk for developing intellectual disability (25).

Crouzon-Pfeiffer syndrome occurs in 1 in 25.000 births and is an autosomal dominant syndrome, predominantly caused by mutations in *FGFR2*, located on chromosome 10 with variable expression. But sometimes the *FGFR1* or the *FGFR3* mutation, A391E, has also been reported in individuals with Crouzon syndrome and acanthosis nigricans (26, 27) (28). The Crouzon syndrome was first described by Octave Crouzon in 1912 and Rudolf Arthur Pfeiffer described in 1964 the Pfeiffer syndrome (29). Historically both were distinguished by the presence of broad and short thumbs and halluces. Currently the distinction between these two syndromes can be seen as irrelevant because of completely identical genetic mutations. Phenotypically they suffer usually from bicoronal synostosis, but other sutures can be affected. In some of the cases the craniosynostosis develops postnatally (30). Exorbitism, midface hypoplasia and malocclusion type III belong to the characteristics of Crouzon-Pfeiffer syndrome. Most Crouzon-Pfeiffer patients have a normal or even high intelligence, but others may suffer from mental retardation (IQ range: 54-133) (25).

Muenke syndrome is an autosomal dominant disorder with incomplete penetrance, caused by the Pro250Arg mutation of the *FGFR3* gene on chromosome 4. The mutation is described by Muenke in 1997, but the phenotype is first described in 1994 by Glass (31, 32) The estimated birth prevalence is 1 in 30.000 births. (4) Most likely this occurrence is underestimated because not all patients are clinically recognized (33-38). Not all cases come to clinical attention because the phenotype is variable and sometimes very mild. But, most often the phenotype consists of unilateral or bilateral coronal synostosis and associated anomalies. Sensorineural hearing loss, hypertelorism, high arched palate, strabismus, carpal bone fusions and brachydactyly are described in this patient group (35, 39). Muenke patients have a mean IQ of 95.2 (range 73-124), which is not significantly

Chapter 1

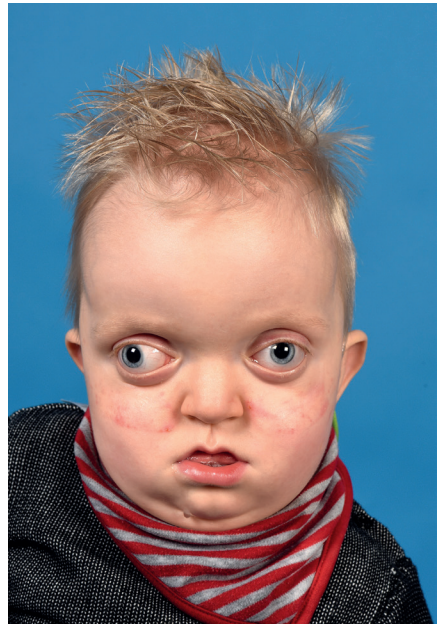
lower compared to normative. Nevertheless a proportion of 0.39 have an intellectual disability in this patient group. On the other hand parents reported higher levels of behavioural problems, emotional problems, social problem and inattention compared to parents of children who have other subtypes (25).

Saethre-Chotzen syndrome has a birth prevalence of 1 in 25.000 births. (4) It is an autosomal dominant syndrome, caused by mutations of deletions in the *TWIST1* gene. Phenotypically it is characterized by coronal synostosis, ptosis of the upper eyelid, external ear anomalies. Limb abnormalities, such as brachydactyly, syndactyly, clinodactyly or broad halluces are also frequently described. Intelligence in Saethre-Chotzen patients can vary enormously. Earlier research described a range from 52-141, with a mean of 100 (25). Yet, it is suggested that patients with *TWIST* deletions have a higher frequency of mental retardation (40)

Complex craniosynostosis includes patients who have multisuture synostosis but without known genetic mutation. This is a very divergent group and a source for genetic research. Discovering more genetic mutations, such as *MSX2*, *IL11RA*, *ERF*, *TCF12* and *ZIC1* makes this a shrinking population (5, 7, 41-43).



A. Apert



B. Crouzon-Pfeiffer



C. Muenke



D. Saethre-Chotzen

Figure 3: Showing Apert, Crouzon - Pfeiffer, Muenke and a Saethre-Chotzen patient. Note the different phenotypes.

CRANIOSYNOSTOSIS AND INTRACRANIAL PRESSURE

Elevated intracranial pressure (ICP) is a well-known, but poorly understood problem in craniosynostosis patients. It is most common in syndromic craniosynostosis in which the prevalence varies. Pre-operatively the incidence varies between 40 to nearly 100% (44-50). In these pre-operative studies the numbers are relatively small, many articles come from the same centers and a big variance is reported in all syndromes. To prevent intracranial hypertension, a cranial vault expansion is done in the first year of life by most craniofacial centers. Nevertheless, early expansion does not completely prevent the development of elevated ICP. Even after surgery patients can develop elevated ICP. In contrast to preoperative results, there is little literature about post-operative elevated intracranial pressure. Results vary from 8 up to 43% of syndromic craniosynostosis patients who develop elevated ICP (44, 51, 52).

Potential causes for elevated ICP are cranio-cerebral disproportion (53), obstructive sleep apnea (OSA), tonsillar herniation of the cerebellum (54) and venous hypertension.

Literature shows that patients with syndromic craniosynostosis have a normal brain volume and intracranial volume, indicating that a cranio-cerebral imbalance is seldom the initial cause for elevated ICP and only so in patients with pansynostosis (55). During follow-up, however, a falling-off in occipitofrontal head circumference growth curve is associated with intracranial hypertension (52).

OSA has an important implication for cerebral blood flow and intracranial pressure dynamics (46, 55). Nearly 70% of patients with a syndromic craniosynostosis suffers from OSA, mainly of mild severity (56), and therefore its contribution to the high prevalence of elevated ICP seems limited. But research did describe an association between intracranial hypertension and moderate / severe obstructive sleep apnea, by causing vasodilatation and thus extra inflow of blood, during the nocturnal episodes of desaturation. (52)

Tonsillar herniation is defined as a herniation of the cerebellar tonsils through the foramen magnum. When the herniation is less than 5mm below the foramen magnum it is called a tonsillar herniation, when it is more than 5mm below the foramen magnum it is called Chiari I malformation (CMI; classic definition)(57-60). Whether tonsillar herniation develops as a result of elevated ICP or (also) causes the ICP is to debate. CMI development is a complex problem. Rijken studied the relation between the size of the foramen magnum and the development of CMI. She states that a reduced foramen magnum size is not related to CMI. But she did prove that patients with a syndromic craniosynostosis do have a smaller foramen magnum compared to control patients. In the Crouzon-Pfeiffer and Apert group the smaller foramen was related to premature closure of the anterior and posterior intra-occipital synchondroses. Hence, the idea that a smaller posterior fossa would cause CMI was proven wrong in this study. It did show that a higher cerebellar volume / posterior fossa volume ratio was found to be a predisposing factor for the development of CMI (61, 62).

Venous hypertension refers to obstruction of the venous outflow of the brain and alterations in the dynamics of flow in the superior sagittal sinus (53). Venous hypertension is commonly described in syndromic craniosynostosis and has been related to a reduced diameter of the jugular foramen. Theories differ, some state that the bony narrowing may lead to obstructed outflow. As a result of the obstructed outflow, venous pressure and consequently CSF pressure raises. (63-65) Others attenuate this by presenting no difference in jugular foramen diameter between craniosynostosis patients with and without intracranial hypertension.(66) Another anomaly that is frequently encountered in syndromic craniosynostosis is the presence of venous collaterals at the level of the posterior fossa. This appears to be a bypass system to allow for additional venous outflow.

CRANIOSYNOSTOSIS AND WHITE MATTER INTEGRITY

The cause for the known developmental and psychological problems are still unexplained for in these patients. Not only genetics, elevated intracranial pressure but also the brains of these patients have been studied using conventional magnetic resonance imaging (MRI). Ventriculomegaly, corpus callosum, hippocampus or septum pellucidum anomalies are seen on MRI. Moreover, white matter alterations and abnormal gyral structure have been reported (67-71). These are all anomalies that could indicate either secondary causes or a primary congenital disorder. In 2007, Raybaud et al. (72) published a review with the aim of resolving the controversy regarding whether the brain abnormalities seen in patients with syndromic craniosynostosis are primary or secondary to the bone deformities. In their review they state that experimental neurobiological evidence supports the hypothesis that the fibroblast growth factor receptor (*FGFR* 1, *FGFR*2, and *FGFR*3) gene mutations, causal of syndromic craniosynostosis, may also be causal of diffusely abnormal white matter development.

Their research shows an interaction of *FGFR* with L1 cell adhesion molecule (*L1CAM*). And this *L1CAM* is related to developmental white matter disorders. Consequently cerebral abnormalities are the result of white matter alterations. White matter has been reported as atrophic or hypoplastic in all syndromes (67, 69-72). Additionally, partial or total agenesis of the pellucid septum has been reported (67-72). Cerebellar involvement, ascribed to a small fossa posterior associated with tonsillar herniation, has also been documented often (67, 68, 70). Raybaud and co-workers concluded that the observed white matter abnormalities, assessed on conventional brain MRI, could constitute a primary disorder (72). Diffusion Tensor Imaging (DTI) is an MRI sequence that allows to study the micro-architectural organization of brain tissue in vivo. DTI can provide an objective and reproducible assessment of the white matter derived from quantitative measures (73, 74). Diffusion tensor imaging is a non-invasive technique that provides microstructural information related to white matter status. DTI gives us the ability to learn the water

Chapter 1

diffusion profile in white matter. Fractional anisotropy (FA) is a common used parameter in DTI and describes the degree of anisotropic diffusion. Fractional anisotropy values ranges from 0 to 1, with 0 being completely isotropic (equal in all directions) and 1 being completely anisotropic (diffusion along only one axis)(75). Muetzel describes associations between white matter microstructure and cognition in a large sample of young children. They observe associations in white matter integrity and general intelligence (76). No studies were performed by combining intellectual, behavioural and emotional functioning with white matter microstructural integrity in syndromic craniosynostosis patients yet.

CRANIOSYNOSTOSIS INITIAL TREATMENT

Early recognition is the first step in good practice. Craniosynostosis is rare and often late or even not recognized. In first and second line craniosynostosis has to be distinguished from non synostotic plagiocephaly (NSOP). Recognition of craniosynostosis patients is hampered by the growing incidence of NSOP since the nineties. This rising incidence is caused by the advise to let children sleep at their back to prevent sudden infant death syndrome. Syndromic craniosynostosis patients do have additional abnormalities as midface hypoplasia, exorbitism and limb abnormalities. Craniosynostosis can be distinguished from NSOP by adequate history taking and physical examination and often rotation of the skullbase on CT. If patients are suspected to have craniosynostosis, a referral to a expertise craniofacial center is indicated.

In our treatment protocol diagnostic imaging will be performed by doing an ultrasound when the diagnosis is uncertain and a CT scan with 3D imaging to confirm the diagnosis. Operation will be done in all patients in the first year of life, and the main reason to operate is to prevent elevated intracranial pressure (77-79). The timing of the operation is diagnosis-dependent. Apert and Crouzon-Pfeiffer patients will generally be operated at the age of 6 months. For these patients an occipital expansion with springs is primary choice, because of the greater increase in intracranial volume compared to fronto-orbital advancement. Additional benefit of doing the first vault expansion at the back is that there is a lower complication rate when doing a monobloc advancement, Le Fort III or facial bipartition in a later stage (80). When doing occipital expansion there must be awareness of the possibility of occipital collaterals as the main mechanism of drainage for the cerebral venous system. Occipital surgery can have major complications in these cases. A pre-operative CT angiography (CTA) is necessary in all cases. Additionally, in patients with severe exorbitism, a monobloc advancement with distraction should be considered as first cranial vault expansion.

Saethre-Chotzen and Muenke patients, where retrusion of the orbital bar is the main clinical feature and midface development is near normal, a fronto-orbital advancement will be performed in their first year of live. Saethre-Chotzen patients will be treated earlier,

between 6-9 months of age, and Muenke patients between 9-12 months of age. The reason to operate Muenke patients later is because of the low risk of elevated intracranial pressure within the first year of life and better esthetical outcome when operated at a later age (81-83)

If there is proof of elevated intracranial pressure, operation will then be rescheduled at an earlier date in all patients.

AIM OF THIS THESIS

At first we give an overview of craniosynostosis nowadays. The first part of this thesis focuses at the genetic origin of craniosynostosis. Genetic research is done in families in whom a syndromic presentation is seen but none of the most common genetic mutations is found. In **Chapter Two** a report of a second mutation in *MSX2* is described following the first and only reported family in the world with a Boston type craniosynostosis (84) It describes mutations in the DNA binding region of the homeobox gene *MSX2* whereas loss of one allele of *BCL11a* in **Chapter Three** provides the link to transcriptional regulation and comorbidities to Primary Immune Deficiency patients. It describes two patients who add different forms of craniosynostosis to the clinical spectrum of the 2p15p16.1 microdeletion syndrome. (85)

The second part concentrates at imaging in craniosynostosis patients. **Chapter Four** reports on venous hypertension as a cause of elevated intracranial pressure. (66)

Chapter Five is a prospective DTI study to assess whether architectural alterations exist in the white matter of operated patients with syndromic craniosynostosis. **Chapter Six** reports white matter alterations in young unoperated patients compared to healthy controls.

Chapter Seven focusses at sleep apnoea problems in syndromic craniosynostosis patients and describes the relationship of hindbrain herniation and occurrence of OSA.

REFERENCES

1. Morriss-Kay GM, Wilkie AO. Growth of the normal skull vault and its alteration in craniosynostosis: insights from human genetics and experimental studies. *J Anat.* 2005;207(5):637-53.
2. Panchal J, Uttchin V. Management of craniosynostosis. *Plast Reconstr Surg.* 2003;111(6):2032-48; quiz 49. Epub 2003/04/25.
3. Cohen MM. Craniosynostosis. Diagnosis, Evaluation, and Management. ed. New York: Raven Press; 1986.
4. Cornelissen M, Ottelander B, Rizopoulos D, van der Hulst R, Mink van der Molen A, van der Horst C, et al. Increase of prevalence of craniosynostosis. *J Craniomaxillofac Surg.* 2016;44(9):1273-9. Epub 2016/08/09.
5. Sharma VP, Fenwick AL, Brockop MS, McGowan SJ, Goos JA, Hoogeboom AJ, et al. Mutations in *TCF12*, encoding a basic helix-loop-helix partner of *TWIST1*, are a frequent cause of coronal craniosynostosis. *Nat Genet.* 2013;45(3):304-7. Epub 2013/01/29.
6. Jabs EW, Muller U, Li X, Ma L, Luo W, Haworth IS, et al. A mutation in the homeodomain of the human *MSX2* gene in a family affected with autosomal dominant craniosynostosis. *Cell.* 1993;75(3):443-50. Epub 1993/11/05.
7. Warman ML, Mulliken JB, Hayward PG, Muller U. Newly recognized autosomal dominant disorder with craniosynostosis. *Am J Med Genet.* 1993;46(4):444-9. Epub 1993/06/01.
8. Twigg SR, Wilkie AO. A Genetic-Pathophysiological Framework for Craniosynostosis. *Am J Hum Genet.* 2015;97(3):359-77. Epub 2015/09/05.
9. Blank CE. Apert's syndrome (a type of acrocephalosyndactyly)-observations on a British series of thirty-nine cases. *Ann Hum Genet.* 1960;24:151-64. Epub 1960/05/01.
10. Cohen MM, Jr., Kreiborg S, Lammer EJ, Cordero JF, Mastroiacovo P, Erickson JD, et al. Birth prevalence study of the Apert syndrome. *Am J Med Genet.* 1992;42(5):655-9. Epub 1992/03/11.
11. Czeizel AE, Elek C, Susanszky E. Birth prevalence study of the Apert syndrome. *Am J Med Genet.* 1993;45(3):392-3. Epub 1993/02/01.
12. Tolarova MM, Harris JA, Ordway DE, Vargervik K. Birth prevalence, mutation rate, sex ratio, parents' age, and ethnicity in Apert syndrome. *Am J Med Genet.* 1997;72(4):394-8. Epub 1997/12/31 23:38.
13. Wilkie AO, Slaney SF, Oldridge M, Poole MD, Ashworth GJ, Hockley AD, et al. Apert syndrome results from localized mutations of *FGFR2* and is allelic with Crouzon syndrome. *Nat Genet.* 1995;9(2):165-72. Epub 1995/02/01.
14. Oldridge M, Zackai EH, McDonald-McGinn DM, Iseki S, Morriss-Kay GM, Twigg SR, et al. De novo alu-element insertions in *FGFR2* identify a distinct pathological basis for Apert syndrome. *Am J Hum Genet.* 1999;64(2):446-61. Epub 1999/02/11.
15. Lajeunie E, Cameron R, El Ghouzzi V, de Parseval N, Journeau P, Gonzales M, et al. Clinical variability in patients with Apert's syndrome. *J Neurosurg.* 1999;90(3):443-7. Epub 1999/03/06.
16. Moloney DM, Slaney SF, Oldridge M, Wall SA, Sahlin P, Stenman G, et al. Exclusive paternal origin of new mutations in Apert syndrome. *Nat Genet.* 1996;13(1):48-53. Epub 1996/05/01.

17. Goriely A, McVean GA, van Pelt AM, O'Rourke AW, Wall SA, de Rooij DG, et al. Gain-of-function amino acid substitutions drive positive selection of *FGFR2* mutations in human spermatogonia. *Proc Natl Acad Sci U S A*. 2005;102(17):6051-6. Epub 2005/04/21.
18. Cohen MM, Jr., Kreiborg S. A clinical study of the craniofacial features in Apert syndrome. *Int J Oral Maxillofac Surg*. 1996;25(1):45-53. Epub 1996/02/01.
19. Park WJ, Theda C, Maestri NE, Meyers GA, Fryburg JS, Dufresne C, et al. Analysis of phenotypic features and *FGFR2* mutations in Apert syndrome. *Am J Hum Genet*. 1995;57(2):321-8. Epub 1995/08/01.
20. Cohen MM, Jr., Kreiborg S. Hands and feet in the Apert syndrome. *Am J Med Genet*. 1995;57(1):82-96. Epub 1995/05/22.
21. Upton J. Apert syndrome. Classification and pathologic anatomy of limb anomalies. *Clin Plast Surg*. 1991;18(2):321-55. Epub 1991/04/01.
22. Da Costa AC, Walters I, Savarirayan R, Anderson VA, Wrennall JA, Meara JG. Intellectual outcomes in children and adolescents with syndromic and nonsyndromic craniosynostosis. *Plast Reconstr Surg*. 2006;118(1):175-81; discussion 82-3. Epub 2006/07/04.
23. Renier D, Arnaud E, Cinalli G, Marchac D, Brunet L, Sebag G, et al. [Mental prognosis of Apert syndrome]. *Arch Pediatr*. 1996;3(8):752-60. Epub 1996/08/01. Pronostic mental du syndrome d'Apert.
24. Renier D, Arnaud E, Cinalli G, Sebag G, Zerach M, Marchac D. Prognosis for mental function in Apert's syndrome. *J Neurosurg*. 1996;85(1):66-72. Epub 1996/07/01.
25. Maliepaard M, Mathijssen IM, Oosterlaan J, Okkerse JM. Intellectual, behavioral, and emotional functioning in children with syndromic craniosynostosis. *Pediatrics*. 2014;133(6):e1608-15. Epub 2014/05/28.
26. Jabs EW, Li X, Scott AF, Meyers G, Chen W, Eccles M, et al. Jackson-Weiss and Crouzon syndromes are allelic with mutations in fibroblast growth factor receptor 2. *Nat Genet*. 1994;8(3):275-9. Epub 1994/11/01.
27. Reardon W, Winter RM, Rutland P, Pulleyn LJ, Jones BM, Malcolm S. Mutations in the fibroblast growth factor receptor 2 gene cause Crouzon syndrome. *Nat Genet*. 1994;8(1):98-103. Epub 1994/09/01.
28. Meyers GA, Orlow SJ, Munro IR, Przylepa KA, Jabs EW. Fibroblast growth factor receptor 3 (*FGFR3*) transmembrane mutation in Crouzon syndrome with acanthosis nigricans. *Nat Genet*. 1995;11(4):462-4. Epub 1995/12/01.
29. Pfeiffer RA. [Dominant Hereditary Acrocephalosyndactylia] Dominant Erbliche Akrocephalosyndaktylie. *Z Kinderheilkd*. 1964;90:301-20. Epub 1964/09/16.
30. Hoefkens MF, Vermeij-Keers C, Vaandrager JM. Crouzon syndrome: phenotypic signs and symptoms of the postnatally expressed subtype. *J Craniofac Surg*. 2004;15(2):233-40; discussion 41-2. Epub 2004/05/29.
31. Muenke M, Gripp KW, McDonald-McGinn DM, Gaudenz K, Whitaker LA, Bartlett SP, et al. A unique point mutation in the fibroblast growth factor receptor 3 gene (*FGFR3*) defines a new craniosynostosis syndrome. *Am J Hum Genet*. 1997;60(3):555-64. Epub 1997/03/01.

Chapter 1

32. Glass IA, Chapman S, Hockley AD. A distinct autosomal dominant craniosynostosis-brachydactyly syndrome. *Clin Dysmorphol*. 1994;3(3):215-23. Epub 1994/07/01.
33. Keller MK, Hermann NV, Darvann TA, Larsen P, Hove HD, Christensen L, et al. Craniofacial morphology in Muenke syndrome. *J Craniofac Surg*. 2007;18(2):374-86. Epub 2007/04/07.
34. Sabatino G, Di Rocco F, Zampino G, Tamburrini G, Caldarelli M, Di Rocco C. Muenke syndrome. *Childs Nerv Syst*. 2004;20(5):297-301. Epub 2004/02/14.
35. de Jong T, Mathijssen IM, Hoogbeem AJ. Additional phenotypic features of Muenke syndrome in 2 Dutch families. *J Craniofac Surg*. 2011;22(2):571-5. Epub 2011/03/16.
36. Dognon A, Florisson C. [Not Available] Generateurs ultra-sonores de laboratoire; quelques exemples d'applications physiques et chimiques. *Bull Soc Chim Biol (Paris)*. 1945;27:97-101. Epub 1945/01/01.
37. Moloney DM, Wall SA, Ashworth GJ, Oldridge M, Glass IA, Francomano CA, et al. Prevalence of Pro250Arg mutation of fibroblast growth factor receptor 3 in coronal craniosynostosis. *Lancet*. 1997;349(9058):1059-62. Epub 1997/04/12.
38. Rannan-Eliya SV, Taylor IB, De Heer IM, Van Den Ouweland AM, Wall SA, Wilkie AO. Paternal origin of *FGFR3* mutations in Muenke-type craniosynostosis. *Hum Genet*. 2004;115(3):200-7. Epub 2004/07/09.
39. de Jong T, Toll MS, de Gier HH, Mathijssen IM. Audiological profile of children and young adults with syndromic and complex craniosynostosis. *Arch Otolaryngol Head Neck Surg*. 2011;137(8):775-8. Epub 2011/08/17.
40. de Heer IM, de Klein A, van den Ouweland AM, Vermeij-Keers C, Wouters CH, Vaandrager JM, et al. Clinical and genetic analysis of patients with Saethre-Chotzen syndrome. *Plast Reconstr Surg*. 2005;115(7):1894-902; discussion 903-5. Epub 2005/06/01.
41. Nieminen P, Morgan NV, Fenwick AL, Parmanen S, Veistinen L, Mikkola ML, et al. Inactivation of IL11 signaling causes craniosynostosis, delayed tooth eruption, and supernumerary teeth. *Am J Hum Genet*. 2011;89(1):67-81. Epub 2011/07/12.
42. Twigg SR, Vorgia E, McGowan SJ, Peraki I, Fenwick AL, Sharma VP, et al. Reduced dosage of *ERF* causes complex craniosynostosis in humans and mice and links ERK1/2 signaling to regulation of osteogenesis. *Nat Genet*. 2013;45(3):308-13. Epub 2013/01/29.
43. Twigg SR, Forecki J, Goos JA, Richardson IC, Hoogbeem AJ, van den Ouweland AM, et al. Gain-of-Function Mutations in *ZIC1* Are Associated with Coronal Craniosynostosis and Learning Disability. *Am J Hum Genet*. 2015;97(3):378-88. Epub 2015/09/05.
44. Bannink N, Joosten KF, van Veelen ML, Bartels MC, Tasker RC, van Adrichem LN, et al. Papilledema in patients with Apert, Crouzon, and Pfeiffer syndrome: prevalence, efficacy of treatment, and risk factors. *J Craniofac Surg*. 2008;19(1):121-7. Epub 2008/01/25.
45. Gault DT, Renier D, Marchac D, Jones BM. Intracranial pressure and intracranial volume in children with craniosynostosis. *Plast Reconstr Surg*. 1992;90(3):377-81.
46. Hayward R, Gonzalez S. How low can you go? Intracranial pressure, cerebral perfusion pressure, and respiratory obstruction in children with complex craniosynostosis. *J Neurosurg*. 2005;102(1 Suppl):16-22.
47. Marucci DD, Dunaway DJ, Jones BM, Hayward RD. Raised intracranial pressure in Apert syndrome. *Plast Reconstr Surg*. 2008;122(4):1162-8; discussion 9-70. Epub 2008/10/02.

48. Renier D, Sainte-Rose C, Marchac D, Hirsch JF. Intracranial pressure in craniostenosis. *J Neurosurg.* 1982;57(3):370-7.
49. Tamburrini G, Di Rocco C, Velardi F, Santini P. Prolonged intracranial pressure (ICP) monitoring in non-traumatic pediatric neurosurgical diseases. *Med Sci Monit.* 2004;10(4):MT53-63. Epub 2004/03/25.
50. Thompson DN, Harkness W, Jones B, Gonzalez S, Andar U, Hayward R. Subdural intracranial pressure monitoring in craniosynostosis: its role in surgical management. *Childs Nerv Syst.* 1995;11(5):269-75.
51. Kress W, Schropp C, Lieb G, Petersen B, Busse-Ratzka M, Kunz J, et al. Saethre-Chotzen syndrome caused by *TWIST 1* gene mutations: functional differentiation from Muenke coronal synostosis syndrome. *Eur J Hum Genet.* 2006;14(1):39-48. Epub 2005/10/28.
52. Spruijt B, Joosten KF, Driessen C, Rizopoulos D, Naus NC, van der Schroeff MP, et al. Algorithm for the Management of Intracranial Hypertension in Children with Syndromic Craniosynostosis. *Plast Reconstr Surg.* 2015;136(2):331-40. Epub 2015/04/25.
53. Hayward R. Venous hypertension and craniosynostosis. *Childs Nerv Syst.* 2005;21(10):880-8.
54. Driessen C, Joosten KF, Florisson JM, Lequin M, van Veelen ML, Dammers R, et al. Sleep apnoea in syndromic craniosynostosis occurs independent of hindbrain herniation. *Childs Nerv Syst.* 2013;29(2):289-96. Epub 2012/09/26.
55. Gonzalez S, Hayward R, Jones B, Lane R. Upper airway obstruction and raised intracranial pressure in children with craniosynostosis. *Eur Respir J.* 1997;10(2):367-75. Epub 1997/02/01.
56. Driessen C, Joosten KF, Bannink N, Bredero-Boelhouwer HH, Hoeve HL, Wolvius EB, et al. How does obstructive sleep apnoea evolve in syndromic craniosynostosis? A prospective cohort study. *Arch Dis Child.* 2013;98(7):538-43. Epub 2013/05/25.
57. Aboulez AO, Sartor K, Geyer CA, Gado MH. Position of cerebellar tonsils in the normal population and in patients with Chiari malformation: a quantitative approach with MR imaging. *J Comput Assist Tomogr.* 1985;9(6):1033-6. Epub 1985/11/01.
58. Amer TA, el-Shmam OM. Chiari malformation type I: a new MRI classification. *Magn Reson Imaging.* 1997;15(4):397-403. Epub 1997/01/01.
59. Elster AD, Chen MY. Chiari I malformations: clinical and radiologic reappraisal. *Radiology.* 1992;183(2):347-53. Epub 1992/05/01.
60. Wu YW, Chin CT, Chan KM, Barkovich AJ, Ferriero DM. Pediatric Chiari I malformations: do clinical and radiologic features correlate? *Neurology.* 1999;53(6):1271-6. Epub 1999/10/16.
61. Rijken BF, Lequin MH, van der Lijn F, van Veelen-Vincent ML, de Rooi J, Hoogendam YY, et al. The role of the posterior fossa in developing Chiari I malformation in children with craniosynostosis syndromes. *J Craniomaxillofac Surg.* 2015;43(6):813-9. Epub 2015/05/17.
62. Rijken BF, Lequin MH, Van Veelen ML, de Rooi J, Mathijssen IM. The formation of the foramen magnum and its role in developing ventriculomegaly and Chiari I malformation in children with craniosynostosis syndromes. *J Craniomaxillofac Surg.* 2015;43(7):1042-8. Epub 2015/06/09.
63. Booth CD, Figueroa RE, Lehn A, Yu JC. Analysis of the jugular foramen in pediatric patients with craniosynostosis. *J Craniofac Surg.* 2011;22(1):285-8. Epub 2011/01/18.

Chapter 1

64. Jeevan DS, Anlsow P, Jayamohan J. Abnormal venous drainage in syndromic craniosynostosis and the role of CT venography. *Childs Nerv Syst.* 2008;24(12):1413-20.
65. Rich PM, Cox TC, Hayward RD. The jugular foramen in complex and syndromic craniosynostosis and its relationship to raised intracranial pressure. *AJNR Am J Neuroradiol.* 2003;24(1):45-51.
66. Florisson JM, Barmpalios G, Lequin M, van Veelen ML, Bannink N, Hayward RD, et al. Venous hypertension in syndromic and complex craniosynostosis: the abnormal anatomy of the jugular foramen and collaterals. *J Craniomaxillofac Surg.* 2015;43(3):312-8. Epub 2015/01/22.
67. Cohen MM, Jr. Pfeiffer syndrome update, clinical subtypes, and guidelines for differential diagnosis. *Am J Med Genet.* 1993;45(3):300-7. Epub 1993/02/01.
68. Proudman TW, Clark BE, Moore MH, Abbott AH, David DJ. Central nervous system imaging in Crouzon's syndrome. *J Craniofac Surg.* 1995;6(5):401-5. Epub 1995/09/01.
69. Quintero-Rivera F, Robson CD, Reiss RE, Levine D, Benson CB, Mulliken JB, et al. Intracranial anomalies detected by imaging studies in 30 patients with Apert syndrome. *Am J Med Genet A.* 2006;140(12):1337-8.
70. Tokumaru AM, Barkovich AJ, Ciricillo SF, Edwards MS. Skull base and calvarial deformities: association with intracranial changes in craniofacial syndromes. *AJNR Am J Neuroradiol.* 1996;17(4):619-30.
71. Yacubian-Fernandes A, Palhares A, Giglio A, Gabarra RC, Zanini S, Portela L, et al. Apert syndrome: analysis of associated brain malformations and conformational changes determined by surgical treatment. *J Neuroradiol.* 2004;31(2):116-22.
72. Raybaud C, Di Rocco C. Brain malformation in syndromic craniosynostoses, a primary disorder of white matter: a review. *Childs Nerv Syst.* 2007;23(12):1379-88.
73. Huppi PS, Dubois J. Diffusion tensor imaging of brain development. *Semin Fetal Neonatal Med.* 2006;11(6):489-97. Epub 2006/09/12.
74. Neil J, Miller J, Mukherjee P, Huppi PS. Diffusion tensor imaging of normal and injured developing human brain - a technical review. *NMR Biomed.* 2002;15(7-8):543-52. Epub 2002/12/19.
75. Basser PJ, Pierpaoli C. Microstructural and physiological features of tissues elucidated by quantitative-diffusion-tensor MRI. *J Magn Reson B.* 1996;111(3):209-19. Epub 1996/06/01.
76. Muetzel RL, Mous SE, van der Ende J, Blanken LM, van der Lugt A, Jaddoe VW, et al. White matter integrity and cognitive performance in school-age children: A population-based neuroimaging study. *Neuroimage.* 2015;119:119-28. Epub 2015/06/13.
77. Mathijssen IM, Arnaud E. Benchmarking for craniosynostosis. *J Craniofac Surg.* 2007;18(2):436-42. Epub 2007/04/07.
78. Marchac D, Arnaud E, Renier D. Frontocranial remodeling without opening of frontal sinuses in a scaphocephalic adolescent: a case report. *J Craniofac Surg.* 2002;13(5):698-705. Epub 2002/09/10.
79. Renier D, Lajeunie E, Arnaud E, Marchac D. Management of craniosynostoses. *Childs Nerv Syst.* 2000;16(10-11):645-58.
80. de Jong T, van Veelen ML, Mathijssen IM. Spring-assisted posterior vault expansion in multisuture craniosynostosis. *Childs Nerv Syst.* 2013;29(5):815-20. Epub 2013/01/29.

81. Arnaud E, Marchac D, Renier D. Reduction of morbidity of the frontofacial monobloc advancement in children by the use of internal distraction. *Plast Reconstr Surg.* 2007;120(4):1009-26. Epub 2007/09/07.
82. Fitzgerald O'Connor EJ, Marucci DD, Jeelani NO, Witherow H, Richards R, Dunaway DJ, et al. Ocular advancement in monobloc distraction. *Plast Reconstr Surg.* 2009;123(5):1570-7. Epub 2009/05/02.
83. Honnebier MB, Cabiling DS, Hetlinger M, McDonald-McGinn DM, Zackai EH, Bartlett SP. The natural history of patients treated for *FGFR3*-associated (Muenke-type) craniosynostosis. *Plast Reconstr Surg.* 2008;121(3):919-31. Epub 2008/03/05.
84. Florisson JM, Verkerk AJ, Huigh D, Hoogeboom AJ, Swagemakers S, Kremer A, et al. Boston type craniosynostosis: report of a second mutation in *MSX2*. *Am J Med Genet A.* 2013;161A(10):2626-33. Epub 2013/08/21.
85. Florisson JM, Mathijssen IM, Dumee B, Hoogeboom JA, Poddighe PJ, Oostra BA, et al. Complex craniosynostosis is associated with the 2p15p16.1 microdeletion syndrome. *Am J Med Genet A.* 2013;161A(2):244-53. Epub 2013/01/11.



CHAPTER 2

Boston-type Craniosynostosis: Report of a Second Mutation in *MSX2*

J.M.G. Florisson
J.M.H. Verkerk
D. Huigh
A.J.M. Hoozeboom
S. Swagemakers
A. Kremer
D. Heijsman
M. H. Lequin
I.M.J. Mathijssen
P. J. van der Spek

American journal of medical genetics Part A. 2013;161A(10):2626-33. Epub 2013/08/21.

ABSTRACT

We describe a family that segregated an autosomal dominant form of craniosynostosis characterized by variable expression and limited extra-cranial features. Linkage analysis and whole genome sequencing were performed to identify the underlying genetic mutation. A c.443C>T missense mutation in *MSX 2*, which predicts p.Pro148Leu was identified and segregated with the disease in all affected family members. One other family with autosomal dominant craniosynostosis (Boston-type) has been reported to have a missense mutation in *MSX*. These data confirm that missense mutations altering the proline at codon 148 of *MSX2* cause dominantly inherited craniosynostosis.

INTRODUCTION

Craniosynostosis may be isolated finding or part of a syndrome and affects 1 in every 2500 live births (1). It may affect only one suture, or when part of a syndrome, usually multiple sutures are involved. This is the case in at least 20% of the patients with craniosynostosis (2). Associated problems, such as widely spaced eyes, malar flattening, and hand or foot anomalies may indicate a genetic cause (1). Well-known syndromes such as Crouzon, Pfeiffer, Apert, Muenke, Saethre-Chotzen or craniofrontonasal dysplasia have characteristic features. Confirmation of the diagnosis can be made by DNA analysis of *FGFR1* [OMIM:136350], *FGFR2* [OMIM:176943], *FGFR3* [OMIM:134934], *TWIST1* [OMIM:601622] and the, recently identified, *TCF12* gene [OMIM:600480] (1, 3).

The first family with a newly recognized form of autosomal dominant craniosynostosis was reported by Warman et al.(4). They describe a family with the trait in 3 generations with variable expressivity of sutural involvement and cranial abnormalities combined with associated problems like headache, poor vision and seizures. Clinical diagnosis was precluded based upon the absence of characteristic changes normally present in these syndromes (5). Using linkage analysis, a locus on chromosome 5qter was assigned by Müller et al. and a causal mutation in the homeodomain of *MSX2* [OMIM:12301] in this family was reported by Jabs et al. who used the term “Boston type” for this type of craniosynostosis (6, 7).

We describe a family that segregated an autosomal dominant form of craniosynostosis characterized by variable expression and limited extra-cranial features, not resembling the unspecified phenotype described for the Boston type craniosynostosis. Linkage analysis and genome sequencing were performed to identify the causative mutation in this family.

MATERIALS AND METHODS

Study Subjects

This research project was reviewed and approved by the Erasmus MC, Institutional Review Board/Medical Ethical Committee (MEC 2005-273). The Next Generation DNA Sequencing (NGS) experiments were performed under the general Medical Ethical Committee approval (MEC 2011-253). This research is in line with the World Medical Association Declaration of Helsinki.

Linkage Analysis

CSV files containing SNP call data from HumanCytoSNP-12v2.1(Illumina, San Diego, CA) arrays were adapted by GenomeStudio (Illumina) to be compatible for calculating LOD scores with Allegro (8). Mendelian inheritance check was performed for all family members, with the program PedCheck (9). The SNPs showing Mendelian inconsistencies

Chapter 2

were excluded from the calculation. Individuals who were encoded by the pedigree information file were used for allele frequencies computation. Any SNPs with a call rate lower than 95% were excluded from the calculations. Multipoint linkage analysis was performed using Allegro with a SNP spacing of 0.2 cM. LOD scores were calculated assuming the disease to be an autosomal dominant disorder with 99% penetrance.

Genome Sequencing:

Genome sequencing was performed by Complete Genomics A BGI Company. (Mountain View, CA) using a sequencing-by-ligation method described previously, on DNA of five family members: three patients (I-2, II-1, III-1) and two unaffected individuals (I-1, II-2) (10). Paired-end reads (30-35 bp) were mapped to the NCBI reference genome build 36.3 and dbSNP build 130. Data were analysed using cga tools version 1.3.0 build 9 (<http://www.completegenomics.com/sequence-data/cgatools/>) and Spotfire 3.3.1 (Tibco). Mapped sequence of the five samples varied in size between 222 and 312 Gigabytes, resulting in an average coverage between 80 and 113-fold per genome. Confident diploid calls could be made for 93 to 95% of the reference genome in all samples.

PCR and Sanger sequencing

Specific primers were developed for Sanger sequence analysis of the exon 2 variant at position c.443 (NM_002449.4) in *MSX2*.

Primers used were:

Forward primer in intron 2: 5'-AGAGATGACGGGGGAGATGG-3'

Reverse primer in exon 2: 5'-TGGGGAAAGGGAGACTGAAGC-3'

Amplification reactions were performed in a total volume of 20 µl, containing 1x AmpliTaq360 PCR buffer, 1.8 mM MgCl₂, 200 µM of each dNTP, 10 µM forward primer, 10 µM reverse primer, 0.5 unit AmpliTaq360 DNA polymerase (Applied Biosystems, Ilfe technologies, Grand Island, NY), and 30 ng genomic DNA. PCR conditions: 5 min 94°C initial denaturation followed by 10 cycles of 30 sec 94°C; 30 sec 70°C -1°C/cycle (touch down); 60 sec 72°C and 35 cycles 30 sec 94°C; 30 sec 60°C; 60 sec 72°C with a final extension for 5 min 72°C.

The PCR reactions were purified with ExoSAP-IT (USB, Affymetrix, Cleveland OH). Direct sequencing of both strands was performed using Big Dye Terminator chemistry v3.1 (Applied Biosystems) as recommended by the manufacturer.

Dye terminators were removed using SephadexG50 (GE Healthcare, Pittsburgh, PA) and loaded on an ABI 3130XL Genetic Analyzer (Applied Biosystems). For sequence analysis the software package Seqscape (Applied Biosystems, version 2.6) was used.

Reference sequences included NM_002449.4; Ensembl Transcript ID ENST00000239243 and NP_002440.2; Ensembl Protein ID: ENSP00000239243.

CLINICAL REPORTS

A young patient (III-1, Fig. 1) of a large Bosnian family presented at the Dutch Craniofacial Centre with multiple sutural craniosynostosis. The pedigree showed that eight members were affected with craniosynostosis (Fig. 1). Twelve family members (I-3 and II-5 not included) were seen at the department of plastic and reconstructive surgery and participated in the study. No consanguinity was known in this family and the inheritance was consistent with an autosomal dominant pattern.

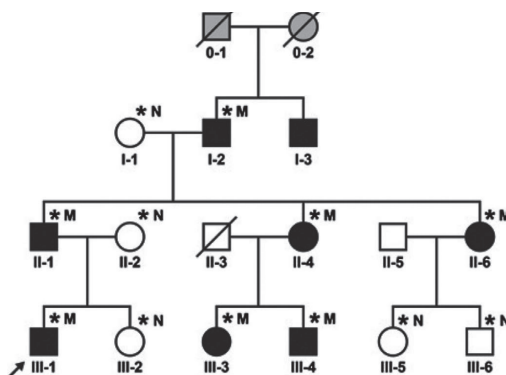


Figure 1: Pedigree of the craniosynostosis family with four generations (0-III). The proband III-1 is indicated with an arrow. I-3 was known to have turricephaly but did not participate in the study. Of I-3, II-3, and II-5 no DNA was available. No information is available about the great grandparents (0-1 and 0-2) or their phenotype. Filled symbols = affected, empty symbols = unaffected, / = deceased, gray symbols = phenotype unknown. Individuals II-1 and III-1 were heterozygous for a deletion in the *LEMD3* gene. An* indicates individuals which were genotyped. A heterozygous mutation in *MSX2* is indicated with an M. Normal homozygous *MSX2* sequence is indicated with an N.

The proband

Patient III-1 was seen at the age of 5 months. He presented with an abnormal skull shape, and a skull circumference of 37.5 cm (< 2th centile) (**Figure 2**). Physical examination showed a turricephaly, narrow forehead, down slanted palpebral fissures and closely spaced eyes. The maxilla showed a minimal underdevelopment. A CT scan showed bilateral coronal suture synostosis, metopic suture synostosis and wormian bones (**Figure 3**). There was a normal ventricular size and no signs of papilledema at fundoscopy. The fingers were short and broad, while the feet were without abnormalities. An X-ray of both hands showed no bony abnormalities. At the age of 6 months a frontosupra-orbital advancement was performed at our clinic. By 3 years of age the skull circumference was 46 cm (< 2th centile), height 104,5 cm (>84th centile) and 18 kg (84th centile). At the age of five years, he appeared to have a normal neurological development. Psychological tests were never performed because he performed well at primary school. At the age of 6 years he reached a length of 122 cm (>50th centile), a weight of 24.3 kg (>84th centile) and a skull circumference of 46.5 cm (< 2th centile).



Figure 2: Facial and hand phenotypic characteristics of the family members. Left panel top to bottom: II-1: Father of proband (age 43 years, never operated) showing a trigonocephaly with closely spaced eyes, III-1: Proband (age 5 months, pre-operative) showing turricephaly, narrow forehead, downslanting palpebral fissures, closely spaced eyes, and mild midface retrusion. II-4: Mother of Patient III-3 (age 41 years, never operated) showing a brachycephaly sk. Right panel top to bottom: Patient III-3 (age 18 years, post-operatively) showing post-operative retrusion of the forehead. Hands of Patient III-3 showing short fingers. X-ray of hands of patient III-3 showing shortening of the distal phalanges.

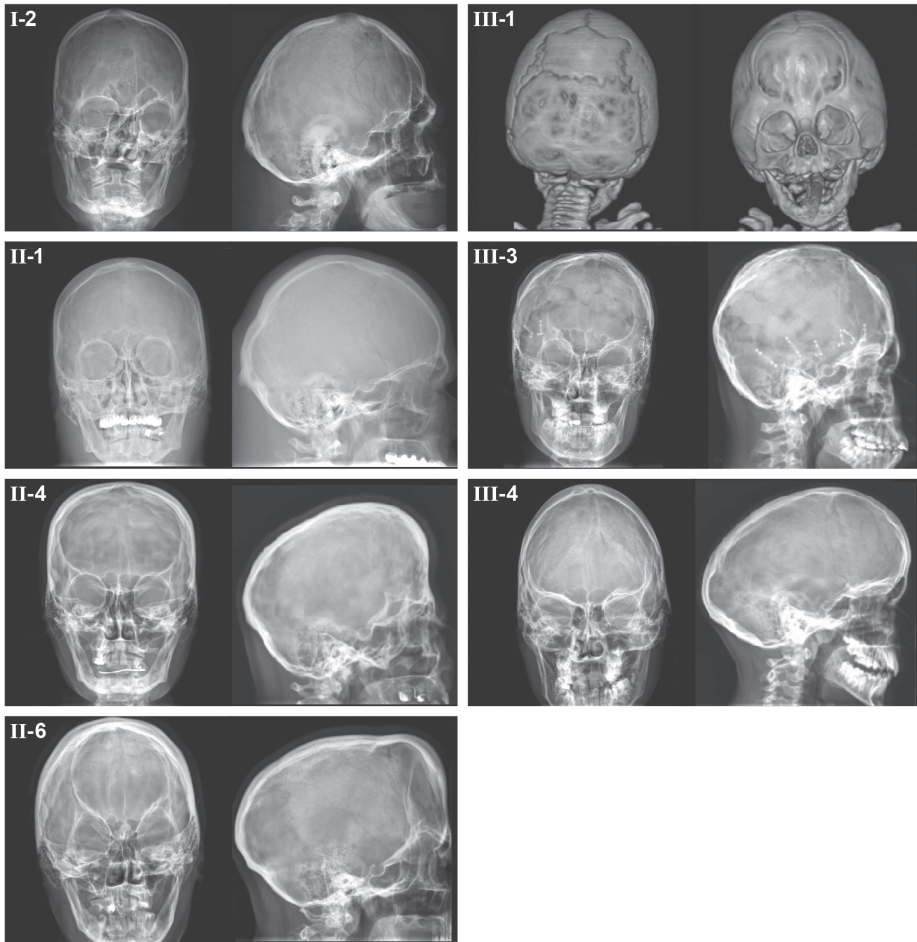


Figure 3: Radiological images: anterior, lateral, and posterior views of the skull. I-2: X-ray of patient I-2, (age 68, never operated) demonstrating left sided coronal suture synostosis and a bony defect at the former site of the anterior fontanel. II-1: X-ray of Patient II-1, (age 43 years, never operated) demonstrating mild trigonocephaly with closely spaced eyes. II-4: X-ray of patient II-4, (age 41, never operated) demonstrating a brachycephaly, due to early closure of the coronal sutures, and a generalized copper beaten aspect. II-6: X-ray of Patient II-6, (age 34, never operated) demonstrating a brachycephaly with closure of the coronal sutures and elevated sphenoid wings and a distorted orbital shape. It also shows a generalized copper beaten aspect. III-1: 3D-CT of the skull of Patient III-1 (age 6 months, pre-operatively), demonstrating turricephaly and metopic and bilateral coronal synostoses. There is bone at the junction of the sagittal and lambdoid sutures, called the interparietal portion of the squamous supraoccipital bone. The generalized copper beaten aspect is present and midface retrusion. III-3: X-ray of Patient III-3 (age 18 years, post-operatively) demonstrating a copper beaten skull. III-4: X-ray of Patient III-4, (age 13 years, never operated) demonstrating scaphocephaly.

Chapter 2

Patient III-3, a cousin of the proband, was born in Bosnia with a complex craniosynostosis. She was operated in her homeland in the first year of life. From this patient no pre-operative X-rays were available. A second skull remodelling was performed after she arrived in The Netherlands because of an obvious retrusion of the forehead. Her hands showed short fingers, mainly caused by shortening of the distal phalanges. Both thumbs had a supination position. She performs well at higher general secondary school and there are no signs of a delayed development. Pictures are shown in Figures 2 and 3.

Patient III-4, a cousin of the proband, is a boy with a sagittal suture synostosis with a mild dolichocephaly, which has never been operated. There was a normal development and there were no other characteristic anomalies. Pictures are shown in Figure 3.

Patient number II-1, the father of the proband III-1, showed a craniosynostosis of the metopic suture, which has never been operated. He showed slightly closely spaced eyes which matched his trigonocephaly. Pictures are shown in Figures 2 and 3. Remarkable in this patient were the short fingers of the hands. The shape of the digits was normal. An X-ray of the hands showed the short fingers and unexpectedly the presence of osteopoikilosis. Short fingers in this patient were caused by shortening of all phalanges, and diagnosed by a clinical geneticist and a plastic surgeon. After testing *LEMD3*, a gene known to be involved in osteopoikilosis, a deletion of exon 5-13 was found in this gene in this patient. All family members were then tested for this deletion by qPCR (data not shown). The *LEMD3* mutation in patient II-1 was an apparently de novo mutation, inherited by his son, Patient III-1. In the son the osteopoikilosis was not visible due to his young age (11, 12). All other family members tested negative for this *LEMD3* mutation.

Both patients II-4 and II-6, who are sisters and were never operated, showed a brachycephalic skull shape. X-rays of the skull of these patients showed premature closure of the coronal sutures with elevated sphenoid wings and thereby a distorted orbital shape. X-rays of these patients showed generalized copper beaten aspect, suggestive of elevated intracranial pressure. Pictures are shown in Figures 2 and 3. Hands and feet did not show any abnormalities.

Patient I-2 is the grandfather of the family. His skull X-ray showed a unilateral coronal suture synostosis and a bony defect at the region of the anterior fontanel. The midface did not show any specific abnormalities. Pictures are shown in Figure 3.

Patient I-3 is known to have a turricephaly but refused to participate in this study. X-rays are not available.

In summary, all patients have a distinct skull phenotype. The main characteristic present in all patients is the craniosynostosis. Other characteristics such as closely spaced eyes, midface retrusion and hand abnormalities were variable. Clinical information is presented in Table I.

Based on the clinical information and the pedigree, it was concluded that the disease segregates in an autosomal dominant mode of inheritance. Linkage analysis combined with genome sequencing was performed to identify the underlying genetic defect.

Table I: Summary of clinical information of the whole family

Individual	Age in years	Sex	Craniosynostosis phenotype	Surgery	Other
I-2	73	M	Unilateral coronal synostosis	-	Defect anterior fontanel
I-3		M	Turricephaly	-	No participation
II-1	47	M	Trigonocephaly	-	Brachydactyly, hypotelorism
II-4	46	F	Brachycephaly	-	
II-6	39	F	Brachycephaly	-	
III-1	7	M	Turricephaly	Yes	Bitemporal depression, hypotelorism
III-3	22	F	Complex craniosynostosis	Yes	Retrusion forehead
III-4	17	M	Scaphocephaly	-	

Linkage analysis

Multipoint linkage analysis using DNA of seven patients (I-2, II-1, II-4, II-6, III-1, III-3, III-4) and five unaffected individuals (I-1, II-2, III-2, III-5, III-6), was performed on the craniosynostosis trait and resulted in four linkage peaks:

chr. 2q11, 0.5 Mb, rs28442891 - rs1441649/112238628 bp - 88295232 bp;
 chr. 2q32, 8.6 Mb, rs10931712 - rs13394087/196677840 bp - 205260409 bp;
 chr. 5q35, 5.9 Mb, rs6555884 - rs3955072/169510630 bp - 174708042 bp;
 chr. 21q22, 1.6 Mb, rs7275820 - rs3787835/37409414 bp - 39189570) with maxLOD scores between 2 and 2.5. These four loci together comprise of 16.7 Mb containing 195 genes (NCBI Build 37) and excluded all known craniosynostosis-associated genes except for *MSX2*.

Genome Sequencing Data Analysis

To evaluate candidate genes from the linkage regions, genome sequencing data of five selected family members was analyzed. The initial analysis was restricted to non-synonymous variants, variants disrupting a splice site, and small insertions or deletions (up to approximately 50 bp) in the coding sequence. Additionally, variants had to be fully called in all five family members, absent from dbSNP version 130, and follow the expected autosomal dominant inheritance mode. This filtering left 134 candidate variants (**Table II**). When focusing on the regions that showed linkage, only two of these variants remained, both single nucleotide variants encoding missense mutations. One variant, in exon 18 of *DNAH7* [OMIM:610061] c.2516C>G (NM_018897.2), predicts p.Pro839Arg (NP_061720.0). The other variant, in exon 2 of *MSX2*, c.443C>T (NM_002449.4), predicts p.Pro148Leu (NP_002440.2). Both single nucleotide variants were predicted to be probably damaging by PolyPhen2, and were not present in our in-

Chapter 2

house database Huvarione or in the data from the 1000 genomes project (13). However, the DNAH7 variant was present once in the Exome Variant Server database.(NHLBI GO ESP6500), whereas the *MSX2* variant was not.

Therefore, the p.Pro148Leu variant in *MSX2* was a candidate given that a mutation on the same position in the *MSX2* protein was described previously in a three-generation American family in which craniosynostosis was segregating in 13 individuals, and described as the Boston-type craniosynostosis(4, 6). Additionally, the proline is evolutionary conserved, see Figure 4A. This suggests that the mutation we found on the same position in *MSX2* is likely to be the variant causing the craniosynostosis in the family reported by us.

Validation of the variant by Sanger Sequencing

The mutation within the *MSX2* gene has been verified by DNA Sanger sequencing in all 12 participating family members and was present in all affected family members and absent in all unaffected family members, see Figure 4B.

Table II: Outlines the bioinformatics filtering steps that have led to the identification of the two single nucleotide variants within the two candidate genes *MSX2* and *DNAH7*

Total variants	n = 6073719
Not in dbSNP 130	n= 892483
Fully called in all 5 family members	n = 581520
Autosomal dominant	n = 34433
In exon / Splice site	n = 284
Nonsynonymous / disrupting splice site	n= 134
In linkage area	n=2

DISCUSSION

The Boston type craniosynostosis [OMIM 604757] is an autosomal dominant disorder described by Muller et al. and Warman et al. and termed as such by Jabs et al.(4, 6, 7)

Subsequently, only one additional family with an *MSX2* mutation has been described. Wilkie et al. screened a cohort of 362 patients with craniosynostosis for mutations (14). Ninety-one mutation negative patients were tested for mutations in *MSX2*. However, this did not indentify any definite pathogenic mutations. Four patients were described with an extra copy of *MSX2* (15-18)

As noted above, Jabs et al. found the first mutation in *MSX2* in a large family with a highly variable phenotype as described earlier by Warman et al. (4, 6). The family that we present is the second family with a mutation in the *MSX2* gene and also shows variable clinical presentation. Still, we observe some striking phenotypic similarities in these two families. Both had frontal bossing and turricephaly in the most severely affected patients. Furthermore, there was an absence of gross limb abnormalities.

Interestingly, the affected amino acid in *MSX2* in the family described here (p.Pro148Leu) was at the same codon as in the family described by Jabs et al. (p.Pro148His) and likely causing a similar and specific gain of function through increased or altered binding of the *MSX2* protein to DNA (6, 19). Given the rarity of this gain of function mutation it is likely that gain of function is only possible through a very limited mutations repertoire within the DNA-binding homeodomain. Most described *MSX2* mutations are loss of function mutations and the haploinsufficiency phenotype is different, causing parietal foramina [OMIM:168500] (20-24)

Osteopoikilosis which is described as a loss of function mutation of the LEMD3 protein, was found only in two members in this family and considered as a coincidental separate anomaly with an apparently *de novo* mutation in patient II-1 (25, 26). Only one patient has been described with a combination of osteopoikilosis and craniosynostosis (27). Therefore, we conclude that it is a coincidence that the patient reported here has osteopoikilosis and craniosynostosis. Brachydactyly, as seen in three of seven patients, may likely be a part of the variable *MSX2* Boston type craniosynostosis.

In conclusion, we identified the second family with a dominant inherited mutation in the *MSX2* gene, 20 years after the original publication. This confirms that missense mutations of codon 148 cause Boston type craniosynostosis and that the phenotype is variable and difficult to recognize on clinical grounds. Since a *MSX2* gene mutation occurs rarely and is clinically difficult to recognize, next generation sequencing may be an effective approach to make a precise diagnosis.

A.

Homo Sapiens (NP_002440.2)	NRKPRT E FTTSQLLALERKFRQKQYLSIAERAEFSSSLNLTETQVKIWFQNRRAKAKRLQ
Pan troglodytes (NP_001129097.2)	NRKPRT E FTTSQLLALERKFRQKQYLSIAERAEFSSSLNLTETQVKIWFQNRRAKAKRLQ
Canis lupus familiaris (NP_001003098.1)	NRKPRT E FTTSQLLALERKFRQKQYLSIAERAEFSSSLNLTETQVKIWFQNRRAKAKRLQ
Bos taurus (NP_001073082.1)	NRKPRT E FTTSQLLALERKFRQKQYLSIAERAEFSSSLNLTETQVKIWFQNRRAKAKRLQ
Mus musculus (NP_038629.2)	NRKPRT E FTTSQLLALERKFRQKQYLSIAERAEFSSSLNLTETQVKIWFQNRRAKAKRLQ
Rattus norvegicus (NP_037114.2)	NRKPRT E FTTSQLLALERKFRQKQYLSIAERAEFSSSLNLTETQVKIWFQNRRAKAKRLQ
Gallus gallus (NP_989890.1)	NRKPRT E FTTSQLLALERKFRQKQYLSIAERAEFSSSLNLTETQVKIWFQNRRAKAKRLQ
Danio rerio (NP_571351.2)	NRKPRT E FTTSQLLALERKFRQKQYLSIAERAEFSSSLTLTETQVKIWFQNRRAKAKRLQ
Macaca mulatta (XP_001082405.1)	NRKPRT E FTTSQLLALERKFRQKQYLSIAERAEFSSSLNLTETQVKIWFQNRRAKAKRLQ
Mutation reported by Jabs et al. 1993	NRKPRT H FTTSQLLALERKFRQKQYLSIAERAEFSSSLNLTETQVKIWFQNRRAKAKRLQ
Mutation this report	NRKPRT L FTTSQLLALERKFRQKQYLSIAERAEFSSSLNLTETQVKIWFQNRRAKAKRLQ

B.

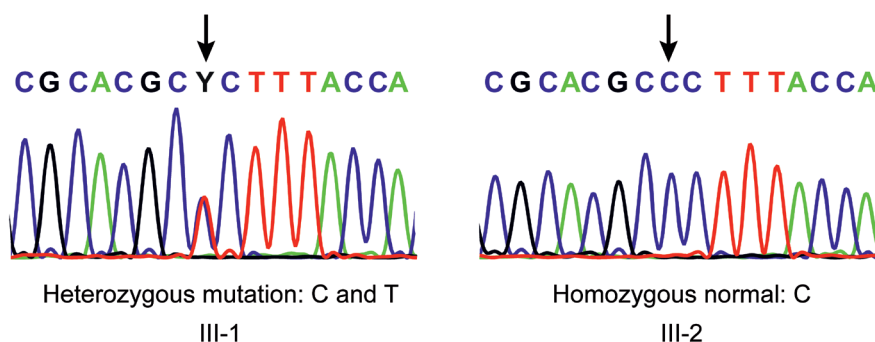


Figure 4: *MSX2* protein (A) and gene (B) sequences. **A:** Alignment of the conserved DNA binding homeobox domain of *MSX2* in different species. In the human protein the DNA binding domain of *MSX2* is 60 aa, from residue 142 to 201. The proline on position 148 is indicated in red. The mutations in the patients described by Jabs et al. [1993] (p.Pro148His) and in the family reported here (p.Pro148Leu) are indicated in gray. **B:** Validation of Mutation with Sanger Sequence Analysis. Sanger sequencing analysis showing the *MSX2* mutation in exon 2 (c.443C>T) in the proband III-1 (left panel). The normal DNA sequence is: CGC ACG CCC TTT ACC A. Homozygous normal sequence from III-2, the unaffected sister of the proband, is shown in the right panel. Sequences shown are representative for the sequence of the other affected and unaffected members from the pedigree as indicated in Figure 1. Mutated and normal sequence is indicated with an arrow.

ACKNOWLEDGEMENTS

The authors extend their sincere appreciation to the patients and their parents for their participation and the enthusiastic support. Moreover, we are grateful for the grants obtained from the Centre for Translational Molecular Medicine in The Netherlands. We would like to acknowledge Rick Tearle and Stephen Lincoln from Complete Genomics a BGI Company (Mountain View, CA) for their support to our NGS training Centre in Rotterdam. We thank Tom de Vries Lentsch for graphical support.

REFERENCES

1. Morriss-Kay GM, Wilkie AO. Growth of the normal skull vault and its alteration in craniosynostosis: insights from human genetics and experimental studies. *J Anat.* 2005;207(5):637-53.
2. Johnson D, Wilkie AO. Craniosynostosis. *European journal of human genetics : EJHG.* 2011;19(4):369-76. Epub 2011/01/21.
3. Sharma VP, Fenwick AL, Brockop MS, McGowan SJ, Goos JA, Hooeboom AJ, et al. Mutations in *TCF12*, encoding a basic helix-loop-helix partner of *TWIST1*, are a frequent cause of coronal craniosynostosis. *Nature genetics.* 2013;45(3):304-7. Epub 2013/01/29.
4. Warman ML, Mulliken JB, Hayward PG, Muller U. Newly recognized autosomal dominant disorder with craniosynostosis. *Am J Med Genet.* 1993;46(4):444-9.
5. Park WJ, Theda C, Maestri NE, Meyers GA, Fryburg JS, Dufresne C, et al. Analysis of phenotypic features and *FGFR2* mutations in Apert syndrome. *American journal of human genetics.* 1995;57(2):321-8. Epub 1995/08/01.
6. Jabs EW, Muller U, Li X, Ma L, Luo W, Haworth IS, et al. A mutation in the homeodomain of the human *MSX2* gene in a family affected with autosomal dominant craniosynostosis. *Cell.* 1993;75(3):443-50.
7. Muller U, Warman ML, Mulliken JB, Weber JL. Assignment of a gene locus involved in craniosynostosis to chromosome 5qter. *Hum Mol Genet.* 1993;2(2):119-22. Epub 1993/02/01.
8. Gudbjartsson DF, Jonasson K, Frigge ML, Kong A. Allegro, a new computer program for multipoint linkage analysis. *Nature genetics.* 2000;25(1):12-3. Epub 2000/05/10.
9. O'Connell JR, Weeks DE. PedCheck: a program for identification of genotype incompatibilities in linkage analysis. *American journal of human genetics.* 1998;63(1):259-66. Epub 1998/06/23.
10. Drmanac R, Sparks AB, Callow MJ, Halpern AL, Burns NL, Kermani BG, et al. Human genome sequencing using unchained base reads on self-assembling DNA nanoarrays. *Science.* 2010;327(5961):78-81. Epub 2009/11/07.
11. Woyciechowsky TG, Monticelo MR, Keiserman B, Monticelo OA. Osteopoikilosis: what does the rheumatologist must know about it? *Clin Rheumatol.*
12. Gass JK, Hellemans J, Mortier G, Griffiths M, Burrows NP. Buschke-Ollendorff syndrome: a manifestation of a heterozygous nonsense mutation in the *LEMD3* gene. *Journal of the American Academy of Dermatology.* 2008;58(5 Suppl 1):S103-4. Epub 2008/06/14.
13. Stubbs A, McClellan EA, Horsman S, Hiltmann SD, Palli I, Nouwens S, et al. Huvariome: a web server resource of whole genome next-generation sequencing allelic frequencies to aid in pathological candidate gene selection. *Journal of clinical bioinformatics.* 2012;2(1):19. Epub 2012/11/21.
14. Wilkie AO, Byren JC, Hurst JA, Jayamohan J, Johnson D, Knight SJ, et al. Prevalence and complications of single-gene and chromosomal disorders in craniosynostosis. *Pediatrics.* 2010;126(2):e391-400. Epub 2010/07/21.

Chapter 2

15. Bernardini L, Castori M, Capalbo A, Mokini V, Mingarelli R, Simi P, et al. Syndromic craniosynostosis due to complex chromosome 5 rearrangement and *MSX2* gene triplication. *American journal of medical genetics Part A*. 2007;143A(24):2937-43. Epub 2007/11/15.
16. Kariminejad A, Kariminejad R, Tzschach A, Ullmann R, Ahmed A, Asghari-Roodsari A, et al. Craniosynostosis in a patient with 2q37.3 deletion 5q34 duplication: association of extra copy of *MSX2* with craniosynostosis. *American journal of medical genetics Part A*. 2009;149A(7):1544-9. Epub 2009/06/18.
17. Shiihara T, Kato M, Kimura T, Hayasaka K, Yamamori S, Ogata T. Craniosynostosis with extra copy of *MSX2* in a patient with partial 5q-trisomy. *American journal of medical genetics Part A*. 2004;128A(2):214-6. Epub 2004/06/24.
18. Wang JC, Steinraths M, Dang L, Lomax B, Eydoux P, Stockley T, et al. Craniosynostosis associated with distal 5q-trisomy: further evidence that extra copy of *MSX2* gene leads to craniosynostosis. *American journal of medical genetics Part A*. 2007;143A(24):2931-6. Epub 2007/10/24.
19. Ma L, Golden S, Wu L, Maxson R. The molecular basis of Boston-type craniosynostosis: the Pro148-->His mutation in the N-terminal arm of the *MSX2* homeodomain stabilizes DNA binding without altering nucleotide sequence preferences. *Hum Mol Genet*. 1996;5(12):1915-20.
20. Mavrogiannis LA, Taylor IB, Davies SJ, Ramos FJ, Olivares JL, Wilkie AO. Enlarged parietal foramina caused by mutations in the homeobox genes *ALX4* and *MSX2*: from genotype to phenotype. *European journal of human genetics : EJHG*. 2006;14(2):151-8. Epub 2005/12/02.
21. Spruijt L, Verdyck P, Van Hul W, Wuyts W, de Die-Smulders C. A novel mutation in the *MSX2* gene in a family with foramina parietalia permagna (FPP). *American journal of medical genetics Part A*. 2005;139(1):45-7. Epub 2005/10/14.
22. Wilkie AO, Tang Z, Elanko N, Walsh S, Twigg SR, Hurst JA, et al. Functional haploinsufficiency of the human homeobox gene *MSX2* causes defects in skull ossification. *Nature genetics*. 2000;24(4):387-90. Epub 2000/03/31.
23. Wuyts W, Reardon W, Preis S, Homfray T, Rasore-Quartino A, Christians H, et al. Identification of mutations in the *MSX2* homeobox gene in families affected with foramina parietalia permagna. *Hum Mol Genet*. 2000;9(8):1251-5. Epub 2000/04/18.
24. Garcia-Minaur S, Mavrogiannis LA, Rannan-Eliya SV, Hendry MA, Liston WA, Porteous ME, et al. Parietal foramina with cleidocranial dysplasia is caused by mutation in *MSX2*. *European journal of human genetics : EJHG*. 2003;11(11):892-5. Epub 2003/10/23.
25. Hellemans J, Debeer P, Wright M, Janecke A, Kjaer KW, Verdonk PC, et al. Germline *LEMD3* mutations are rare in sporadic patients with isolated melorheostosis. *Human mutation*. 2006;27(3):290. Epub 2006/02/14.
26. Mumm S, Wenkert D, Zhang X, McAlister WH, Mier RJ, Whyte MP. Deactivating germline mutations in *LEMD3* cause osteopoikilosis and Buschke-Ollendorff syndrome, but not sporadic melorheostosis. *Journal of bone and mineral research : the official journal of the American Society for Bone and Mineral Research*. 2007;22(2):243-50. Epub 2006/11/08.
27. Reid EM, Baker BL, Stees MA, Stone SP. Buschke-Ollendorff syndrome: a 32-month-old boy with elastomas and craniosynostosis. *Pediatric dermatology*. 2008;25(3):349-51. Epub 2008/06/26.



CHAPTER 3

Complex Craniosynostosis is associated with the 2p15p16.1 Microdeletion Syndrome

J.M.G. Florisson
I.M.J. Mathijssen
B. Dumee
A.J.M. Hoogeboom
P.J. Poddighe
B.A. Oostra
J.P. Frijns
L. Koster
A. de Klein
B. Eussen
B.B.A. de Vries
S. Swagemakers
P. J. van der Spek
J.M.H. Verkerk

American journal of medical genetics Part A. 2013;161A(2):244-53. Epub 2013/01/11.

ABSTRACT

In a screening project of patients with (complex) craniosynostosis using genomic arrays, we identified two patients with craniosynostosis and microcephaly with a deletion in the 2p15p16.1 chromosomal region. This region has been associated with a new microdeletion syndrome, for which patients have various features in common, including microcephaly and intellectual disability. Deletions were identified using Affymetrix 250K SNP array and further characterized by fluorescence in situ hybridisation (FISH) analysis and qPCR. The deletions in our two patients overlapped within the 2p15p16.1 microdeletion syndrome area and were 6.8 and 6.9 Mb in size, respectively. FISH and qPCR confirmed the presence of only 1 copy in this region.

Finemapping of the breakpoints indicated precise borders in our patients and were further finemapped in two other previously reported patients.

Clinical features of patients with deletions in the 2p15p16.1 region vary. Including data from our patients, now 8 out of 9 reported patients have microcephaly, one of the major features, and all had intellectual disability. The current reported two patients add different forms of craniosynostosis to the clinical spectrum of this recently recognized microdeletion syndrome.

keywords: chromosome 2p15p16.1, craniosynostosis, microcephaly, microdeletion, 250K SNP array

INTRODUCTION

Genomic array studies have recently revealed a new microdeletion syndrome on chromosome 2p15p16.1 (1-6)

In total seven patients have been described with overlapping deletions, varying from 570 kb to 5.7 Mb, using various comparative genomic hybridization (CGH) array analyses (bacterial artificial chromosome (BAC), oligo or SNP based techniques).

Of these seven cases, the one with the small 570 kb deletion seems to have a significant milder phenotype compared to the other six with larger deletions varying from 3.2 Mb to 5.7 Mb. In the latter six cases common clinical features are moderate to severe developmental delay, mild to moderate intellectual disability, microcephaly and characteristic and recognizable facial dysmorphisms. In addition five were known to have optic nerve hypoplasia, three had a hydronephrosis, two had cortical dysplasia and hand/foot abnormalities were reported in four patients. Liang et al. proposed two critical regions: the distal 570 kb for developmental delay and some of the facial dysmorphisms and the proximal 2.1 Mb for autistic behavior, short stature, microcephaly, additional facial dysmorphisms, optic nerve hypoplasia and hydronephrosis (4). The patient reported by Prontera et al., with a deletion of 3.5 Mb, had many clinical features overlapping with the other described patients, but that deletion encompasses only few genes (5).

Here we report on two additional patients with overlapping de novo deletions in the same chromosomal area, detected by 250 K SNP array analysis. These patients do not only show the common features of the 2p15p16.1 microdeletion syndrome, but additionally show a complex form of craniosynostosis. We have fine mapped the deletion breakpoints of our patients and the two previously reported patients described by de Leeuw et al. and Chabchoub et al using qPCR(1, 2). Additionally we have further defined the published borders of the deletion breakpoints by mapping data in USCS build 37.

MATERIALS AND METHODS

Clinical assessment

All patients seen at the Dutch craniofacial center for syndromic forms of craniosynostosis undergo genetic screening for microscopic chromosomal abnormalities and/or *FGFR1*, *FGFR2*, *FGFR3* mutations or *TWIST1* mutations or deletions. In the patients described in this paper, who were suspected for a syndromic form of craniosynostosis, no such mutation was found. We performed SNP array analysis for these patients.

SNP Array analysis

Whole genome analysis was performed by microarray analysis using Affymetrix 250K Nspl SNP arrays. The assays were carried out according to the manufacturer's instructions

Chapter 3

(Affymetrix GeneChip Mapping assay: www.affymetrix.com). Genotype data analysis was performed in Nexus 5 (Biodiscovery) using the Rank Segmentation algorithm.

FISH analysis

FISH analysis was performed on chromosomes of patients 1 and 2 and their parents.

The BAC clones used were selected from the University of California Santa Cruz UCSC browser and purchased from BACPAC Resources.

DNA was digested (Mbol) and labeled with Bio-16-dUTP or dig-11-dUTP by a Random Prime labeling system (Invitrogen, Carlsbad, CA). The FISH experiments were performed according to standard protocols with minor modifications. FISH slides were analyzed with a Axioplan 2 Imaging microscope (Zeiss, Sliedrecht, The Netherlands). Images were captured using the fluorescent software Isis (MetaSystems, Altlussheim, Germany).

Names and location (build 37) of the BAC clones used were:

RP11-373L24; 2p16.1; 61073681 - 61282740 bp

RP11-772D22; 2p15; 62167828 - 62350291 bp

RP11-355B11; 2p15; 61660124 - 61819815 bp

CTB-8L3; 2p25.3; sub-telomeric chromosome 2 probe used as a control

Quantitative PCR analysis

Relative copy numbers were determined by using real-time PCR analysis. 25 ng of patient or control DNA was used in a 25 µl reaction containing 1x iTaq SYBR Green Supermix with ROX (Bio-Rad) and 200 nM of each primer. To verify results, three replicates were performed for each sample. Real-time PCR was performed on a 7300 Real Time PCR system (Applied Biosystems), cycle conditions: 10 min 95°C initial denaturation, followed by 40 cycles 15 sec denaturation; annealing/extension and data collection 1min 60°C. Data were analyzed using the software package 7300 System SDS Software RQ Study Application v1.2.3 (Applied Biosystems). Q-PCR Primer sequences used and their location on chromosome 2 are summarized in supplementary eTable SI. (See Supporting Information online)

RESULTS

Clinical description of the patients

We describe two patients who were referred to the Dutch Craniofacial Centre in Rotterdam.

Patient 1 is a male patient who was born after 42 weeks of gestation with a weight of 3240 grams. At three months of age he had a small skull and a deviating skull circumference of -3 SD, based on curve "head circumference for age [growth analyser, The Netherlands 1997]. He showed a protrusion of the central forehead and a triangular shaped head

when viewed from above (**Figure 1A**) and had a palpable metopic ridge, hypotelorism and supraorbital retrusion, all characteristics in concordance with a combined trigonocephaly and microcephaly. The face showed strabismus, mild epicanthal folds, mild ptosis, short palpebral fissures, smooth and long philtrum, everted lower lip and retrognathia. The hands showed no abnormalities; both feet show a clinodactyly of the 4th ray (**Figure 1A**). A 3D CT scan image at the age of three months showed a synostosis of the metopic and the sagittal sutures (**Figure 1B**). The coronal sutures and the lambdoid sutures were still open. Additionally the CT scan showed that the trigonocephaly caused the hypotelorism. Furthermore impressions of the inner table of the skull, mainly situated at the occipital and the parietal regions, were seen. The brain parenchyma and the ventricles showed a normal aspect. A MRI scan performed at the age of 2 years and 10 months (1.5 Tesla GE system, General Electric) showed a simplified gyral pattern in the supra tentorial region, a hypoplastic corpus callosum and a rather small aspect of the cerebellum and the pons (**Figure 1C**).

Patient 1 was operated for his craniosynostosis at the age of 7 months in our clinic. A parietal and frontal correction was performed without any complications. At the age of three years, his motor and mental developments were delayed. At the age of 22 months he started walking with support, which normally starts around the age of 13 -15 months and there was no speech at all. His cognitive development was more severely retarded than his motor development. At the age of 33 months he had a mental development matching a 7.5-month-old-child, and a motor development matching a 15-month-old child [mental and motor scale of Bayley Scales of Infant Development - Second Edition (BSID-II)]. Both parents had a normal phenotype.

Patient 2 was operated abroad and after that seen at our clinic at the age of 6 months. She was born after 36 weeks of gestational age with a weight of 2150 gram. Directly after birth different deformities were noticed (**Figure 1D**). The head showed an abnormal skull shape, matching the sagittal suture and left coronal suture synostosis. The skull circumference at birth was 29 cm (<P3). The nose had a very broad nasal root and the philtrum was flat. Blepharophimosis and long down slanting eyelashes were noticed. The ears showed an hypoplastic helical rim, and the palate was flat. The hands showed tapering fingers and a camptodactyly of all the digits but mainly the third and fourth digit. The 5th finger was small on both hands (**Figure 1E**). She had a very short neck and one café au lait spot on the left buttock. There was a severe motor and mental developmental delay. Motor development at the age of 13 years was restricted to walking for several hours, climbing stairs was possible with support. Verbally the patient was restricted to signs and the use of single words. Psychological testing was performed at the age of 10 years and matched functioning at an age level of 17 months. Both parents and the brother and sister of the patient had a normal phenotype.

This study was approved by the medical ethical committee of the Erasmus MC, MEC-2005-273.

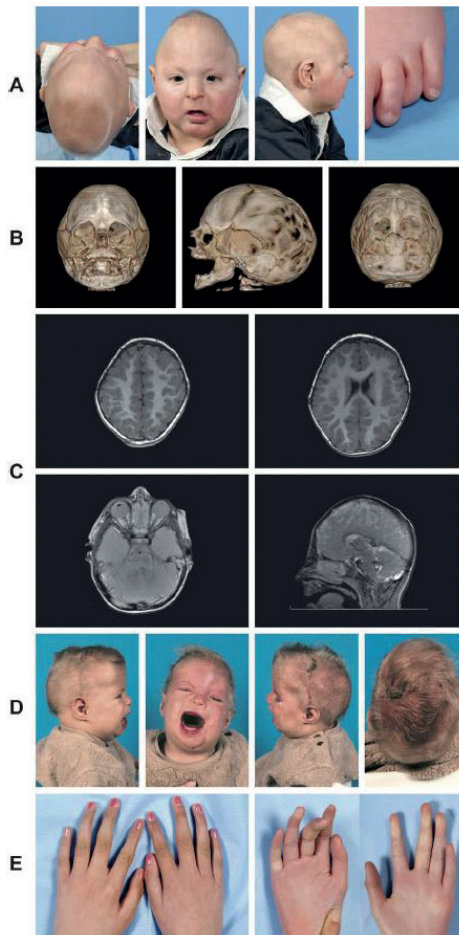


Figure 1: Clinical data of patient 1 and 2. **A:** patient 1 at the age of six months. Note the trigonocephalic form of the skull and the small size of the head, the strabismus and epicanthal folds on both eyes and clinodactyly of the fourth ray on the feet. **B:** 3D CT scan of patient 1 at the age of 3 months showing a synostosis of the metopic and sagittal suture, hypotelorism and impressions at the occipital and parietal bones. **C:** MRI of patient 1 at the age of 2 years and 10 months shows a simplified gyral pattern in the supra tentorial region and a hypoplastic corpus callosum. The cerebellum and pons are rather small. **D:** patient 2 at the age of 6 months. Note the abnormal skull shape and small size of the head, a very broad nasal root and a flat philtrum, blepharophimosis, long eyelashes and an expired helix fold of the ears. **E.** Hands of patient 2 at the age of 12 years. Tapering of the fingers is clearly seen (in the dorsal view) as is the campodactyly of the third and fourth ray on the hands.

SNP array analysis and validation with FISH analysis

DNA of patient 1 and 2 was analyzed on Affymetrix 250K Nsp1 SNP array. Both patients showed a deletion of respectively 6.9 and 6.8 Mb in chromosome 2, showing an overlap in the p15p16 area (**Figure 2A and B**). The deletions were confirmed by FISH analysis with chromosome 2p15p16.1 and 2p25 BAC probes (**Figure 3A and B**) in both patients. The deletions were absent in their parents (data not shown), indicating a de novo deletion in both children.

Complex craniosynostosis is associated with the 2p15p16.1 microdeletion syndrome

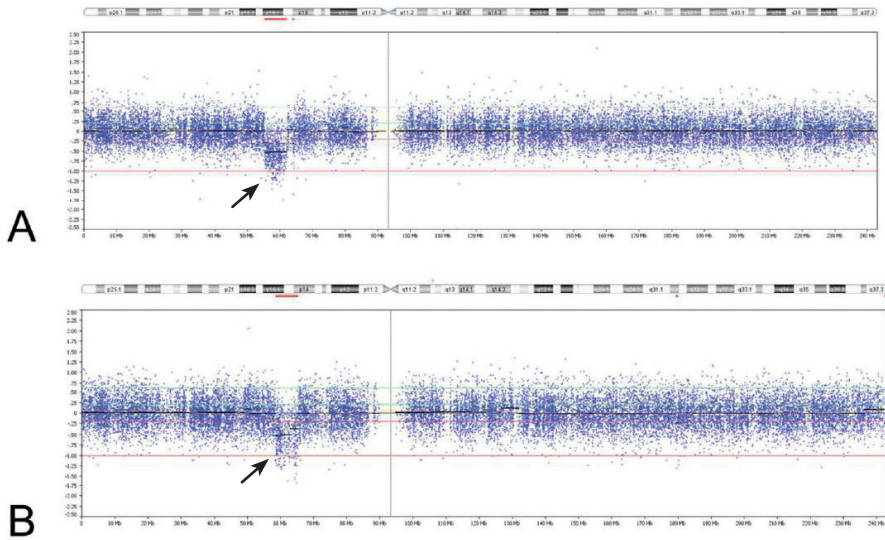


Figure 2: Identification of the 2p15p16 deletions by analysis of Affymetrix 250 K NSPI SNP data in Nexus 5 (Biodiscovery) in **A:** patient 1 (6,9 Mb) and **B:** patient 2 (6,8 Mb). Blue dots represent the log2 ratio's of SNP probe intensities of experiment and control samples. Arrows indicate the presence of copy number loss at 2p15p16.

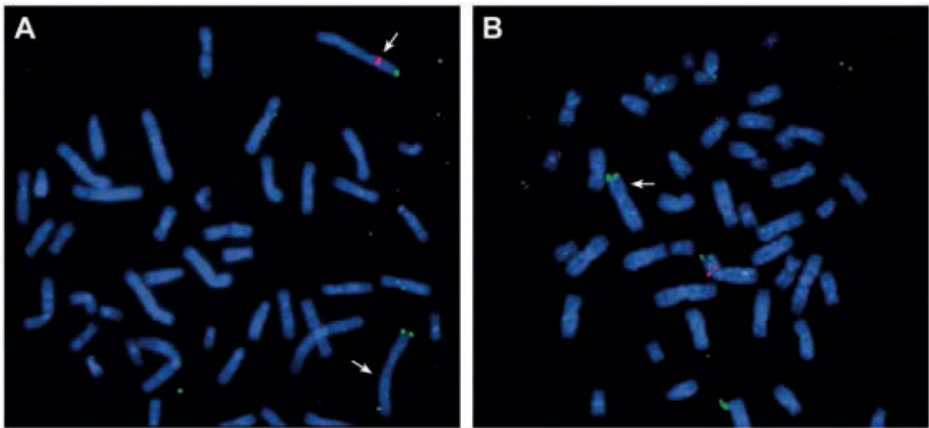


Figure 3: Fluorescence in situ hybridization analysis on metaphases obtained from cultured lymphocytes of patient 1 (A) and patient 2 (B). **A:** BAC probe RP11-373L24 (2p16) in red, 1 copy present and CTB-8L3 (2p25.3, control probe) in green, 2 copies present. (1948.012). **B:** BAC probe RP11-772D22 (2p15) in red, 1 copy present and CTB-8L3 (2p25.3, control probe) in green, 2 copies present. (0603.002)

3

DEFINING DELETION BORDERS AND REGION

qPCR

Breakpoints of the deletions of patient 1 and 2 were further mapped by qPCR. In addition we have fine mapped the breakpoints for the chromosome 2 deletion patients described by Chabchoub et al. and de Leeuw et al. by qPCR, as the breakpoints in these patients were based on 1Mb resolution BAC array data, with the BACs not covering the complete chromosomal 2p15p16.1 area (1, 2). Primers including base pair positions for qPCR are indicated in supplementary eTable S1 (See supporting information online). Histogram displaying results of the qPCR are shown in supplementary eFigure S1 (See supporting information online). Results are indicated in Table I. The distal breakpoint in our patient 1 is between MTIF2 (2 copies; primerset cr2_s13_F2/R2) and CCDC88A (1 copy; cr2_s15_F1/R1). The proximal breakpoint is between COMMD1 (1 copy; primerset cr2_s5_COMMD1_Fp1/Rp1) and B3GNT2 (2 copies; cr2_s14_F1/R1). The deletion area encompasses 35 genes (excluding the pseudogenes). The distal breakpoint in patient 2 is between FANCL (2 copies; primerset cr2_p1_F/R) and FLJ30838 (1 copy, primerset cr2_p2_F/R). The proximal breakpoint is between RAB1A (1 copy; primerset cr2_s13_F4/R4) and ACTR2 (2 copies; primerset cr2_s13_F5/R5) with the deletion encompassing 43 genes (excluding pseudogenes). The deletion overlap for these two patients with microcephaly and craniosynostosis encompasses 23 genes, from FLJ30838 to COMMD1.

The distal breakpoint for the patient described by Chabchoub et al. is between REL (2 copies, primerset cr2_s12_F3/R3) and PUS10 (1 copy, primerset cr2_s8_PUS10_Fp1/Rp1) (1). The proximal breakpoint is between SNORA70B (1 copy, primerset cr2_s9_Fp3/Rp3) and LOC647077 (2 copies, primerset cr2_betweenXPO+FAMM_F/R), possibly in the XPO1 gene based on the published BAC data (1). By qPCR we could not determine the copy number in the area between SNORA70B and LOC647077 due to normal copy number variation in this area (Database of Genomic Variants; <http://projects.tcag.ca/cgi-bin/variation/gbrowse/hg19>). The distal breakpoint for the patient described by de Leeuw et al. is between CCDC85A (2 copies, primerset cr2_betweenVRK2+LOC1001F/R) and the VRK2 gene (1 copy, primerset cr2_s12_F1/R1)² (2). The proximal breakpoint is the same as for the patient described by Chabchoub et al. (1).

Deletions of all patients, encompassing genes in the area, are indicated in **Figure 4**.

Complex craniosynostosis is associated with the 2p15p16.1 microdeletion syndrome

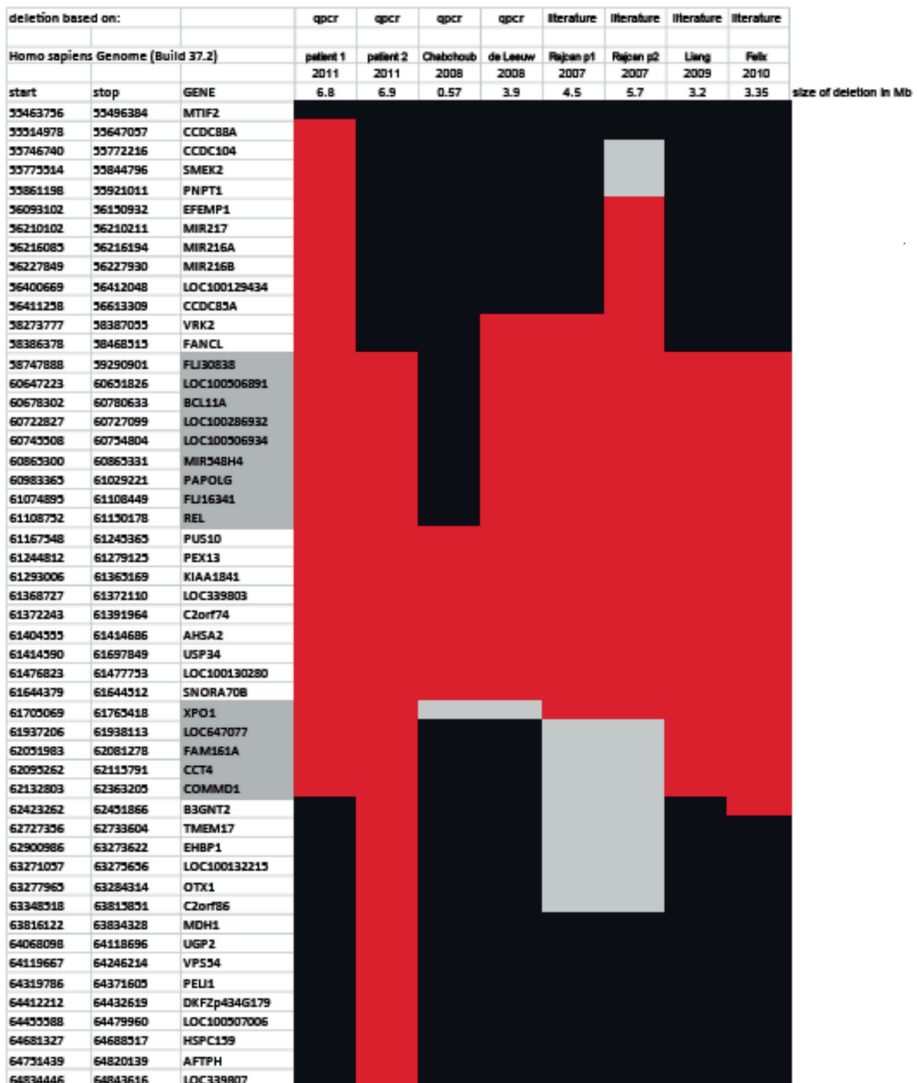


Figure 4: Microdeletion area chromosome 2p15p16 .

Deletions (in red) are indicated in our patient 1 and 2 and in all patients described in literature until now. Genes in the region with basepair positions (build 37, hg19) are indicated on the left. The light-grey area around Xpo 1 could not be resolved by q-PCR, due to normal copy number variation in this region. The minimal distal deletion borders in the two subjects from Rajcan-Separovic et al. are indicated as described in Liu et al. [2011]. Unresolved areas are indicated in light-gray.

Basepair positions from the deletions described in the literature were all converted to build 37, hg 19. The deletion from Prontera et al. seems small in the figure, because in their 3.5 Mb deletion area, only 3 genes are located (distances are not drawn to scale).

Table 1: results breakpoint analysis by qPCR: deletion areas are indicated in gray

Name primer pair forward/reverse	patient 1	patient 2	Chabchoub	de Leeuw	gene
1-2: cr2_s13_F2/R2	2				MTIF2
3-4: cr2_s15_F1/R1	1				CCDC88A
5-6: cr2_s13_F3/R3					
7-8: cr2_betweenVRK2+LOC1001_F/R				2	CCDC85A
9-10: cr2_s12_F1/R1				1	VRK2
11-12: cr2_p1_F/R		2			FANCL
13-14: cr2_p2_F/R		1			FLJ30838
15-16: cr2_s12_F3/R3			2		REL
17-18: cr2_s8_Pus10_Fp1/Rp1			1		PUS10
19-20: cr2_s9_Fp3/Rp3			1	1	SNORA70B
21-22: cr2_betweenXPO+FAMM_F/R			2	2	LOC647077
23-24: cr2_s5_COMMD1_Fp1/Rp1	1				COMMD1
25-26: cr2_s14_F1/R1	2				B3GNT2
27-28: cr2_s13_F4/R4		1			RAB1A
29-30: cr2_s13_F5/R5		2			ACTR2

Enhancers

In the region from 55463756 – 65498387, 42 Human Vista enhancer elements are located (7). These are highly conserved elements with possible gene distant-acting enhancer activity. These 42 are all between FANCL and PAPOLG, the region that is deleted in seven and partially deleted in one of the patients (**supplementary eFigure S2 – See supporting information online**). Fourteen of these elements have expression as assessed in transgenic mice, in amongst others brain (hs394,hs399,hs779,hs975,hs1076 ,hs1119,hs1535), facial mesenchym (hs836) eye (hs393), and ear (hs1071). This indicates that these enhancers possibly play a role in the observed phenotype and have a function in these tissues in regulating other genes.

DISCUSSION

We describe two patients with overlapping deletions in the 2p15p16.1 region, an area that is recently recognized as a new microdeletion syndrome (1-6). These patients have the largest deletions in this area described so far, but the common overlapping deleted region is similar to the deletions described in the patients by Liang et al. and Felix et al. (3, 4). Notably, the current patients add craniosynostosis as a new clinical characteristic to this novel microdeletion syndrome (**Table II**), though both patients have different forms. Patient 1 has a synostosis of the metopic and the sagittal suture in addition to a trigonocephalic head, whereas patient 2 has a synostosis of the left coronal and sagittal suture. Patient 1 additionally showed brain abnormalities in the form of a simplified gyral pattern in the supra tentorial region, a hypoplastic corpus callosum and a small cerebellum and pons. Because patient 2 was operated in another centre abroad, no original MRI or CT data was available. We propose that the craniosynostosis in these patients is primary,

Complex craniosynostosis is associated with the 2p15p16.1 microdeletion syndrome

and not secondary to the microcephaly, as this last would generally result in pansynostosis rather than sagittal, coronal or metopic synostosis. Except for the craniosynostosis, clinically both patients do resemble the 2p15p16.1 microdeletion syndrome. However, for some clinical features, for example, optic nerve hypoplasia and hydronephrosis, the children may still be too young to express these abnormalities (**Table II**).

Rajcan-Separovic et al. reported brachycephaly as a dysmorphic feature in their patients, although it is not clear what the underlying cause of this feature in these patients is (6). In addition to our patient 1, also the two patients from Rajcan-Separovic et al. showed brain abnormalities; perisylvian migration disorder (Patient 1(6)) and generally thickened cortex with hyperintense subcortical tissue suggesting dysmyelination or cortical dysplasia; enlarged 4th ventricle, mild hypoplasia of the inferior cerebellar vermis and small anterior pituitary and pons (Patient 2(6)). These partly overlap with the brain features in our patient.

We have determined the deletion borders in our two patients and the patients described by Chabchoub et al. and de Leeuw et al. by qPCR (1, 2). The data of these authors was based on BAC data, and therefore, the borders were not determined precisely. According to the Leeuw et al, XPO1 is outside their deletion area, according to Chabchoub et al, XPO1 is included in their deletion area (1, 2). However, by qPCR we have not been able to resolve whether XPO1 is deleted in the 2 patients described by these authors. This is likely due to copy number variation in that area (Database of Genomic Variants; <http://projects.tcag.ca/cgi-bin/variation/gbrowse/hg19>).

The patient described by Chabchoub et al., with the smallest deletion, is also intellectually disabled, similar to the other patients with a deletion in this area (1). However, he is the only one without microcephaly. Additionally, several other clinical features observed in the majority of 2p15p16.1 microdeletion patients, for example, some facial dysmorphisms, optic nerve hypoplasia and hydronephrosis, could not be observed in this patient (**Table II**). This milder phenotype is in line with the small size of its deletion which is only 570 kb versus the 3.2 to 6.9 Mb in all the other so far reported cases. The patient reported by Prontera et al., with a deletion of 3.5 Mb, has many clinical features overlapping with the other described patients, including microcephaly and intellectual disability, but no craniosynostosis or structural brain abnormalities and that deletion encompasses only 1 uncharacterized and 2 known genes (5). Additionally, this patient has 2 other chromosomal rearrangements that could possibly influence the clinical phenotype. All nine patients have moderate to severe mental disability, though not all deletions overlap, indicating that genes in different regions can have influence on mental disability. For the microcephaly, the only gene that seems left, is the uncharacterized gene LOC100506891. Considering the presence of craniosynostosis in our two patients, we propose that the candidate region for this feature lies within the region between FANCL and B3GNT2. Additionally, features may depend on the different sizes of deletions found in the different patients and may show variable expression depending on genetic background(8). Also the enhancer elements present in the area may play a role.

Table 2: Continued.

	Present		Chabchoub et al.	De Leeuw et al.	Rajcan-Separovic et al.	Rajcan-Separovic et al.	Liang et al.	Felix et al.	Pontero Et al	Total		
	Patient 1										Patient 2	
	Patient 1	Patient 2									Subject 1	Subject 2
Facial features												
Bitemporal narrowing	+	+	NM	+	+	+	-	NM	+	6/9		
Receding short forehead	-	±	-	+	+	+	-	+	-	5/9		
Strabismus	+	-	-	+	-	-	-	--	-	3/9		
Ptosis	+	+	-	+	+	+	+	+	+	8/9		
Telecanthus	+	+	+	+	+	+	+	+	+	9/9		
Widened inner canthal distance	+	+	-	+	+	+	+	NM	+	7/9		
Short palpebral fissures	-	-	-	+	+	+	+	+	+	6/9		
Down slanting palpebral fissures	-	-	-	+	+	+	-	NM	-	3/9		
Epicanthal folds	+	+	+	+	-	+	+	NM	+	7/9		
Broad/high nasal root	+	+	+	+	+	+	±	+	+	9/9		
Prominent nasal tip	-	-	+	-	+	+	-	NM	+	4/9		
Long, straight eyelashes	-	+	NM	+	+	+	-	+	-	5/9		
Long, thin eyebrows	-	+	NM	-	+	+	-	NM	-	2/9		
Large ears	+	-	+	-	+	+	-	+	+	6/9		
Smooth and/or long philtrum	+	+	-	+	+	+	+	+	+	8/9		
Smooth upper vermillion border	-	-	+	+	+	+	-	NM	+	5/9		
Everted lower lip	-	-	+	+	+	+	-	NM	+	5/9		
High narrow palate	-	-	+	+	+	+	-	+	+	6/9		
Retrognathia	-	-	NM	+	-	+	+	Micrognathia	-	3/9		

Tabel 2: Continued.

	Present	Present	Chabchoub et al.	De Leeuw et al.	Rajcan-Separovic et al.		Liang et al.	Felix et al.	Pontero Et al	Total
					Subject 1	Subject 2				
					Patient 1	Patient 2				
Other physical features										
Widened inter nipple distance	-	-	NM	+	+	+	-	+	+	5/9
Extra nipple	-	-	NM	-	-	+	-	NM	-	1/9
Camptodactyly digit(s)	+	+	-	-	+	+	-	+	-	5/9
Metatarsus abductus	-	-	-	-	+	+	+	+	-	4/9
Spasticity legs	-	-	-	-	+	+	+	NM	+	4/9
Other										
Optic nerve hypoplasia	-	-	NM	+	+	+	+	-	-	4/9
Disturbed vision	-	-	NM	+	-	+	NA	+	NM	3/9
Hearing loss	-	+	NM	-	-	+	-	-	-	2/9
Frequent upper respiratory infections	-	-	NM	+	+	-	-	-	-	2/9
Laryngomalacia	-	-	NM	-	-	+	-	NM	-	1/9
Hydronephrosis	-	-	-	+	+	+	-	-	-	3/9
Hypogonadism	-	-	NM	-	-	+	-	-	-	1/9

NM= not mentioned, NA = not assessed

Complex craniosynostosis is associated with the 2p15p16.1 microdeletion syndrome

Some genes have a known function in brain. BCL11A (CTIP1) [OMIM:606557], a gene that plays a role in globin gene regulation is also highly expressed in brain and thought to be involved in axon outgrowth and branching (9-11). BCL11A is deleted in seven of the nine patients. As information on brain development on MRI is available in six of the patients, it is at this point not possible to conclude whether absence of this gene plays a major role in the formation of brain abnormalities seen in these patients. XPO1 (or CRM1) [OMIM:602559] is evolutionary conserved and expressed in the developing brain and proposed to be involved in motor neuron development and survival (12). Additionally it is implicated to have a role during mitosis (13).

Notably, REL [OMIM:164910] binds to CREBBP [OMIM:600140] and EP300 [OMIM:602700], two genes involved in Rubinstein-Taybi syndrome [OMIM:180849 and 61384], where intellectual disability and microcephaly are part of the phenotypic characteristics, and structural brain abnormalities have been reported in a minority of cases (14).

Array CGH and SNP array screening has led to the characterization of many heterozygous (novel) microdeletion and microduplication syndromes(15). Intellectual disability is often a feature of these syndromes, as is microcephaly(8, 15-17) Additionally microcephaly is found as an isolated feature, but can also be associated with many syndromes (18). Also, disruption of one gene can lead to a combination of phenotypic features including microcephaly and intellectual disability(19-21). For most microdeletion syndromes it is difficult to pinpoint one clinical feature to the absence of a specific gene in a deletion encompassing many genes and this is supported by comparing with the clinical phenotype in this study (22-26). Mouse models carrying targeted deletions of genes within these regions may help to elucidate the function of the individual genes (27). Deletions in the 2p15p16.1 area show variable clinical expression and may lead to microcephaly, intellectual disability and additionally to craniosynostosis, depending on the size and extension of the deletion combined with genetic background.

ACKNOWLEDGEMENTS

The authors extend their sincere appreciation to patient 1 and 2 and their parents for their support of this study. We thank Tom de Vries Lentsch for graphical support.

REFERENCES

1. Chabchoub E, Vermeesch JR, de Ravel T, de Cock P, Fryns JP. The facial dysmorphism in the newly recognised microdeletion 2p15-p16.1 refined to a 570 kb region in 2p15. *Journal of medical genetics*. 2008;45(3):189-92. Epub 2008/03/04.
2. de Leeuw N, Pfundt R, Koolen DA, Neefs I, Scheltinga I, Mieloo H, et al. A newly recognised microdeletion syndrome involving 2p15p16.1: narrowing down the critical region by adding another patient detected by genome wide tiling path array comparative genomic hybridisation analysis. *Journal of medical genetics*. 2008;45(2):122-4. Epub 2008/02/05.
3. Felix TM, Petrin AL, Sanseverino MT, Murray JC. Further characterization of microdeletion syndrome involving 2p15-p16.1. *American journal of medical genetics Part A*. 2010;152A(10):2604-8. Epub 2010/08/28.
4. Liang JS, Shimojima K, Ohno K, Sugiura C, Une Y, Yamamoto T. A newly recognised microdeletion syndrome of 2p15-16.1 manifesting moderate developmental delay, autistic behaviour, short stature, microcephaly, and dysmorphic features: a new patient with 3.2 Mb deletion. *Journal of medical genetics*. 2009;46(9):645-7. Epub 2009/09/03.
5. Prontera P, Bernardini L, Stangoni G, Capalbo A, Rogaia D, Romani R, et al. Deletion 2p15-16.1 syndrome: case report and review. *American journal of medical genetics Part A*. 2011;155A(10):2473-8. Epub 2011/09/13.
6. Rajcan-Separovic E, Harvard C, Liu X, McGillivray B, Hall JG, Qiao Y, et al. Clinical and molecular cytogenetic characterisation of a newly recognised microdeletion syndrome involving 2p15-16.1. *Journal of medical genetics*. 2007;44(4):269-76. Epub 2006/09/12.
7. Visel A, Minovitsky S, Dubchak I, Pennacchio LA. VISTA Enhancer Browser--a database of tissue-specific human enhancers. *Nucleic acids research*. 2007;35(Database issue):D88-92. Epub 2006/11/30.
8. Girirajan S, Rosenfeld JA, Cooper GM, Antonacci F, Siswara P, Itsara A, et al. A recurrent 16p12.1 microdeletion supports a two-hit model for severe developmental delay. *Nature genetics*. 2010;42(3):203-9. Epub 2010/02/16.
9. Kuo TY, Hong CJ, Chien HL, Hsueh YP. X-linked mental retardation gene CASK interacts with Bcl11A/CTIP1 and regulates axon branching and outgrowth. *Journal of neuroscience research*. 2010;88(11):2364-73. Epub 2010/07/14.
10. Kuo TY, Hsueh YP. Expression of zinc finger transcription factor Bcl11A/Evi9/CTIP1 in rat brain. *Journal of neuroscience research*. 2007;85(8):1628-36. Epub 2007/04/25.
11. Sankaran VG, Menne TF, Xu J, Akie TE, Lettre G, Van Handel B, et al. Human fetal hemoglobin expression is regulated by the developmental stage-specific repressor BCL11A. *Science*. 2008;322(5909):1839-42. Epub 2008/12/06.
12. Kolle G, Georgas K, Holmes GP, Little MH, Yamada T. CRIM1, a novel gene encoding a cysteine-rich repeat protein, is developmentally regulated and implicated in vertebrate CNS development and organogenesis. *Mechanisms of development*. 2000;90(2):181-93. Epub 2000/01/21.
13. Hutten S, Kehlenbach RH. CRM1-mediated nuclear export: to the pore and beyond. *Trends in cell biology*. 2007;17(4):193-201. Epub 2007/02/24.
14. Roelfsema JH, Peters DJ. Rubinstein-Taybi syndrome: clinical and molecular overview. *Expert reviews in molecular medicine*. 2007;9(23):1-16. Epub 2007/10/19.

15. Slavotinek AM. Novel microdeletion syndromes detected by chromosome microarrays. *Human genetics*. 2008;124(1):1-17. Epub 2008/05/31.
16. Reddy S, Dolzhanskaya N, Krogh J, Velinov M. A novel 1.4 Mb de novo microdeletion of chromosome 1q21.3 in a child with microcephaly, dysmorphic features and mental retardation. *European journal of medical genetics*. 2009;52(6):443-5. Epub 2009/09/24.
17. Walczak-Sztulpa J, Wisniewska M, Latos-Bielenska A, Linne M, Kelbova C, Belitz B, et al. Chromosome deletions in 13q33-34: report of four patients and review of the literature. *American journal of medical genetics Part A*. 2008;146A(3):337-42. Epub 2008/01/19.
18. Abuelo D. Microcephaly syndromes. *Seminars in pediatric neurology*. 2007;14(3):118-27. Epub 2007/11/06.
19. Campbell IM, Kolodziejska KE, Quach MM, Wolf VL, Cheung SW, Lalani SR, et al. TGFBR2 deletion in a 20-month-old female with developmental delay and microcephaly. *American journal of medical genetics Part A*. 2011;155A(6):1442-7. Epub 2011/05/14.
20. Mukhopadhyay A, Kramer JM, Merx G, Lugtenberg D, Smeets DF, Oortveld MA, et al. CDK19 is disrupted in a female patient with bilateral congenital retinal folds, microcephaly and mild mental retardation. *Human genetics*. 2010;128(3):281-91. Epub 2010/06/22.
21. Williams SR, Mullegama SV, Rosenfeld JA, Dagli AI, Hatchwell E, Allen WP, et al. Haploinsufficiency of MBD5 associated with a syndrome involving microcephaly, intellectual disabilities, severe speech impairment, and seizures. *European journal of human genetics : EJHG*. 2010;18(4):436-41. Epub 2009/11/12.
22. Klaassens M, de Klein A, Tibboel D. The etiology of congenital diaphragmatic hernia: still largely unknown? *European journal of medical genetics*. 2009;52(5):281-6. Epub 2009/05/26.
23. Kumar D. Disorders of the genome architecture: a review. *Genomic medicine*. 2008;2(3-4):69-76. Epub 2009/03/12.
24. Masurel-Paulet A, Andrieux J, Callier P, Cuisset JM, Le Caignec C, Holder M, et al. Delineation of 15q13.3 microdeletions. *Clinical genetics*. 2010;78(2):149-61. Epub 2010/03/20.
25. Stankiewicz P, Lupski JR. Structural variation in the human genome and its role in disease. *Annual review of medicine*. 2010;61:437-55. Epub 2010/01/12.
26. Vissers LE, de Vries BB, Veltman JA. Genomic microarrays in mental retardation: from copy number variation to gene, from research to diagnosis. *Journal of medical genetics*. 2010;47(5):289-97. Epub 2009/12/03.
27. Abrams JM, Jiao Y. Keeping it simple: what mouse models of Wolf-Hirschhorn syndrome can tell us about large chromosomal deletions. *Disease models & mechanisms*. 2009;2(7-8):315-6. Epub 2009/06/26.
28. Liu X, Malenfant P, Reesor C, Lee A, Hudson ML, Harvard C, et al. 2p15-p16.1 microdeletion syndrome: molecular characterization and association of the OTX1 and XPO1 genes with autism spectrum disorders. *European journal of human genetics : EJHG*. 2011;19(12):1264-70. Epub 2011/07/14.



CHAPTER 4

Venous hypertension in syndromic and complex craniosynostosis: The abnormal anatomy of the jugular foramen and collaterals.

J.M.G. Florisson
G. Bampalios
M.H. Lequin
M.L.C. van Veelen
N. Bannink
R.D. Hayward
I.M.J. Mathijssen

Journal of cranio-maxillo-facial surgery : official publication of the European Association for Cranio-Maxillo-Facial Surgery. 2015;43(3):312-8. Epub 2015/01/22.

ABSTRACT

Why craniosynostosis patients develop elevated intracranial pressure (ICP) is still a mystery. Multiple factors seem to be involved and a reduced jugular foramen diameter is one of the factors cited in literature(1, 2). Our aim was to investigate jugular foramen size and its relation to venous hypertension and elevated ICP in craniosynostosis patients. Secondly, we evaluated whether occipital collateral veins develop as a compensatory mechanism for elevated ICP.

We conducted a prospective study in 41 children with craniosynostosis who underwent a 3D-CT-angiography. We evaluated the anatomical course of the jugular vein, the diameter of the jugular foramen and its surface area and matched those to the presence of papilledema. Additionally, we studied the anatomical variations of the cerebral venous drainage system including the presence and pattern of collateral veins in relation to papilledema, diagnosis and age.

The diameter and the surface of the jugular foramen were significantly smaller or it was completely occluded in 14.6% of our patients. Abnormal venous collaterals were most often observed in patients with Apert, Crouzon-Pfeiffer and Saethre Chotzen syndrome, even in children under two years of age. There was no significant difference in the number of collateral veins in patients with or without papilledema. Collaterals appear to reflect an inborn abnormality of the venous system, rather than a compensating mechanism for elevated ICP.

This study confirms the presence of jugular foraminal narrowing in craniosynostosis patients and an abnormal venous system, which may predispose to elevated ICP.

INTRODUCTION

Elevated intracranial pressure (ICP) is a well-known, but mal-understood problem in craniosynostosis patients (3). It is most common in syndromic craniosynostosis in which the prevalence varies between 40 to nearly 100% (4-10). A routine early cranial vault expansion does not completely prevent the development of elevated ICP. Even after surgery, up to 43% of syndromic craniosynostosis patients develop elevated ICP (4, 11, 12). Potential causes for elevated ICP are cranio-cerebral disproportion (13), obstructive sleep apnea (OSA), tonsillar herniation of the cerebellum (14) and venous hypertension.

Literature shows that patients with syndromic craniosynostosis have a normal brain volume and intracranial volume, indicating that a cranio-cerebral imbalance is seldom the cause for elevated ICP and only so in patients with pansynostosis¹². OSA has an important implication for cerebral blood flow and pressure dynamics (6, 15). Although nearly 70% of patients with a syndromic craniosynostosis suffers from OSA, it is mainly of mild severity (16) and therefore its contribution to the high prevalence of elevated ICP seems limited. Whether tonsillar herniation develops as a result of elevated ICP or (also) causes the ICP to rise is still controversial.

Venous hypertension refers to obstruction of the venous outflow of the brain and alterations in the dynamics of flow in the superior sagittal sinus (13). Venous hypertension is commonly described in syndromic craniosynostosis and has been related to a reduced diameter of the jugular foramen. The bony narrowing may lead to obstructed outflow. As a result of the obstructed outflow, venous pressure and consequently CSF pressure raises. (1, 2, 17) Another anomaly that is frequently encountered in syndromic craniosynostosis is the presence of venous collaterals at the level of the posterior fossa. This appears to be a bypass system to allow for additional venous outflow.

Our prospective study evaluates if the jugular foramen is narrower in children with syndromic or complex craniosynostosis and whether its (reduced) size is associated with elevated ICP. Secondly, the anatomical variations of the cerebral venous drainage system including the occipital collateral veins are studied to evaluate whether collaterals develop as a compensatory mechanism for venous hypertension.

MATERIAL AND METHODS

Patients

This prospective study was undertaken between January 2007 and January 2013 at the Craniofacial Center of the Sophia Children's Hospital in Rotterdam, The Netherlands. This is the single national referral center for syndromic craniosynostosis for a population of 16 million people. We included all consecutive patient with syndromic or complex craniosynostosis

Chapter 4

whose diagnoses was based on genetic analysis and included Apert, Crouzon/Pfeiffer, Muenke and Saethre-Chotzen syndrome. A craniosynostosis was defined as complex when there were at least two sutures prematurely closed without genetic anomalies of the *FGFR2, 3* or *TWIST1* genes. All patients routinely underwent 3D-CT scanning as a part of their diagnostic and preoperative assessment. Medical Ethical approval was given to extend their 3D-CT-scan to 3D-CT angiography (2005-273) after consent by the parents.

Different patient groups were defined for analysis. In the first group (I) patients with a syndromic or complex craniosynostosis without papilledema at routine fundoscopy were enrolled. In the second group (II) are syndromic or complex craniosynostosis patients with papilledema. The third study group (III) are patients who had a CT angiography for other indications such as hemiplegia, sickle cell disease and headache and these patients had no craniosynostosis or signs of elevated ICP. This group was used for control measures of the bony and vascular part of the jugular foramen.

3D-CT scan

All patients underwent a 3D-CT angiography, made by a Siemens CT 128 slice scanner and the imaging data sets were accessible for analysis by means of multi-planar reformatted images. All scans were made using the same protocol. (941044Q)

The 3D-CT was analyzed for the following parameters:

- 1: Whether or not the jugular vein coursed through the jugular foramen.
- 2: The diameter and the surface area of the jugular foramen.
- 3: The presence and pattern of venous collaterals

Ad 1. The principal researcher (JF) and a pediatric radiologist (ML) described the anatomic course of the jugular vein and determined whether the vein passed the foramen.

Ad 2. To measure the diameter of the jugular vein a set of reformatted images was obtained in the line of the jugular foramen (Figure 1). Figure 1A and 1B show the jugular foramen is clearly visible at the coronal and transversal images. Figure 1C shows how the axis is set to allow standardized measurements of the jugular foramen. The 3D-CT allowed verification in the third dimension to assess if the jugular foramen was accurately measured. All the exact measurements were done in the parasagittal images (Figure 2). The narrowest point of the inflow of the jugular vein is measured at the right and left side, which is marked by the red line in figure 2. The outflow of the jugular foramina is marked by the blue line and is also measured at each side. The bilateral inflow and outflow measurements provide a total of 4 measurements per CT scan, from which we have calculated the mean right and left sided diameter and a mean combined diameter (sum of the mean right and left sided diameter)(2). Theoretically, the blood flow is most compromised by either inflow or outflow, depending on which was the most narrow. Therefore we also analyzed the results by using the mean of the right and left sided smallest measurement from each side.

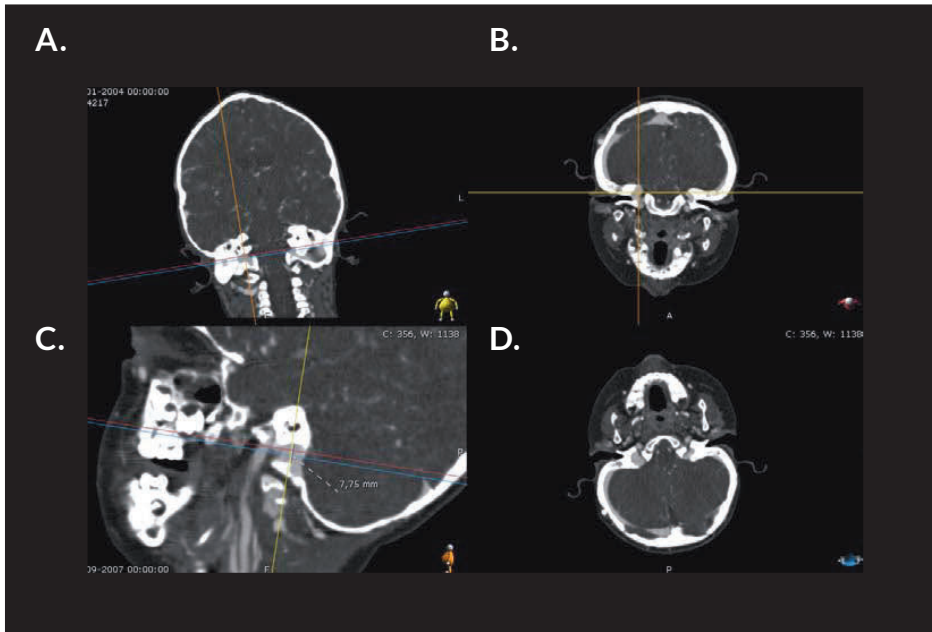


Figure 1: Reformatted images of the jugular foramen in coronal (A), axial (B), sagittal (C) and axial view (D)



Figure 2: Measurement of the jugular foramen. Red line; narrowest point of inflow of jugular vein. Blue line; outflow of the jugular foramina.

Chapter 4

We also measured the surface area of the jugular vein by performing a vessel segmentation analysis which automatically detects and measures the shortest axis of the annotated vessel inside the foramen (in orthogonal planes). It also measures the total area of the vessel in every orthogonal plane and acquires a 3D view of the jugular foramen (Fig 3). For analysis, we have used the surface area at the most narrow point in the foramen. (MeVisLab 2.1 - MeVis Medical Solutions and Fraunhofer MEVIS)

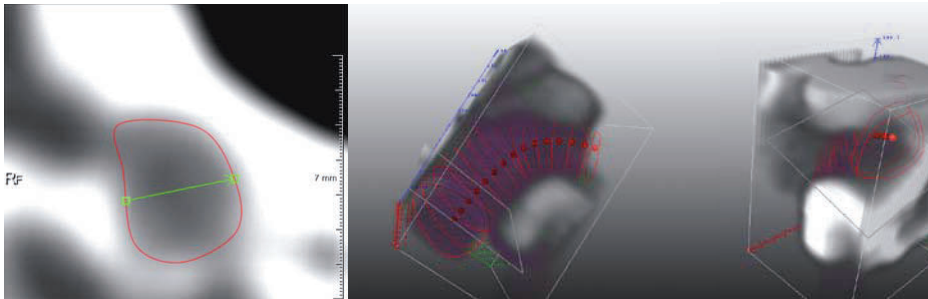


Figure 3: Measurement of the total area and smallest diameter of the jugular vein (A) and 3D acquisitions of the jugular foramen (B - C) using vessel segmentation analysis in orthogonal planes.

The principal researcher performed all measurements and a pediatric radiologist who was blinded for the measurements of the first observer additionally captured the first ten patients.

Ad 3. The anatomical definitions for collateral venous drainage mechanisms as described by Jeevan et al. were used to judge the venous collateral drainage pattern (A-G)(17). Moreover, the principal researcher and pediatric radiologist scored all scans for the inferior sagittal sinus, pericalosal veins, the pterygoid sinus and the transverse sinus (I t/m K) as follows: 0 points when there was a normal pattern of drainage, 1 when there were several collaterals or very wide veins, and 2 points when there were a lot of collaterals and extremely wide veins. When possible, right and left site were scored (Figure 4). All scores for each patient were added, ranging from 0 to 34. Total scores for each patient are given and compared between group I, II and III. Total scores were also compared for the separate craniosynostosis syndromes. The following anatomical definitions were used in identifying the collateral venous drainage mechanisms:

- A: Parietal emissary vein connects the superior sagittal sinus with the veins of the scalp.
- B: Occipital emissary vein arises from the medial border of the transverse sinus or torcula herophili and drains to the occipital vein and internal vertebral plexus.
- C: Mastoid emissary vein drains the lateral sinus (medial lateral portion of the transverse and sigmoid sinus) to the occipital vein or to the posterior auricular vein.
- D: Condylod emissary vein drains the lower genu of the sigmoid sinus or jugular sinus to the deep cervical vein through the condyloid canal.

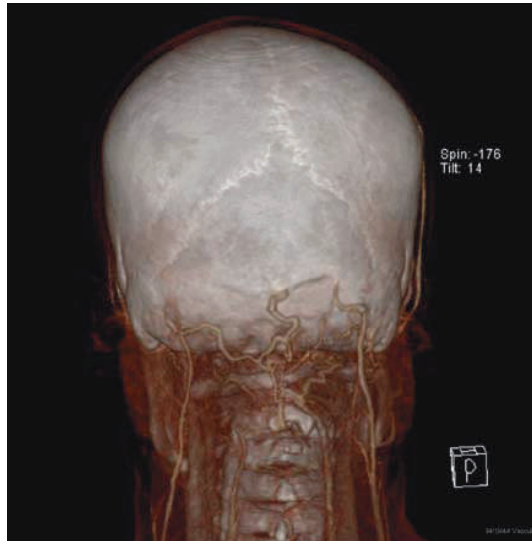


Figure 4: Example of a patient with many collaterals.

- E: Occipital sinus is situated in the attached margin of the falx cerebelli and is generally single, but occasionally there are two. It drains from the torcula downwards to the internal vertebral plexus.
- F: Marginal sinus is located between the layers of the dura at the rim of the foramen magnum. This sinus encircles the foramen magnum, communicating with the basal venous plexus of the clivus anteriorly and with the occipital sinus posteriorly. It normally drains to the sigmoid sinus or jugular bulb by a series of small sinuses. Anastomotic connections to the internal vertebral venous plexus as well as to paravertebral and/ or deep cervical veins are typically present.
- G: Venous collaterals of the ophthalmic vein into the facial vein
- H: Inferior Sagittal Sinus
- I: Pericallosal vein
- J: Pterygoid sinus plexus
- K: Transverse sinus

Fundoscopy

Papilledema was used as a sign of elevated ICP. Funduscopy is done on a yearly base at least up to the age of 6 by a pediatric ophthalmologist. Papilledema was defined as blurring of the margins of the optic disk after exclusion of hyperopia by cycloplegic retinoscopy, because a hyperopic papil can resemble papilledema without being a sign of elevated ICP. All funduscopies taken at the same time as the CT scan were included. The correlation between the occurrence and type of venous collaterals in our study group I and II and the presence of papilledema was examined.

Statistical analysis

SPSS Software was used for statistical analyses (IBM SPSS Statistics for Windows, Version 21.0. Armonk, NY: IBM Corp). Mann-Whitney U test was used for statistical analysis off the differences of diameter in between the groups, and $p < 0,05$ was regarded as significant.

RESULTS

We included a total number of 58 patients: 41 patients with a syndromic or complex form of craniosynostosis (11 Apert syndrome, 15 Crouzon-Pfeiffer syndrome, 7 Muenke syndrome, 3 Saethre-Chotzen syndrome, 5 complex craniosynostosis), and 17 control patients. Fundoscopy showed papilledema in 15 patients with syndromic craniosynostosis. The baseline characteristics of the subpopulations of patients are summarized in Table 1 and 2.

Table 1: Patient characteristics of the study groups: Study group I= patients with syndromic craniosynostosis without papilledema. Study group II = patients with syndromic craniosynostosis with papilledema. Study group III = control group

Study group	I	II	III
N	26	15	17
Male/Female	15/11	7/8	9/8
Mean Age (Years)	6,22	5,60	7,94
(minimum – maximum)	(0,13-18,96)	(1,50-13,89)	(0,19-16,4)

Table 2: Patient distribution of diagnosis in study groups : Study group I= patients with syndromic craniosynostosis without papilledema. Study group II = patients with syndromic craniosynostosis with papilledema.

Study group	I	II
Apert	10	1
Crouzon-Pfeiffer	6	9
Muenke	6	1
Saethre-Chotzen	1	2
Complex	3	2

The course of the jugular vein through the jugular foramen

In six ($6/41 = 14,6\%$) patients with syndromic and complex craniosynostosis patients we noticed an anatomic variance where the jugular vein did not pass the jugular foramen. Of these 6 patients, 2 had Apert syndrome, 1 had Crouzon-Pfeiffer syndrome, 1 had Muenke syndrome, 1 had Saethre-Chotzen syndrome and 1 had a complex craniosynostosis. Papilledema was present in 5 of these 6 patients. These patients were also included in the analyses of the jugular foramen. Their characteristics are presented below:

The first patient with Apert syndrome demonstrated an asymmetric jugular foramen. The right foramen is smaller than the left. The jugular veins are both hypoplastic. Multiple venous collaterals are shown. Total collateral score is 15, with mainly collaterals at the mastoid emissary vein, the condyloid emissary vein, the marginal sinus, the venous collaterals of the ophthalmic vein, the inferior sagittal sinus, the pterygoid sinus plexus. There is a dilatation of the ventricles.

The second patient has Apert syndrome. The left jugular foramen is wide compared to the right foramen and the right jugular vein is hypoplastic. The ventricles are large and there is some scalloping of the skull. At the time of the CT scan, at the age of 2 years and 8 months, papilledema was detected. In the following years his papilledema disappeared but it reappeared at the age of 5 years, accompanied by an aggravation of his Chiari malformation. The total collateral score is 16 and the collaterals are mainly occipital, mastoid and condyloid emissary vein, the marginal and the inferior sagittal sinus, and the pterygoid sinus plexus.

The third patient, with Crouzon syndrome, showed a hypoplastic transverse sinus and sigmoid and jugular vein on the left side. The jugular foramen had a normal anatomy. He had persistent papilledema. The scan showed no Chiari malformation. The total collateral score was 8 with the collaterals mainly seen at the inferior sagittal sinus, the ophthalmic vein, the occipital sinus, the condyloid and mastoid emissary vein. Three years later, at the age of 6 years, a Chiari malformation had developed.

The fourth patient has Muenke syndrome. The transverse sinus and sigmoid sinus, the jugular vein and foramen on the left side are hypoplastic. Ventricles are wide but matching his macrocephaly. No signs of elevated intracranial pressure were present. The total collateral score was 9.

The fifth patient with Saethre-Chotzen syndrome has an asymmetrical jugular vein, and the right jugular vein was more wide compared to the left. The left jugular foramen and the jugular vein were hypoplastic as were the transverse sinus and sigmoid sinus. There size of the ventricles was normal. At the time of the CT scan there was papilledema. Many collaterals gave this patient a total collateral score of 11.

The sixth patient has complex craniosynostosis. The transverse sinus and sigmoid sinus, the jugular foramen and the vein are hypoplastic on the left side. No signs of elevated intracranial pressure are present. At the time of scanning there was no Chiari malformation. One year later, at the age of 4 he developed a tonsillar herniation. At that time invasive intracranial pressure measurement was done and showed elevated intracranial pressure: baseline pressure at daytime 10 mmHg and raised from 5 to 16 mmHg during sleep, 4 plateaux were observed with a pressure above 35 mmHg and a duration of longer than 20 minutes. Few collaterals were present with a total collateral

score of 5. Collaterals were seen at the site of the mastoid and condyloid emissary vein and the occipital and inferior sagittal sinus.

Diameter of jugular foramen

There were no differences when comparing the measurements of the jugular foramen made by the two different researchers. First we compared all syndromic craniosynostosis patients with our control group. The diameter of the jugular foramen in patients with syndromic craniosynostosis was significantly smaller compared to controls. Patients had a mean combined diameter of 9.09 mm and controls had a mean combined diameter of 12.05 mm. ($p = 0,002$).

Subgroup analyses shows that patients with syndromic craniosynostosis without papilledema (study group I; 8.74) have a smaller diameter of the jugular foramen compared to controls (study group III; 12.05) ($p = 0.01$ Mann-Whitney). Patients with syndromic craniosynostosis and papilledema (group II) do also have a significantly smaller mean combined diameter of the jugular foramen compared to our controls in group III ($p = 0.017$ Mann-Whitney) (Table 3)

Table 3: Diameter of the jugular foramen.

Study group	I	II	III
N	26	15	17
Mean combined diameter	8,74*	9,69*	12.05
(p value compared to group III)	0.001	0.017	
Minimum mean combined diameter	4,54	7,12	7,17
Maximum mean combined diameter	13,04	13,17	16,45
Minimum diameter	1.23*	1.93	2.34
(p value compared to group III)	0.001	> 0.05	

Group I= patients with syndromic craniosynostosis without papilledema. group II = patients with syndromic craniosynostosis with papilledema. group III = control group.

* = significant $p < 0.05$

Correlation between surface area of jugular foramen and papilledema

The surface area of the jugular foramen at its most narrow part of patients with papilledema is not significantly different from that of patients without papilledema. ($p > 0.05$ Mann Whitney U test) (Table 4). We do find significant differences between the 2 syndromic craniosynostosis groups and the control group, with a much smaller jugular foramen in the craniosynostosis patients.

Table 4: Diameter and surface area of the jugular foramen.

Study Group	I	II	III
N	25	14	17
Mean combined surface area measurements (p value compared to group IV; MWU test)	7,03* (p < 0.001)	8,5* (p = 0.002)	11,4
Smallest surface area right (p value compared to group III; MWU test)	15.8* (p < 0.001)	24.9* (p < 0.05)	44,5
Smallest surface area left (p value compared to group III; MWU test)	19.1* (p < 0.05)	21.7* (p < 0.05)	39.0
Mean diameter right (p value compared to group III; MWU test)	3,34* (p < 0.001)	4,34* (p < 0.05)	6.01
Mean diameter left (p value compared to group III; MWU test)	3,69* (p = 0.001)	4,13* (p < 0.05)	5,38

Group I= patients with syndromic craniosynostosis without papilledema. group II = patients with syndromic craniosynostosis with papilledema. group III = control group.

MWU: Mann-Whitney U test

* significant p<0.05

Venous collaterals and the relationship with papilledema

The scores for the 11 items on venous collaterals are shown in table 5. Most abnormalities were seen at the condyloid emissary vein that drains the lower genu of the sigmoid sinus or jugular sinus to the deep cervical vein through the condyloid canal (98 %), the occipital sinus (93%) and the inferior sagittal sinus (95%) (Table 5). A high degree of symmetry is found for the areas that were scored bilateral. In the control group only the mastoid and the condyloid canals are sometimes enlarged. (31% and 44% respectively). The total collateral score is 10.6 for the craniosynostosis patients and 2.0 for the control group. This is a highly significant difference (p < 0.002).

To investigate the development of collaterals with increasing age, the results are plotted in figure 5. Study group I (syndromic craniosynostosis without papilledema) has a slight upward trend line for the development of collaterals. Study group II (syndromic craniosynostosis with papilledema) shows a flat line. Remarkable is that the youngest patients under the age of 2 years already have high numbers of collaterals.

Table 5: Incidence of collateral venous drainage in syndromic craniosynostosis patients

Collaterals	Craniosynostosis patients (N = 41)	Number of patients with Collateral (%)	Controls (N = 16)	Number of patients with Collateral (%)
A	1	(2%)	0	(0%)
B right	10	(24%)	0	(0%)
B left	6	(15%)	0	(0%)
C right	28	(68%)	5	(31%)
C left	24	(59%)	4	(25%)
D right	40	(98%)	7	(44%)
D left	40	(98%)	7	(44%)
E	38	(93%)	0	(0%)
F right	22	(54%)	0	(0%)
F left	22	(54%)	0	(0%)
G right	8	(20%)	0	(0%)
G left	9	(22%)	0	(0%)
H	39	(95%)	0	(0%)
I	1	(2%)	2	(13%)
J right	23	(56%)	4	(25%)
J left	26	(63%)	4	(25%)
K	5	(12%)	2	(13%)

A: parietal emissary vein, B: occipital emissary vein, C: mastoid emissary vein, D: condyloid emissary vein, E: occipital sinus, F: marginal sinus, G: venous collaterals of the ophthalmic vein to the facial vein, H: inferior sagittal sinus, I: pericallosal vein, J: pterygoid sinus plexus, K: transverse sinus

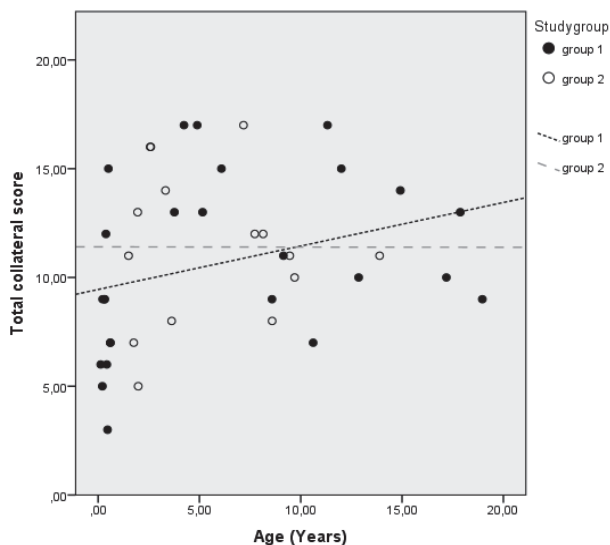


Figure 5: shows the development of the total collateral score over time. Study group 1= patients with syndromic craniosynostosis without papilledema. Study group 2 = patients with syndromic craniosynostosis with papilledema.

Table 6 shows the presence of occipital collaterals and the presence of papilledema at the time of CT scan or developing later during life. This table also shows that 20 out of 41 patients have papilledema at the time of the CT scan or develop papilledema later in time. Patients with or without papilledema have the same amount of collaterals. A more specific result is obtained if we investigate the development of collaterals for each syndrome (table 7).

Results are shown for the total score of collaterals, and for only the occipital collaterals as they are most commonly encountered.

The total score of collaterals is highest for the diagnoses Apert, Crouzon-Pfeiffer and Saethre Chotzen syndromes. The score for occipital collaterals only is highest for the diagnoses Apert and complex craniosynostosis, followed by Crouzon-Pfeiffer, Saethre Chotzen. In contrast, patients with Muenke syndrome and the controls have no occipital collaterals.

Table 6: Crosstab of the mean score of total collaterals and a history of papilledema.

	Mean Total Collaterals	N (Number of patients)
No papilledema	11.0	21
Papilledema	11.0	20
	11.0	41

Table 7: Table shows the mean of the occipital collateral score (range 0 to 2) and mean total collateral (range 0 to 22) Score for each diagnose

Diagnosis (N)	Occipital collateral score (Mean)	Total collateral score (Mean)
Apert (11)	0,55	11,36
Crouzon-Pfeiffer (15)	0,33	11,27
Muenke (7)	0,00	10,71
Saethre- Chotzen (3)	0,33	14,00
Complex (5)	0,60	7,60
Controls (17)	0,00	2,00

DISCUSSION

Two hypothesis were tested in this study: first that a narrow jugular foramen is causally related to elevated intracranial pressure in children with syndromic or complex craniosynostosis, and second that presence of collateral veins is a compensation mechanism for elevated ICP.

In contradiction to our first hypothesis, our study shows no difference in diameter of the jugular foramen between the syndromic craniosynostosis patients with and without papilledema. This is also in contrast with earlier published research(2). Rich et al. (2003) published a study in which they showed significantly narrower jugular foramina in children

Chapter 4

with raised ICP based on invasive ICP measurements, in a similar craniosynostosis study group. This difference might be explained by using different methods: first, we have a study population of 58 patients and Rich uses 31 patients in his study. This may influence the results and gives more power to our study. Second, Rich et al. has a difference in age of approximately 2 years between his patient group with elevated ICP and the control group. That difference is limited to 8 months in our study and we have shown that age is an important factor influencing the diameter of the jugular foramen. Third, the previous study uses a control group of 10 patients with non syndromic craniosynostosis. Nevertheless, 2 of these patients do have a bilateral coronal synostosis and should have been excluded. Fourth, the previous study used conventional CT scans without angiography and without reformatted images. Particularly the use of CT-A enabled us to recognize the 6 patients in whom the jugular vein did not cross the foramen. Fifth, we used papilledema as an indicator of raised ICP and Rich uses invasive ICP measurements. It is known that papilledema is age dependent and its absence doesn't mean the ICP is normal. (18)

We show that syndromic and complex craniosynostosis patients have a smaller jugular foramen compared to healthy control patients. This finding is in agreement with Booth et al. who reveal a significant decrease in jugular foramen in craniosynostosis patients compared to age-matched controls(1).

Our second hypothesis, presence of collateral veins is a compensation mechanism for elevated ICP, is based on several studies. Extensive venous collaterals have been found in patients with syndromic craniosynostosis, especially occipitally (13). Occipital collaterals indicate an abnormal drainage from intracranially to extracranially (19), which is regarded to be a significant contributor to increased ICP (13, 17). To test our hypothesis we investigated the venous drainage at 11 anatomical points. In agreement with Jeevan and co-workers we can confirm that patients with syndromic craniosynostosis often demonstrate prominent venous anatomy. We hypothesized that venous collaterals develop to reduce the blood component of the intracranial volume and thus lower the ICP. Apert, Crouzon-Pfeiffer and Saethre Chotzen are the patients with the highest development of collaterals. In agreement with our hypothesis, they are also the patients who develop elevated intracranial pressure. Similarly, patients with Muenke syndrome rarely show collaterals as they seldom develop elevated ICP. These findings support our hypothesis. However, no significant differences are found in between the craniosynostosis groups with and without papilledema.

Furthermore, our study also shows the presence of collaterals in very young patients. Even patients under the age of two years already have prominent venous collaterals. This implies that collateral development is an intrinsic disorder. The known mutations (*FGFR2*, *TWIST1*) may lead in these children to a congenital abnormal venous pattern. We are therefore more convinced that the collaterals signify an inborn disorder of the venous system, which makes these patients more prone to venous hypertension.

Intrinsic impairment in development could involve a dysfunction of the *FGFR2* gene in embryogenesis. In the fourth week, a process of folding converts the neural plate to a hollow neural tube, which sinks into the body wall and differentiates into brain and spinal cord, followed by formation of a cartilaginous neurocranium. During this process a cartilage template has been formed, vascularized and osteoclasts and osteoblasts are recruited to replace the cartilage scaffold with bone (20, 21). The jugular foramen is situated between the petrous portion of temporal and occipital bones and originates from persistence of the embryologic foramen lacerum posticus, the space between the basi-occiput and auditory canal. Additionally, animal studies have shown *FGFR-2* expression at the neural tube and cranial base during embryogenesis (22-25). Several studies reported abnormalities of the skull (26-30) and skull base (28, 31, 32) in Crouzon syndrome in humans, and in mice (33-35). Hence, it is likely that *FGFR-2* gene mutations have an effect on brain and skull development.

Furthermore, we found an aberrant course of the jugular foramen and a very different venous pattern in 6 of our patients (15%). In 4 of these patients there were signs of elevated intracranial pressure. Only in our Muenke patient we did not find any signs of elevated intracranial pressure.

These collateral veins are very important for these patients, as is shown in the dramatic case report of a girl with Pfeiffer syndrome(36). As the scalp incision for a cranial vault expansion was made, an enormous trans-osseous venous channel emerging in the midline parieto-occipital region was transected. Bleeding was controlled, but the patient developed intractable intracranial hypertension. The surgery was abandoned; the patient died shortly thereafter. At autopsy, the authors found that most of the normal pathways for intracranial venous drainage were severely narrowed and that the trans-osseous venous channel had been the major pathway for venous drainage in this patient. It is therefore extremely important that the venous outflow pattern is taken into consideration when planning surgery for these patients, particularly in case of posterior or suboccipital interventions.

CONCLUSION

In conclusion, we show that a smaller jugular foramen is common in patients with syndromic craniosynostosis, irrespective of presence of papilledema. The jugular foramen diameter may be aberrant because of different embryological development instead of being influenced by intracranial pressure. The high number of collaterals already present in very young patients with syndromic craniosynostosis and the aberrant course of the jugular foramen in 15% of patients in the current study implies an embryologic origin of the anomalous venous drainage, rather than a response to elevated ICP.

This research project reveals a piece of the puzzle of elevated intracranial pressure in patients with syndromic craniosynostosis.

ACKNOWLEDGEMENTS

The authors would like to thank T. van Walsum and BIGR (Biomedical Imaging Group Rotterdam) for their support.

REFERENCES

1. Booth CD, Figueroa RE, Lehn A, Yu JC. Analysis of the jugular foramen in pediatric patients with craniosynostosis. *J Craniofac Surg*. 2011;22(1):285-8. Epub 2011/01/18.
2. Rich PM, Cox TC, Hayward RD. The jugular foramen in complex and syndromic craniosynostosis and its relationship to raised intracranial pressure. *AJNR Am J Neuroradiol*. 2003;24(1):45-51.
3. Zakhary GM, Montes DM, Woerner JE, Notarianni C, Ghali GE. Surgical correction of craniosynostosis. A review of 100 cases. *J Craniomaxillofac Surg*. 2014. Epub 2014/06/28.
4. Bannink N, Joosten KF, van Veelen ML, Bartels MC, Tasker RC, van Adrichem LN, et al. Papilledema in patients with Apert, Crouzon, and Pfeiffer syndrome: prevalence, efficacy of treatment, and risk factors. *J Craniofac Surg*. 2008;19(1):121-7. Epub 2008/01/25.
5. Gault DT, Renier D, Marchac D, Jones BM. Intracranial pressure and intracranial volume in children with craniosynostosis. *Plast Reconstr Surg*. 1992;90(3):377-81.
6. Hayward R, Gonzalez S. How low can you go? Intracranial pressure, cerebral perfusion pressure, and respiratory obstruction in children with complex craniosynostosis. *J Neurosurg*. 2005;102(1 Suppl):16-22.
7. Marucci DD, Dunaway DJ, Jones BM, Hayward RD. Raised intracranial pressure in Apert syndrome. *Plast Reconstr Surg*. 2008;122(4):1162-8; discussion 9-70. Epub 2008/10/02.
8. Renier D, Sainte-Rose C, Marchac D, Hirsch JF. Intracranial pressure in craniostenosis. *J Neurosurg*. 1982;57(3):370-7.
9. Tamburrini G, Di Rocco C, Velardi F, Santini P. Prolonged intracranial pressure (ICP) monitoring in non-traumatic pediatric neurosurgical diseases. *Med Sci Monit*. 2004;10(4):MT53-63. Epub 2004/03/25.
10. Thompson DN, Harkness W, Jones B, Gonzalez S, Andar U, Hayward R. Subdural intracranial pressure monitoring in craniosynostosis: its role in surgical management. *Childs Nerv Syst*. 1995;11(5):269-75.
11. Pagnoni M, Fadda MT, Spalice A, Amodeo G, Ursitti F, Mitro V, et al. Surgical timing of craniosynostosis: what to do and when. *J Craniomaxillofac Surg*. 2014;42(5):513-9. Epub 2013/10/01.
12. Wiberg A, Magdum S, Richards PG, Jayamohan J, Wall SA, Johnson D. Posterior calvarial distraction in craniosynostosis - an evolving technique. *J Craniomaxillofac Surg*. 2012;40(8):799-806. Epub 2012/05/09.
13. Hayward R. Venous hypertension and craniosynostosis. *Childs Nerv Syst*. 2005;21(10):880-8.
14. Driessen C, Joosten KF, Florisson JM, Lequin M, van Veelen ML, Dammers R, et al. Sleep apnoea in syndromic craniosynostosis occurs independent of hindbrain herniation. *Child's nervous system : ChNS : official journal of the International Society for Pediatric Neurosurgery*. 2013;29(2):289-96. Epub 2012/09/26.
15. Gonzalez S, Hayward R, Jones B, Lane R. Upper airway obstruction and raised intracranial pressure in children with craniosynostosis. *Eur Respir J*. 1997;10(2):367-75. Epub 1997/02/01.

Chapter 4

16. Driessen C, Joosten KF, Bannink N, Bredero-Boelhouwer HH, Hoeve HL, Wolvius EB, et al. How does obstructive sleep apnoea evolve in syndromic craniosynostosis? A prospective cohort study. *Arch Dis Child*. 2013;98(7):538-43. Epub 2013/05/25.
17. Jeevan DS, Anlsow P, Jayamohan J. Abnormal venous drainage in syndromic craniosynostosis and the role of CT venography. *Childs Nerv Syst*. 2008;24(12):1413-20.
18. Tuite GF, Chong WK, Evanson J, Narita A, Taylor D, Harkness WF, et al. The effectiveness of papilledema as an indicator of raised intracranial pressure in children with craniosynostosis. *Neurosurgery*. 1996;38(2):272-8.
19. Al-Otibi M, Jea A, Kulkarni AV. Detection of important venous collaterals by computed tomography venogram in multisutural synostosis. Case report and review of the literature. *J Neurosurg*. 2007;107(6 Suppl):508-10.
20. Mann SS, Naidich TP, Towbin RB, Doundoulakis SH. Imaging of postnatal maturation of the skull base. *Neuroimaging Clin N Am*. 2000;10(1):1-21, vii. Epub 2000/02/05.
21. Rice DP, Rice R, Thesleff I. Fgfr mRNA isoforms in craniofacial bone development. *Bone*. 2003;33(1):14-27. Epub 2003/08/16.
22. Bansal R, Lakhina V, Remedios R, Tole S. Expression of FGF receptors 1, 2, 3 in the embryonic and postnatal mouse brain compared with Pdgfralpha, Olig2 and Plp/dm20: implications for oligodendrocyte development. *Dev Neurosci*. 2003;25(2-4):83-95. Epub 2003/09/11.
23. Walshe J, Mason I. Expression of *FGFR1*, *FGFR2* and *FGFR3* during early neural development in the chick embryo. *Mech Dev*. 2000;90(1):103-10. Epub 1999/12/10.
24. Wright TJ, Hatch EP, Karabagli H, Karabagli P, Schoenwolf GC, Mansour SL. Expression of mouse fibroblast growth factor and fibroblast growth factor receptor genes during early inner ear development. *Dev Dyn*. 2003;228(2):267-72. Epub 2003/10/01.
25. Saarimaki-Vire J, Peltopuro P, Lahti L, Naserke T, Blak AA, Vogt Weisenhorn DM, et al. Fibroblast growth factor receptors cooperate to regulate neural progenitor properties in the developing midbrain and hindbrain. *J Neurosci*. 2007;27(32):8581-92. Epub 2007/08/10.
26. Hoefkens MF, Vermeij-Keers C, Vaandrager JM. Crouzon syndrome: phenotypic signs and symptoms of the postnatally expressed subtype. *J Craniofac Surg*. 2004;15(2):233-40; discussion 41-2. Epub 2004/05/29.
27. Johnson D, Wilkie AO. Craniosynostosis. *European journal of human genetics : EJHG*. 2011;19(4):369-76. Epub 2011/01/21.
28. Kreiborg S, Marsh JL, Cohen MM, Jr., Liversage M, Pedersen H, Skovby F, et al. Comparative three-dimensional analysis of CT-scans of the calvaria and cranial base in Apert and Crouzon syndromes. *J Craniomaxillofac Surg*. 1993;21(5):181-8. Epub 1993/07/01.
29. Wilkie AO. Craniosynostosis: genes and mechanisms. *Hum Mol Genet*. 1997;6(10):1647-56. Epub 1997/01/01.
30. Sgouros S. Skull vault growth in craniosynostosis. *Childs Nerv Syst*. 2005;21(10):861-70. Epub 2005/03/26.
31. Goodrich JT. Skull base growth in craniosynostosis. *Childs Nerv Syst*. 2005;21(10):871-9. Epub 2005/05/21.
32. Sgouros S, Natarajan K, Hockley AD, Goldin JH, Wake M. Skull base growth in craniosynostosis. *Pediatr Neurosurg*. 1999;31(6):281-93. Epub 2000/03/07.

33. Martinez-Abadias N, Motch SM, Pankratz TL, Wang Y, Aldridge K, Jabs EW, et al. Tissue-specific responses to aberrant FGF signaling in complex head phenotypes. *Dev Dyn*. 2013;242(1):80-94. Epub 2012/11/23.
34. Gong SG. The Fgfr2 W290R mouse model of Crouzon syndrome. *Childs Nerv Syst*. 2012;28(9):1495-503. Epub 2012/08/09.
35. Perlyn CA, DeLeon VB, Babbs C, Govier D, Burell L, Darvann T, et al. The craniofacial phenotype of the Crouzon mouse: analysis of a model for syndromic craniosynostosis using three-dimensional MicroCT. *Cleft Palate Craniofac J*. 2006;43(6):740-8. Epub 2006/11/16.
36. Thompson DN, Hayward RD, Harkness WJ, Bingham RM, Jones BM. Lessons from a case of kleeblattschadel. Case report. *J Neurosurg*. 1995;82(6):1071-4. Epub 1995/06/01.



CHAPTER 5

Assessment of white matter micro-structural integrity in children diagnosed with syndromic craniosynostosis: A diffusion tensor imaging study

J.M.G. Florisson

J. Dudink

I.V.Koning

W.C.J. Hop

M.L.C. van Veelen

I.M.J.Mathijssen

M.H. Lequin

Radiology. 2011;261(2):534-41. Epub 2011/08/20.

Advances in knowledge

A significant reduction in water diffusion anisotropy was found in children with syndromic or complex craniosynostosis. A primary congenital brain disorder rather than the size or deformities of the skull or the associated hydrocephalus might be a better explanation for the mental deficiency common in craniosynostosis patients.

Implications for patient care

Our findings may indicate a need to a different approach and may initiate a different treatment of the different craniosynostosis syndromes.

ABSTRACT

Purpose: To assess whether architectural alterations exist in the white matter of patients with syndromic and complex craniosynostosis.

Materials and Methods: The Medical Ethics Committee approved this study. Written informed consent was obtained from parents or guardians before imaging. A prospective study was performed in children with syndromic and complex craniosynostosis aged six to fourteen years. Forty-five patients were included: four had Apert syndrome, 14 Crouzon-Pfeiffer syndrome, eight had Muenke syndrome, 11 Saethre-Chotzen syndrome and eight had complex craniosynostosis patients. In addition, seven control subjects were evaluated. For Diffusion Tensor Imaging, an echo planar sequence was used with a diffusion gradient ($b = 1000 \text{ sec/mm}^2$) applied in 25 noncollinear directions. Regions of interest (ROIs) were placed in the following white matter structures: pontine crossing tract (PCT), corticospinal tracts (CST), medial cerebral peduncles (MCP), uncinat fasciculus measured bilaterally (UNC), anterior commissure (AC), bilateral measurements of the frontal and occipital white matter (FW and OW), fornix (FX), corpus callosum measured in the genu (GCC) and splenium (SCC) and the corpus cingulum measured bilaterally (CG). Eigenvalues were measured in all ROIs and Fractional Anisotropy (FA) was calculated.

Results: Across all measured regions of interest FA values were generally lower in all patients combined than in the control subjects ($p < 0.001$). There were no significant differences among subgroups of patients.

Conclusion: DTI measurements of white matter tracts reveal significant white matter integrity differences between children with craniosynostosis and healthy control subjects. This could imply that the developmental delays seen in these patients could be caused by the presence of a primary disorder of the white matter microarchitecture.

INTRODUCTION

Craniosynostosis is a birth defect characterized by premature fusion of at least one cranial suture, with a birth prevalence of approximately 3-5 per 10,000 live born infants (1). In 40% (1:6250) craniosynostosis is a part of a syndrome (2). Children with syndromic craniosynostosis often have unexplained neuropsychological impairment and a lower intelligence quotient (IQ) (3). The decreased intracranial volume and elevated intracranial pressure resulting from the restricted skull growth have been held responsible for these impairments. As a consequence, most children with craniosynostosis receive corrective surgery to enlarge the cranial cavity in the first year of life. Remodeling the cranial vault in an attempt to increase the intracranial volume and control intracranial hypertension while improving the patient's appearance has been the mainstay of surgery for syndromic craniosynostosis (4). Some craniosynostosis patients show developmental delay despite timely surgical intervention, the underlying cause of the delay is unclear.

Apert syndrome is an autosomal dominant syndrome and is caused by one of two fibroblast growth factor receptor 2 (*FGFR2*) mutations in more than 98 % of the cases. This syndrome is characterized by symmetric complex syndactyly of hands and feet, bicoronal synostosis, exorbitism, hypertelorism and midface hypoplasia. Crouzon-Pfeiffer syndrome is also an autosomal dominant syndrome and predominantly caused by mutations in *FGFR2*, but incidentally caused by mutations in the *FGFR1* or *FGFR3*. Crouzon-Pfeiffer syndrome is characterized by midface hypoplasia, exorbitism and various forms of craniosynostosis. Muenke syndrome is an autosomal dominant disorder with incomplete penetrance, caused by the P250R mutation of the *FGFR3* gene. These patients are characterized by macrocephaly, unilateral or bilateral craniosynostosis, and hearing loss. Saethre-Chotzen syndrome is an autosomal dominant disorder with incomplete penetrance, predominantly caused by mutations or deletions in the *TWIST* gene. The phenotype associated with this syndrome incorporates coronal synostosis, upper eyelid ptosis, external ear anomalies and limb abnormalities, such as brachydactyly, syndactyly, and clinodactyly or broad halluces. A mutation may not be found in all patients with a phenotypically syndromic craniosynostosis. Complex craniosynostosis is defined as fusion of two or more cranial sutures without presence of the known mutations in either *FGFR* or *TWIST*. The intelligence of patients with a syndromic form of craniosynostosis may vary from normal to severe mental retardation.

To search for an explanation for their developmental delay, the brains of these patients have been studied repeatedly with conventional magnetic resonance (MR) imaging. White matter alterations and an abnormal gyral structure have been reported (5-9), and these anomalies could indicate either secondary causes or a primary congenital disorder. In 2007, Raybaud et al. (10) published a review with the aim of resolving the controversy regarding whether the brain abnormalities seen in patients with syndromic craniosynostosis are primary or secondary to the bone deformities. In their review they state that experimental

Chapter 5

neurobiological evidence supports the hypothesis that the fibroblast growth factor receptor *FGFR1*, *FGFR2*, and *FGFR3* mutations, causal of syndromic craniosynostosis, may also be causal of diffusely abnormal white matter development. Specifically, they show that developmental white matter disorders are related to mutations in the L1 cell adhesion molecule (L1CAM). Furthermore they stated that L1CAM cannot play its role without a close interaction with *FGFR* genes. Combining these facts they suggest that cerebral abnormalities in syndromic craniosynostosis are an expression of a primary disorder of the white matter. White matter has been reported as atrophic or hypoplastic in all syndromes (5, 7-10). In addition, partial or total agenesis of the pellucid septum has been reported (5-10). Cerebellar involvement, ascribed to a small fossa posterior associated with tonsillar herniation, has also been documented often (5, 6, 8). Raybaud and coworkers concluded that the observed white matter abnormalities, assessed on conventional brain MR images, could constitute a primary disorder (10).

Diffusion Tensor MR imaging enables us to study the micro-architectural organization of brain tissue in vivo. Diffusion-tensor imaging can provide an objective and reproducible assessment of the white matter derived from quantitative measures (11, 12). This offers the opportunity to visualize and quantify the white matter of children with craniosynostosis. The aim of this prospective Diffusion-tensor imaging study was to assess whether architectural alterations exist in the white matter of patients with syndromic and complex craniosynostosis.

METHODS

The Medical Ethics Committee approved this study. Prior to scanning, written informed consent was obtained from the parents or guardians of all patients and control subjects.

Subjects

Data for this study were obtained in the context of a larger prospective ongoing study on craniosynostosis. (Collected by J.M.G.F. and I.M.J.M with 4 and 12 years of experience in plastic surgery, respectively). Craniosynostosis is characterized by premature fusion or agenesis of calvarial sutures. Because of the craniosynostosis, normal growth of the skull related to the affected suture is restricted. To accommodate the growing brain, compensatory skull growth occurs in the other directions resulting in cranial deformation. Children with syndromic or complex craniosynostosis were enrolled. Children included in the diffusion-tensor imaging study had to be between 6 and 14 years. All participants were recruited from the Sophia children's hospital, a national referring center for craniosynostosis patients. Fifty-six patients underwent both MR imaging and genetic testing. For comparison, we included seven healthy control subjects with normal neuropsychological test results and without abnormalities on conventional MR images. Grounds for excluding subjects from the group included the presence of severe artifacts

and/or distortions due to braces and metallic remains from surgery. Consequently, 11 of 56 patients (20%; mean age, 11.7 years, 8.5 – 13.9 years) were excluded. Two of those patients had Apert syndrome, two had Crouzon-Pfeiffer syndrome, two had Muenke syndrome, three had Saethre-Chotzen syndrome, and two had a complex form of craniosynostosis.

In addition, our patient group was further categorized according to the level of the individual syndromes as well as on genetic grounds. The patients with syndromic and complex craniosynostosis were analyzed separately in comparison to the control subjects. Moreover, patients were further classified into three groups on the basis of genetics. The first group consisted of patients with *FGFR* mutations (*FGFR* group). This group included patients with Apert, Crouzon/Pfeiffer, or Muenke syndromes. The second group consisted of patients with mutations and deletions in *TWIST* (*TWIST* group) and included all patients with the Saethre-Chotzen syndrome. The third group consisted of patients with no demonstrable genetic mutation and included patients with complex craniosynostosis (complex craniosynostosis group). Patients in these three genetically classified groups were compared with each other and with the control subjects.

Image acquisition

All imaging data, including those from diffusion-tensor imaging, were acquired from brain MR images obtained with a 1.5-T unit (GE Medical Systems, Milwaukee, Wis). Diffusion-tensor imaging data were obtained by using a multi-repetition single-shot echo planar sequence with a section thickness of 3 mm and no gap. Diffusion-tensor images were obtained in 25 gradient directions with the following parameters: sensitivity, $b = 1000$ sec/mm², repetition time, 15000 msec; echo time, 82.1 msec; one signal acquired; 240 x 240 mm² field of view, and 128 x 128 matrix. This resulted in a voxel size of 1.8 x 1.8 x 3.0 mm³.

Data Collection

ROIs of standard shape (round) and size (36 voxels) were placed manually in 10 predetermined anatomic locations in both hemispheres by a researcher experienced in diffusion-tensor imaging (I.V.K., with one year of experience; M.H.L., with 15 years of experience in pediatric neuroradiology; and J.D., with 8 years of experience in pediatrics and neurologic research). The anatomic locations used were as follows: pontine crossing tract (PCT), corticospinal tracts (CST), medial cerebral peduncles (MCP), uncinate fasciculus measured bilaterally (UNC), anterior commissure (AC), bilateral measurements of the frontal and occipital white matter (FW and OW), fornix (FX), corpus callosum measured in the genu (GCC) and splenium (SCC) and the corpus cingulum measured bilaterally (CG). To optimize ROI placement, standard DTI color maps of white matter atlases (13, 14) were used to determine the most suitable section for every structure individually (Fig 1). The investigators involved in ROI placement were blinded to clinical presentation and outcome.

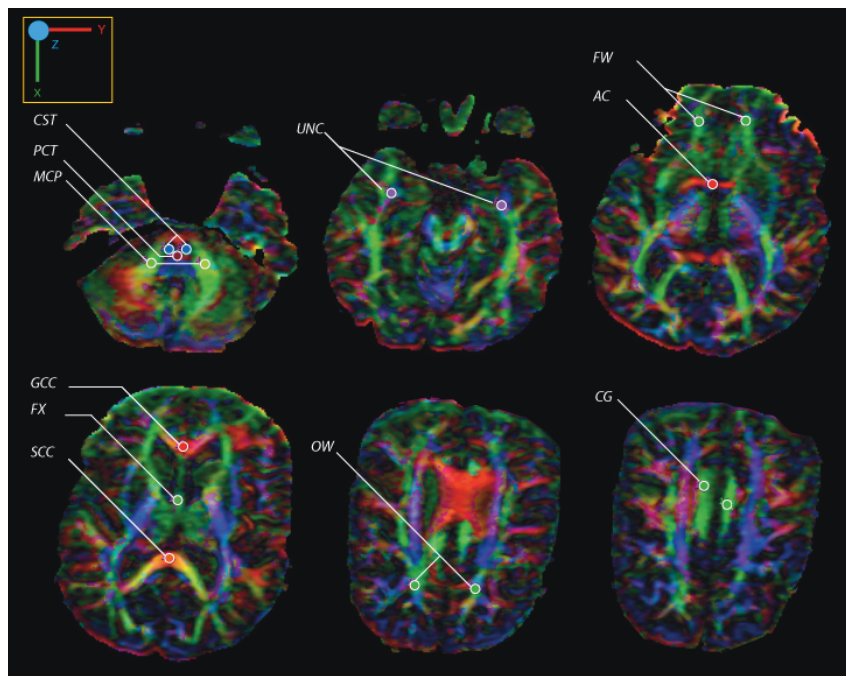


Figure 1: FA colormaps examples at different levels used for our ROI placements in one of our patients. Abbreviations used; PCT=pontine crossing tract; CST=corticospinal tract; MCP=medial cerebral peduncle; UNC=uncinate fasciculus; AC=anterior commissure; FX=fornix; MWM=mean white matter; GCC=genu of corpus callosum; SCC=splenium of corpus callosum; CG=corpus cingulum.

Statistical Analysis

To explore eigenvalues, λ_1 , λ_2 and λ_3 obtained from the left and right hemispheres per region, per subject, were averaged to yield a mean score. Mean White Matter (MWM) is given by the mean of the right and left frontal and occipital white matter measurements. From the mean eigenvalues, Fractional Anisotropy (FA) and the Apparent Diffusion Coefficient (ADC) were computed. ADC was computed by the formula $(\lambda_1 + \lambda_2 + \lambda_3)/3$. FA was calculated by using the formula derived by Basser et al. (15).

Software (The Statistical Package for the Social Sciences version 15.0 for Windows (SPSS, Chicago, Ill) and Statistical Analysis Software (SAS) was used for statistical analysis.

Multivariate comparisons of the measured FA values at the 10 structures between the groups (*FGFR* group, *TWIST* group, complex craniosynostosis group and healthy control subjects) were performed by using repeated measurements analysis of variance (ANOVA) (SAS PROC MIXED, SAS Institute). Dunnett adjustment was applied to the pairwise comparison of patient groups with the control group to correct for multiple comparisons.

ADCs at the various structures were compared between the entire patient group and control subjects by using the Mann-Whitney test because data showed skew distributions at some structures; no multiplicity correction was made. A two-sided P value of less than 0.05 was considered indicative of a statistically significant difference.

To determine the intraobserver reliability of the ROI placement, one observer (I.V.K.) repeated the placement on a subset of 10 images at intervals of 2, 4 and 6 weeks. Single-measure two-way mixed intra-class correlation coefficients (ICCs) were calculated to quantify the variability of data obtained (16).

Statistical analysis was done by an experienced statistician. (W.C.J.H. with 30 years of experience)

RESULTS

Subjects

Forty-five children with syndromic or complex craniosynostosis (mean age 9.5 years; range 6.0 – 13.3 years) and seven healthy control subjects (mean age 10.7 years; range 7.5 – 14.8 years) met the inclusion criteria. The age and sex distributions for our patient groups and control subjects are displayed in Table 1.

Table 1: Age and Sex distribution.

Diagnosis	Total	Male (n)	Female (n)	Mean Age (yrs)
<i>FGFR</i>	26	11	15	9.8
Apert	4	1	3	10.3
Crouzon/Pfeiffer	14	7	7	10.1
Muenke	8	3	5	8.9
<i>Twist</i>	11	8	3	9.3
Complex	8	4	4	8.8
Total Patients	45	23	22	9.5
Controls	7	4	3	10.7

Intra-observer Reliability of Region-of-Interest Placement

Reproducibility of ROI placement in 10 subjects by one observer was moderate to very strong, with ICCs of 0.30 - 0.94. However, the wide range of ICCs in these regions is disconcerting. The ICC was highest in the corticospinal tract (left: 0.94; right: 0.89) and corpus callosum (genu: 0.87; splenium: 0.92). An exception was the occipital white matter, which displayed a very weak ICC (left: 0.06; right: 0.38). The ICC for the MWM (mean of left and right frontal and occipital white matter) was moderate (0.66).

Integrity of Brain Parenchyma in syndromic craniosynostosis patients

To examine the microstructural integrity of the brain, we used the eigenvalues to calculate the FA values and ADCs.

Fractional Anisotropy

Table 2 shows mean FA values according to syndrome and genetic background. Within the *FGFR* group, there were no significant differences (overall $P=0.426$ ANOVA) among patients with Apert, Crouzon-Pfeiffer, and Muenke syndromes. Therefore, further analyses were done to compare the three patient groups with the control group.

Figure 2 shows mean FA values for the various structures in the three patient groups and the control group. ANOVA showed significant differences regarding FA values among the *FGFR*, *TWIST*, complex craniosynostosis, and control groups (overall $P<0.001$). Mean FA values (\pm standard error of the mean) across the ten structures were 0.46, (± 0.01), 0.47(± 0.01), 0.47(± 0.01) and 0.51(± 0.01) for the *FGFR*, *TWIST*, Complex craniosynostosis and control groups, respectively. ANOVA further showed that the differences between these four groups did not significantly depend on the measured structure (interaction group X structure: $p=0.241$), which indicates that the profiles of means for the groups as shown in Figure 2 do not significantly deviate from parallelism. Further pair-wise comparisons of the separate patient groups with the control group showed significant differences for *FGFR* group (adjusted $P < 0.001$) and the complex craniosynostosis group (adjusted $P < 0.013$). The difference between the *TWIST* and control group approached statistical significance (adjusted $P=0.051$). There were no significant differences between the *FGFR*, *TWIST* and Complex craniosynostosis groups (overall $P=0.162$). The combined mean FA values for all patient groups were lower than those in the control group (difference -0.046 ; 95% confidence interval: -0.07 to -0.02 ; $p<0.001$). We obtained the same results when the age of the subjects at MR imaging was taken into account in the ANOVA models as a covariate.

Eigenvalues and ADCs.

Comparison of ADCs in the various structures between the entire patient group and the control group is shown in Table 3. For all structures, the median values were larger in the patient group than in the control group.

Table 2: FA values in White matter structures according to syndrome and genetic background.

Mutation Struct./Diagn.	FGFR 2/3			Twist			Unknown			None		Total	
	Standard Deviation	Apert (n=4)	Crouzon/ Pfeiffer (n=14)	Muenke (n=8)	SC (n=11)	Standard Deviation	Complex (n=8)	Standard Deviation	Controls (n=7)	Standard Deviation	Patients (n=45)	Standard Deviation	Patients (n=45)
PCT	0.32	0.06	0.32	0.31	0.3	0.07	0.32	0.08	0.31	0.09	0.31	0.09	0.31
CST	0.42	0.06	0.37	0.38	0.41	0.07	0.41	0.07	0.41	0.12	0.41	0.12	0.41
MCP	0.62	0.08	0.59	0.64	0.69	0.04	0.63	0.05	0.71	0.07	0.65	0.07	0.65
UNC	0.34	0.09	0.37	0.32	0.41	0.08	0.35	0.06	0.40	0.03	0.37	0.03	0.37
AC	0.28	0.11	0.4	0.25	0.31	0.07	0.26	0.08	0.30	0.09	0.28	0.09	0.28
FX	0.38	0.08	0.37	0.44	0.39	0.04	0.41	0.09	0.46	0.07	0.40	0.07	0.40
GCC	0.55	0.09	0.6	0.62	0.6	0.05	0.64	0.09	0.64	0.07	0.59	0.07	0.59
SCC	0.70	0.08	0.69	0.74	0.72	0.10	0.75	0.06	0.81	0.04	0.73	0.04	0.73
CG	0.5	0.08	0.51	0.51	0.48	0.06	0.49	0.09	0.55	0.05	0.51	0.05	0.51
MWM	0.42	0.06	0.41	0.44	0.44	0.08	0.41	0.10	0.47	0.02	0.43	0.02	0.43

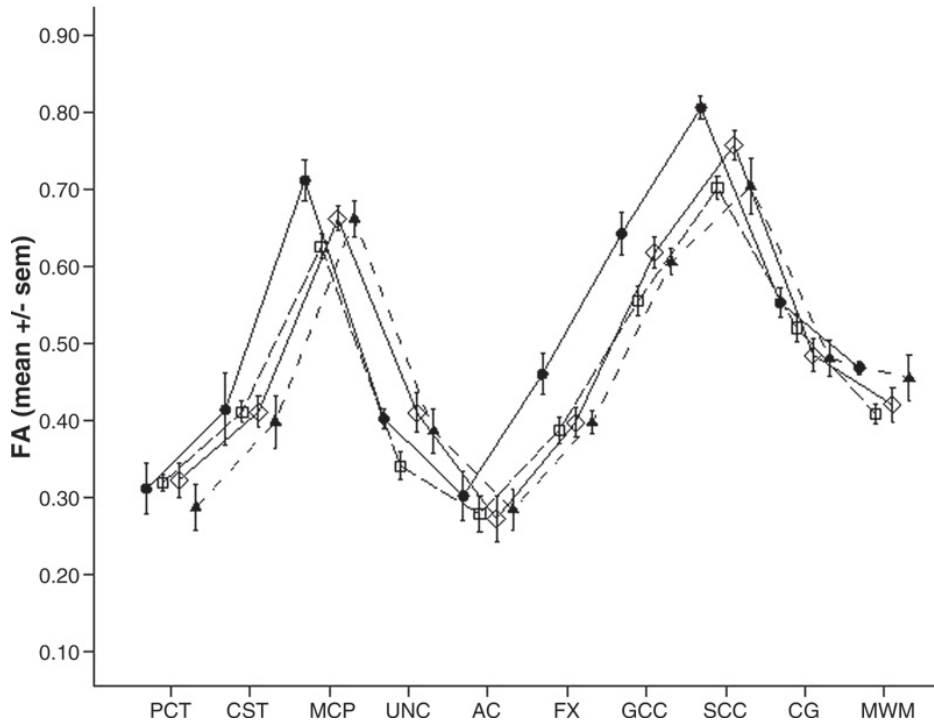


Figure 2: Mean fractional anisotropy (FA) values according to patient group *FGFR* (▲, n=26), *TWIST* (□, n=11), Complex (◇, n=8), Controls (●, n=7)

Table 3: Median with range of apparent diffusion coefficient (ADC in mm²/second) values of patients and control subjects.

Structure	Patients	Controls	P
PCT	7.9 (6.9-9.2)	7.2 (6.5-7.6)	< 0.001
CST	8.0 (6.7-10.4)	7.2 (5.8-7.8)	< 0.001
MCP	7.8 (6.7-10.0)	6.8 (5.6-7.4)	< 0.001
UNC	8.9 (7.3-9.9)	7.8 (7.2-9.0)	< 0.001
AC	12.3 (7.4-25.6)	10.2 (8.6-12.7)	0.019
FX	15.4 (11.4-27.4)	11.9 (10.9-15.4)	0.017
GCC	9.9 (8.4-14.7)	8.9 (7.8-9.1)	< 0.001
SCC	8.5 (7.0-14.0)	7.6 (6.5-8.6)	0.015
CG	7.8 (6.8-8.8)	6.9 (6.4-7.2)	< 0.001
MWM	8.1 (7.7-8.8)	7.3 (6.9-7.6)	< 0.001

DISCUSSION

The aim of our study was to assess whether architectural alterations exist in the white matter of patients with syndromic and complex craniosynostosis. We generally found lower FA values in all white matter structures for patients compared to controls. Although a decrease in diffusion anisotropy, meaning lower FA value, is not unique for our study population but commonly observed concurrent with central nervous system pathology (17-22). Song 2002 et al. (23) demonstrated that a detailed examination of directional diffusivities could shed light on underlying pathology. Also our FA value results suggest the presence of changes in white matter microstructural integrity in specific white matter regions in children diagnosed with syndromic or complex craniosynostosis. This seems to be in agreement with previously published data on white matter alterations, like thin corpus callosum, and septal anomalies, visible on conventional MRI scans (5-10).

There was a difference in FA values between the entire patient group and the control subjects, but there were no significant differences in FA values in specific regions of interest among the subgroups of individual syndromes and the complex form of craniosynostosis. The degree of white matter alterations seen in individual syndromes could not explain the wide range of neuropsychological outcome severities reported in the literature (24). Some studies suggest that difference in neurological outcome may be due to an increase in intracranial pressure, rather than a primary white matter disturbance (3, 4). For instance, patients diagnosed with Crouzon and Apert syndromes are known to be at higher risk for at least one episodes of increased intracranial pressure during their lives (especially during their first four years of life). This cannot be the only explanation, however, because our patients, with Muenke syndrome, which is known to almost never cause an increase in intracranial pressure, (24) also had decreased anisotropy values in the white matter tracts, suggesting a primary cause. The effect of hydrocephalus on white matter structures seems to be dependent of the location of that structure. Anisotropic changes in the corpus callosum could be a direct effect of the hydrocephalus (25), yet mostly this is reversible with surgical correction or ventricular shunts (26). The fact that we found anisotropic changes in structures throughout the whole brain of patients with craniosynostosis, who had already undergone surgery, is one more step towards the hypothesis of a primary disorder.

Our findings of lower FA values suggesting microstructural disturbances are supported by recent neurobiological evidence. The L1 cell adhesion molecule (L1CAM) gene plays a major role in the development of white matter. Its mutation causes similar defects of the corpus callosum, septum pellucidum, centrum semi-ovale and corticospinal tracts in humans and mice (27, 28). The growth hormone *FGFR*, defects of which cause syndromic craniosynostosis, is essential for L1CAM to operate (29, 30). Hence, in addition to its effect on the cranial sutures, *FGFR* seems to act on growth and maturation of white matter tracts, leading to primary alterations in the development of the white matter (10).

Chapter 5

The trend towards higher λ_2 and λ_3 eigen values and the higher ADC values in our patient group may also elucidate more about the microarchitecture of the white matter. Changes in these diffusion parameters may indicate diffusion changes radial (perpendicular) to white matter tracts. These findings may potentially be used to differentiate myelin loss from axonal injury (23). In agreement with prior animal and human studies (31-33), besides lower FA values, higher eigenvalues in combination with significantly increased ADC values in our craniosynostosis patients suggest increased radial diffusivity, indicating myelin deficiency. However, we do not have a radiologic-pathologic correlation in our study to confirm this, and detailed biophysical mechanisms underlying differential changes in directional diffusivities remain to be elucidated (23).

Our study has limitations, which include the age ranges and difference in mean ages of patients and control subjects. Results of diffusion-tensor imaging maturation studies suggest consistent, significant positive and negative correlations of, respectively, FA and ADC with age throughout the brain (34-41). However the age range for our study was 6 to 14 years; at 6 years old, the brain has matured thoroughly enough to yield stable anisotropic indices, and DTI values seem to change only slightly afterwards (39). Also, adjusted for age the differences between the various subgroups remained the same.

Using relatively new post-processing tools such as tract-based spatial statistics (TBSS, www.fmrib.ox.ac.uk), assessment of anisotropic indices can be performed automatically. However, we encountered image registration problems when using TBSS because of the severe skull malformations of the patients included in the study. ROI and voxel-based analysis have previously shown good consonance (42), so ROI placement was determined to be the most suitable method for our study.

CONCLUSION

DTI was demonstrated to be a helpful supplement to conventional MRI for identifying white matter anomalies in children diagnosed with syndromic or complex craniosynostosis, adding to the evidence for a primary disorder of the white matter microenvironment. Further research is needed to assess the benefits of surgical interventions in syndromal craniosynostosis patients by focusing on pre-surgical (fetal and/or neonatal) imaging of the brain with diffusion-tensor imaging.

SUMMARY STATEMENT

DTI was demonstrated to be a helpful supplement to conventional MRI for identifying white matter anomalies in children diagnosed with syndromic or complex craniosynostosis, adding to the evidence for a primary disorder of the white matter microenvironment.

REFERENCES

1. Boulet SL, Rasmussen SA, Honein MA. A population-based study of craniosynostosis in metropolitan Atlanta, 1989-2003. *Am J Med Genet A*. 2008;146A(8):984-91. Epub 2008/03/18.
2. Bannink N, Joosten KF, van Veelen ML, Bartels MC, Tasker RC, van Adrichem LN, et al. Papilledema in patients with Apert, Crouzon, and Pfeiffer syndrome: prevalence, efficacy of treatment, and risk factors. *J Craniofac Surg*. 2008;19(1):121-7. Epub 2008/01/25.
3. Da Costa AC, Walters I, Savarirayan R, Anderson VA, Wrennall JA, Meara JG. Intellectual outcomes in children and adolescents with syndromic and nonsyndromic craniosynostosis. *Plast Reconstr Surg*. 2006;118(1):175-81; discussion 82-3. Epub 2006/07/04.
4. Thompson DN, Jones BM, Harkness W, Gonzalez S, Hayward RD. Consequences of cranial vault expansion surgery for craniosynostosis. *Pediatr Neurosurg*. 1997;26(6):296-303. Epub 1997/06/01.
5. Cohen MM, Jr. Pfeiffer syndrome update, clinical subtypes, and guidelines for differential diagnosis. *Am J Med Genet*. 1993;45(3):300-7. Epub 1993/02/01.
6. Proudman TW, Clark BE, Moore MH, Abbott AH, David DJ. Central nervous system imaging in Crouzon's syndrome. *J Craniofac Surg*. 1995;6(5):401-5. Epub 1995/09/01.
7. Quintero-Rivera F, Robson CD, Reiss RE, Levine D, Benson CB, Mulliken JB, et al. Intracranial anomalies detected by imaging studies in 30 patients with Apert syndrome. *Am J Med Genet A*. 2006;140(12):1337-8. Epub 2006/05/13.
8. Tokumaru AM, Barkovich AJ, Ciricillo SF, Edwards MS. Skull base and calvarial deformities: association with intracranial changes in craniofacial syndromes. *AJNR Am J Neuroradiol*. 1996;17(4):619-30. Epub 1996/04/01.
9. Yacubian-Fernandes A, Palhares A, Giglio A, Gabarra RC, Zanini S, Portela L, et al. Apert syndrome: analysis of associated brain malformations and conformational changes determined by surgical treatment. *J Neuroradiol*. 2004;31(2):116-22. Epub 2004/04/20.
10. Raybaud C, Di Rocco C. Brain malformation in syndromic craniosynostoses, a primary disorder of white matter: a review. *Childs Nerv Syst*. 2007;23(12):1379-88. Epub 2007/09/21.
11. Huppi PS, Dubois J. Diffusion tensor imaging of brain development. *Semin Fetal Neonatal Med*. 2006;11(6):489-97. Epub 2006/09/12.
12. Neil J, Miller J, Mukherjee P, Huppi PS. Diffusion tensor imaging of normal and injured developing human brain - a technical review. *NMR Biomed*. 2002;15(7-8):543-52. Epub 2002/12/19.
13. Mori S, Wakana S, Van Zijl PCM. MRI atlas of human white matter. 1st ed. Amsterdam, The Netherlands ; San Diego, CA: Elsevier; 2004. p. p.
14. Wakana S, Jiang H, Nagae-Poetscher LM, van Zijl PC, Mori S. Fiber tract-based atlas of human white matter anatomy. *Radiology*. 2004;230(1):77-87. Epub 2003/12/03.
15. Basser PJ, Pierpaoli C. Microstructural and physiological features of tissues elucidated by quantitative-diffusion-tensor MRI. *J Magn Reson B*. 1996;111(3):209-19. Epub 1996/06/01.

Chapter 5

16. Shrout PE, Fleiss JL. Intraclass correlations: uses in assessing rater reliability. *Psychol Bull.* 1979;86(2):420-8. Epub 1979/03/01.
17. Castriota Scanderbeg A, Tomaiuolo F, Sabatini U, Nocentini U, Grasso MG, Caltagirone C. Demyelinating plaques in relapsing-remitting and secondary-progressive multiple sclerosis: assessment with diffusion MR imaging. *AJNR Am J Neuroradiol.* 2000;21(5):862-8. Epub 2000/05/18.
18. Filippi M, Cercignani M, Inglese M, Horsfield MA, Comi G. Diffusion tensor magnetic resonance imaging in multiple sclerosis. *Neurology.* 2001;56(3):304-11. Epub 2001/02/15.
19. Jones DK, Lythgoe D, Horsfield MA, Simmons A, Williams SC, Markus HS. Characterization of white matter damage in ischemic leukoaraiosis with diffusion tensor MRI. *Stroke.* 1999;30(2):393-7. Epub 1999/02/05.
20. Neil JJ, Shiran SI, McKinstry RC, Scheffert GL, Snyder AZ, Almlí CR, et al. Normal brain in human newborns: apparent diffusion coefficient and diffusion anisotropy measured by using diffusion tensor MR imaging. *Radiology.* 1998;209(1):57-66. Epub 1998/10/14.
21. Werring DJ, Clark CA, Barker GJ, Thompson AJ, Miller DH. Diffusion tensor imaging of lesions and normal-appearing white matter in multiple sclerosis. *Neurology.* 1999;52(8):1626-32. Epub 1999/05/20.
22. Werring DJ, Toosy AT, Clark CA, Parker GJ, Barker GJ, Miller DH, et al. Diffusion tensor imaging can detect and quantify corticospinal tract degeneration after stroke. *J Neurol Neurosurg Psychiatry.* 2000;69(2):269-72. Epub 2000/07/15.
23. Song SK, Sun SW, Ramsbottom MJ, Chang C, Russell J, Cross AH. Dysmyelination revealed through MRI as increased radial (but unchanged axial) diffusion of water. *Neuroimage.* 2002;17(3):1429-36. Epub 2002/11/05.
24. de Jong T, Bannink N, Bredero-Boelhouwer HH, van Veelen ML, Bartels MC, Hoeve LJ, et al. Long-term functional outcome in 167 patients with syndromic craniosynostosis; defining a syndrome-specific risk profile. *J Plast Reconstr Aesthet Surg.* 2009. Epub 2009/11/17.
25. Yuan W, Mangano FT, Air EL, Holland SK, Jones BV, Altabe M, et al. Anisotropic diffusion properties in infants with hydrocephalus: a diffusion tensor imaging study. *AJNR Am J Neuroradiol.* 2009;30(9):1792-8. Epub 2009/08/08.
26. Air EL, Yuan W, Holland SK, Jones BV, Bierbrauer K, Altabe M, et al. Longitudinal comparison of pre- and postoperative diffusion tensor imaging parameters in young children with hydrocephalus. *J Neurosurg Pediatr.* 2010;5(4):385-91. Epub 2010/04/07.
27. Demyanenko GP, Tsai AY, Maness PF. Abnormalities in neuronal process extension, hippocampal development, and the ventricular system of L1 knockout mice. *J Neurosci.* 1999;19(12):4907-20. Epub 1999/06/15.
28. Finckh U, Schroder J, Ressler B, Veske A, Gal A. Spectrum and detection rate of L1CAM mutations in isolated and familial cases with clinically suspected L1-disease. *Am J Med Genet.* 2000;92(1):40-6. Epub 2000/05/08.
29. Doherty P, Walsh FS. CAM-FGF receptor interactions: a model for axonal growth. *Mol Cell Neurosci.* 1996;8(2-3):99-111. Epub 1996/01/01.
30. Kamiguchi H, Lemmon V. Neural cell adhesion molecule L1: signaling pathways and growth cone motility. *J Neurosci Res.* 1997;49(1):1-8. Epub 1997/07/01.

31. Nair G, Tanahashi Y, Low HP, Billings-Gagliardi S, Schwartz WJ, Duong TQ. Myelination and long diffusion times alter diffusion-tensor-imaging contrast in myelin-deficient shiverer mice. *Neuroimage*. 2005;28(1):165-74. Epub 2005/07/19.
32. Ono J, Harada K, Mano T, Sakurai K, Okada S. Differentiation of dys- and demyelination using diffusional anisotropy. *Pediatr Neurol*. 1997;16(1):63-6. Epub 1997/01/01.
33. Takahashi M, Ono J, Harada K, Maeda M, Hackney DB. Diffusional anisotropy in cranial nerves with maturation: quantitative evaluation with diffusion MR imaging in rats. *Radiology*. 2000;216(3):881-5. Epub 2000/08/31.
34. Ashtari M, Cervellione KL, Hasan KM, Wu J, McIlree C, Kester H, et al. White matter development during late adolescence in healthy males: a cross-sectional diffusion tensor imaging study. *Neuroimage*. 2007;35(2):501-10. Epub 2007/01/30.
35. Ben Bashat D, Ben Sira L, Graif M, Pianka P, Hendler T, Cohen Y, et al. Normal white matter development from infancy to adulthood: comparing diffusion tensor and high b value diffusion weighted MR images. *J Magn Reson Imaging*. 2005;21(5):503-11. Epub 2005/04/19.
36. Bonekamp D, Nagae LM, Degaonkar M, Matson M, Abdalla WM, Barker PB, et al. Diffusion tensor imaging in children and adolescents: reproducibility, hemispheric, and age-related differences. *Neuroimage*. 2007;34(2):733-42. Epub 2006/11/10.
37. Eluvathingal TJ, Hasan KM, Kramer L, Fletcher JM, Ewing-Cobbs L. Quantitative diffusion tensor tractography of association and projection fibers in normally developing children and adolescents. *Cereb Cortex*. 2007;17(12):2760-8. Epub 2007/02/20.
38. Giorgio A, Watkins KE, Douaud G, James AC, James S, De Stefano N, et al. Changes in white matter microstructure during adolescence. *Neuroimage*. 2008;39(1):52-61. Epub 2007/10/09.
39. Lobel U, Sedlacik J, Gullmar D, Kaiser WA, Reichenbach JR, Mentzel HJ. Diffusion tensor imaging: the normal evolution of ADC, RA, FA, and eigenvalues studied in multiple anatomical regions of the brain. *Neuroradiology*. 2009;51(4):253-63. Epub 2009/01/10.
40. Nagy Z, Westerberg H, Klingberg T. Maturation of white matter is associated with the development of cognitive functions during childhood. *J Cogn Neurosci*. 2004;16(7):1227-33. Epub 2004/09/30.
41. Schmithorst VJ, Wilke M, Dardzinski BJ, Holland SK. Correlation of white matter diffusivity and anisotropy with age during childhood and adolescence: a cross-sectional diffusion-tensor MR imaging study. *Radiology*. 2002;222(1):212-8. Epub 2002/01/05.
42. Snook L, Plewes C, Beaulieu C. Voxel based versus region of interest analysis in diffusion tensor imaging of neurodevelopment. *Neuroimage*. 2007;34(1):243-52. Epub 2006/10/31.



CHAPTER 6

Corpus callosum and cingulate bundle white matter abnormalities in non-operated craniosynostosis patients – a Diffusion Tensor Imaging study

C.A. de Planque

J.M.G. Florisson

R.C. Tasker

B. Rijken

M.L.C. van Veelen

I.M.J. Mathijssen

M.H. Lequin

M.H.G. Dremmen

* The first two authors contributed equally to the paper

Submitted

ABSTRACT

Background and purpose: In 7 to 15 year old operated children with syndromic craniosynostosis we have shown the presence of microstructural anomalies in brain white matter. To learn more about the cause of these anomalies, the aim of the study is to determine diffusivity values in white matter tracts in non-operated children with syndromic craniosynostosis, aged under 4 years compared to healthy controls.

Materials and methods: DTI datasets of 57 non-operated patients with syndromic craniosynostosis with a median [range] age of 0.4 [0.27-3.16] years, were compared with 7 control subjects aged 1.39 [0.56 to 2.84] years. Major white matter tract pathways were reconstructed with ExploreDTI from datasets of 1.5 Tesla MRI system with 25 diffusion gradient orientations. Eigenvalues of these tract data were examined, with subsequent assessment of radial diffusivity values of the corpus callosum and cingulate bundle. Having syndromic craniosynostosis (versus control), sex, frontal occipital horn ratio and tract volume were treated as independent variables.

Results: Having syndromic craniosynostosis is associated with increased radial diffusivity in the genu and body of the corpus callosum and hippocampal and body of the cingulum bundle ($p < 0.05$), where tract volume and frontal occipital horn ratio are significantly associated interacting factors.

Conclusion: Before any surgery, young syndromic craniosynostosis patients aged under 4 years have increased radial diffusivity values in the corpus callosum and cingulate bundle compared to aged matched controls. This difference suggest intrinsic and mechanic causes, with frontal occipital horn ratio being a significantly associated factor.

INTRODUCTION

Patients with syndromic craniosynostosis (sCS) are at risk of developing intellectual disabilities and problems in behavioural and emotional function. Whether these derangements are caused by disturbances in brain development is unknown.¹ Mutations in genes encoding the fibroblast growth factor receptors (*FGFR*) – which are expressed during early embryonic development – are known to be responsible for the pattern of abnormal skull development in sCS.^{2,3} These gene mutations induce premature fusion of skull sutures and also affect the development of brain tissue and CSF circulation.⁴⁻⁶ It is known that mutations in *FGFR-1* or *FGFR-2* are associated with decreased myelin thickness,^{7,8} but is this finding a consequence of mechanical distortion of the brain due to abnormal shape, ventriculomegaly and/or cerebellar tonsillar herniation, or does this finding reflect an intrinsic cause?^{9-12 13,14}

Previously, we have reported abnormalities in brain white matter microstructure using MRI DTI in a group of older operated sCS patients aged 7 to 15 years. We identified significantly higher white matter mean diffusivity (MD), axial diffusivity (AD) and radial diffusivity (RD) in the cingulate bundle, corpus callosum, fornix and cortical spinal tract.¹⁵ These findings suggested the presence of abnormal white matter microstructural tissue properties in sCS patients and now lead us to consider two key questions: 1) Are these abnormalities already present in young non-operated sCS patients? 2) If so, does it reflect exposure to some mechanically-related cause like worsening ventriculomegaly or does such an abnormality have an intrinsic cause?

In this report we have examined DTI-based white matter microarchitecture in white matter tracts in young non-operated children with sCS. Our hypothesis is that there are abnormalities in white matter microstructure already evident early in brain development.

MATERIAL AND METHODS

This study is an extension of our previously reported work about operated sCS patients versus controls.¹⁵ The Institution Research Ethics Board at Erasmus University Medical Center Rotterdam, The Netherlands, approved this study (MEC-2014-461), which is part of ongoing work at the Dutch Craniofacial Center involving protocolized care, brain imaging, clinical assessment and data summary and evaluation.

Subjects

MRIs from non-operated sCS and multisuture craniosynostosis patients (i.e., 2 or more prematurely closed skull sutures without a known genetic cause), aged under 4 years were included. Control subjects, within the same age range as our patients, were identified.

MRI Acquisition

All brain MRI data were acquired with a 1.5 Tesla unit (General Electric Healthcare, Milwaukee, Wisconsin), including three-dimensional (3D) T1-weighted fast spoiled gradient-recalled sequence, high-resolution 3D T2-weighted spin echo sequence, and DTI sequences. DTI was obtained using a multi repetition single-shot echo-planar sequence with a section thickness of 3 mm without a gap. Images were obtained in 25 gradient directions with the following parameters: sensitivity, b : 1000s/mm²; TR: 15,000ms; TE: 82.1ms; FOV: 240 x 240 mm²; and matrix: 128 x 128, resulting in a voxel size of 1.8 x 1.8 x 3.0 mm. This protocol was identical in both sCS patients and controls, and kept equal throughout the entire study period.

DTI Data Collection

DTI processing was performed using ExploreDTI (<http://exploredti.com/>). The processing consisted of correction of subject motion and eddy current distortions, and a weighted linear least-squares estimation of the diffusion tensor with the robust extraction of kurtosis indices with linear estimation (REKINDLE) approach.^{16, 17} White matter tracts for fiber tractography included projection fibers (corticospinal tract), commissural fibers (corpus callosum), tracts of the brain stem (medial cerebellar peduncle) and the tracts of the limbic system (fornix and cingulate bundle).

A ROI approach was used for white matter tract analysis, with the *MRI Atlas of Human White Matter* as a guideline.¹⁸ “OR/SEED” and “AND” operators were used when tracts were allowed to pass through, and “NOT” operators were used when tracts were not allowed to pass through. Occasionally, “NOT” operators were used to avoid aberrant or crossing fibers from other bundles. To secure measuring identical parts of the different white matter tracts, 2 AND operators at both ends of a bundle to extract always the same segment of the particular white matter tract were used. We measured the tracts as reported previously.¹⁵

DTI Metrics

The white matter metrics from DTI, voxel-by-voxel, are mathematically based on 3 mutually perpendicular eigenvectors, whose magnitude is given by 3 corresponding eigenvalues sorted in order of decreasing magnitude as λ_1 , λ_2 and λ_3 . An ellipsoid is created by the long axis of λ_1 and the small axes λ_2 and λ_3 , from where the measured length of the three axes are the eigen values. These eigenvalues are used to generate quantitative maps of fractional anisotropy (FA), the derivation of MD, RD and AD. FA represents the amount of diffusional asymmetry in a voxel, which is presented from 0 (infinite isotropy) to 1 (infinite anisotropy). AD stands for the diffusivity along the neural tract: λ_1 . The diffusivity of the minor axes, λ_2 and λ_3 , is called the perpendicular or radial diffusivity. The mean of these diffusivity λ_1 , λ_2 and λ_3 is known as MD. FA, MD, AD and RD are used as indirect markers of white matter microstructure of these young patients.¹⁹ However, the mathematical coupling in the FA, MD, RD and AD equations means that our statistical

approach will first need to assess for differences in the eigenvalues before analysing the impact of summary measures of diffusivity. The following equations were used:

$$FA = \sqrt{\frac{3}{2} \cdot \frac{\sqrt{(\lambda_1 - MD)^2 + (\lambda_2 - MD)^2 + (\lambda_3 - MD)^2}}{\sqrt{\lambda_1^2 + \lambda_2^2 + \lambda_3^2}}}$$

$$MD = \frac{(\lambda_1 + \lambda_2 + \lambda_3)}{3}$$

$$RD = \frac{(\lambda_2 + \lambda_3)}{2}$$

$$AD = \lambda_1$$

unit of measure

FA	scalar value ranging between 0-1
MD	mm ² /sec
RD	mm ² /sec
AD	mm ² /sec

Frontal Occipital Horn Ratio

Since ventriculomegaly is an abnormality in sCS patients the analyses we used the *Frontal Occipital Horn Ratio* (FOHR) to correct for ventricular size.²⁰ The measurements were assessed in a standardized way by a single trained rater. Lateral ventricular was evaluated in the axial plane and the FOHR is calculated as the sum of the bifrontal horn bioccipital horn dimensions, divided by twice the biparietal dimension.

Reliability and Reproducibility

Inter-observer reliability of measurements was determined by comparing the results of two trained raters blinded to subject information. Both performed all structural measurements twice in 10 subjects, 5 patients and 5 control subjects. Interrater reliability was based on 10 repeated ratings and found to be high.

Partial volume effects due to brain deformity and abnormal ventricular size and shape potentially influenced the DTI fiber tractography data in patients with sCS. Therefore, our fiber tractography algorithms were adapted to track reliable and comparable fiber tracts in all subjects.

The FA threshold was set at 0.1, and the maximum angle threshold, at 45°. This DTI fiber tractography protocol has been used in craniosynostosis patients and controls.¹⁵ Of note,

even though a FA threshold of 0.2 is commonly used,²¹ a threshold of 0.1 made it possible to track all structures in the control group and almost all structures in the sCS group. However, the FA threshold of 0.1 meant that more aberrant tracts were generated and additional AND and NOT ROIs were required to exclude aberrant fibers. Additionally, by extracting particular segments from a white matter tract (by using 2 AND operators), we could measure identical white matter structures and make fair comparisons between patients with sCS and control subjects.

Statistical Analysis

Analyses were carried out using R Studio Version 1.1.442 – © 2009-2018 RStudio, Inc. Parametric statistics were used when the distribution of the data did not violate assumptions of normality. To minimize false positives resulting from multiple tests, multivariate analysis of variance (MANOVA) was used to determine whether patients and controls differed in patterns of λ_1 , λ_2 and λ_3 in the examined tracts. For λ_1 , λ_2 and λ_3 a η^2 was calculated, in which Cohen's guideline for "high" is $\eta^2 > 0.14$ ²². The significant lambda values gave information from which tract FA, or which diffusivity value, could be affected in patients versus controls (see above, *DTI Metrics*).

Subsequent analyses used linear regression in 6 brain regions (corpus callosum [body and genu] and the left and right cingulate bundle [body and hippocampal]) with sCS/control, sex, FOHR and tract volume added to the model as independent variables. β -Coefficients were calculated (stats package) for each regression and a significance level of 0.05 was considered for all tests.

RESULTS

Patient characteristics

Fifty-seven non-operated sCS patients with median [range] age 0.4 [0.27 to 3.16] years included cases with Apert (n =10), Crouzon-Pfeiffer (n =17), Muenke (n = 8), and Saethre-Chotzen (n =11) syndromes, and complex craniosynostosis patients (n = 11). There were 7 control subjects aged 1.39 [0.56 to 2.84] years (**Table 1**).

Eigen values λ_1 , λ_2 and λ_3

Table 2 summarizes the η^2 of λ_1 , λ_2 , λ_3 by white matter tract. Left and right hemispheres show regional asymmetries. The genu and body of the corpus callosum, and the hippocampal and body of the cingulum bundle show a $\eta^2 > 0.14$ in λ_2 and λ_3 . The left corticospinal tract shows a $\eta^2 > 0.14$ for λ_1 .

The summary shape of the tensors of each voxel in a 3D ellipsoid is shown in **Figure 1** with the mean λ_1 , λ_2 , λ_3 of patients and controls for the corpus callosum genu, corpus callosum body and left cingulate bundle. We see the three major, medium and minor axis of the

diffusion displacement. All 3 ellipsoids show any degree of anisotropy, orientation in 3D space. The control group shows smaller ellipsoids in comparison with sCS patients. The corpus callosum shows a more anisotropic ellipsoid than the cingulate bundle, which has a more Gaussian appearance.

Table 1. Patient Characteristics

	Apert	Crouzon-Pfeiffer	Muenke	Saethre-Chotzen	Complex	Total Craniosynostosis	Controls
no. of subjects	10	17	8	11	11	57	7
M/F sex	06:04	08:09	01:07	05:06	02:09	27:30:00	03:04
Mean age (SD)	0.27 (0.10)	1.00 (0.93)	0.37 (0.09)	0.59 (0.36)	0.40 (0.22)	0.59 (0.60)	1.51 (0.72)
Min age	0.049	0.24	0.26	0.027	0.047	0.027	0.56
Max age	0.41	3.16	0.51	1.28	0.92	3.16	2.84

Table 2. Overview of η^2 of MANOVAs λ_1 , λ_2 and λ_3 in patients vs controls

	λ_1	λ_2	λ_3
CST left	0.2	0.05	0.07
CST right	0.13	0.06	0.1
Corpus Callosum Genu	0.12	0.16	0.19
Corpus Callosum body	0.12	0.18	0.21
Corpus Callosum Splenium	0.04	0.09	0.12
MCP	0	0.04	0.03
Fornix Left	0.06	0.05	0.06
Fornix Right	0.12	0.1	0.09
Cingulum Hippocampal left	0.19	0.19	0.16
Cingulum Hippocampal right	0.11	0.15	0.1
Cingulum body left	0.08	0.31	0.17
Cingulum body right	0.04	0.27	0.21

*Cohens guideline: 0.01 = small, 0.06 = medium, > 0.14 = large

Abbreviations: CST – Cortical Spinal tract, MCP – Medular Cerebral Peduncle, λ - lambda

Radial diffusivity analyses

Since the genu and body of the corpus callosum, and the hippocampal and body of the cingulum bundle show a $\eta^2 > 0.14$ in λ_2 and λ_3 , subsequent analyses focused on RD (see **Figure 1**).

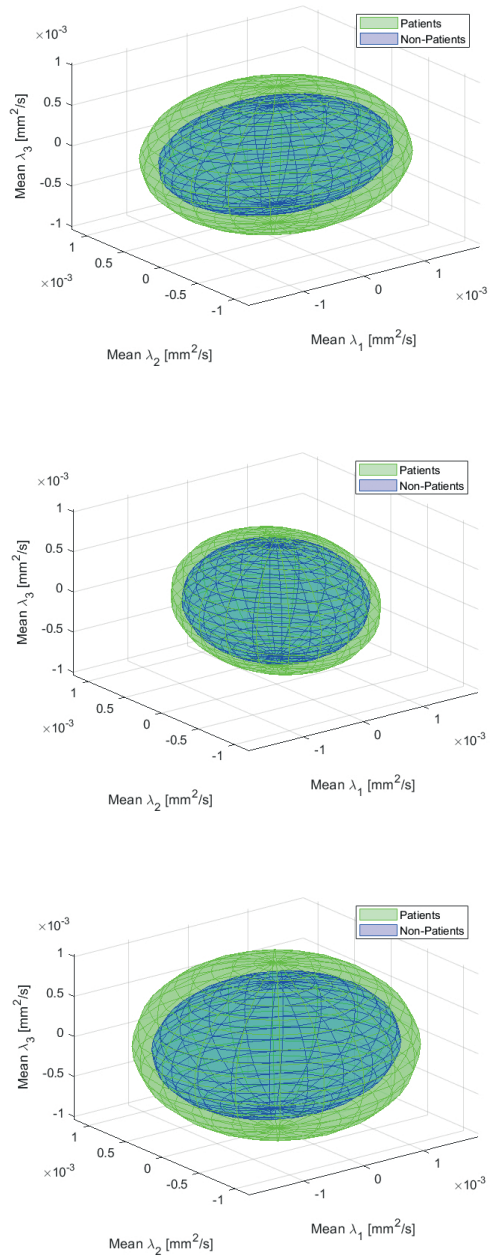


Figure 1 Legend:

Figure 1a. Corpus Callosum Genu

Figure 1b. Corpus Callosum Body

Figure 1c. Cingulate Bundle Body Left

Table 3 shows an increase of $22.80 \times 10^{-5} \text{ mm}^2/\text{sec}$ in RD (95% CI $12.03 \times 10^{-5} \text{ mm}^2/\text{sec} - 33.57 \times 10^{-5} \text{ mm}^2/\text{sec}$, $p = .000$) in the corpus callosum body and an increase of $19.34 \times 10^{-5} \text{ mm}^2/\text{sec}$ in RD (95% CI $8.17 \times 10^{-5} \text{ mm}^2/\text{sec} - 30.51 \times 10^{-5} \text{ mm}^2/\text{sec}$, $p = .001$) in the corpus callosum genu in sCS patients compared to the control group. An 0.1 rise in FOHR gives a rise of $17.22 \times 10^{-5} \text{ mm}^2/\text{sec}$ in RD for the corpus callosum body (95% CI $10.74 \times 10^{-5} - 23.69 \times 10^{-5} \text{ mm}^2/\text{sec}$, $p = .000$) and a rise of $17.91 \times 10^{-5} \text{ mm}^2/\text{sec}$ for the corpus callosum genu (95% CI $12.23 \times 10^{-5} - 23.58 \times 10^{-5} \text{ mm}^2/\text{sec}$, $p = .000$). No gender differences are demonstrated in both tracts of the corpus callosum.

As seen in **Table 3**, the sCS group shows an increase of $12.66 \times 10^{-5} \text{ mm}^2/\text{sec}$ in RD (95% CI $6.03 \times 10^{-5} \text{ mm}^2/\text{sec} - 19.28 \times 10^{-5} \text{ mm}^2/\text{sec}$, $p = .000$) in the body of the cingulate bundle of the left hemisphere and an increase of $10.71 \times 10^{-5} \text{ mm}^2/\text{sec}$ in RD (95% CI $5.19 \times 10^{-5} \text{ mm}^2/\text{sec} - 16.24 \times 10^{-5} \text{ mm}^2/\text{sec}$, $p = .000$) in the body of the cingulate bundle of the right hemisphere, compared to the control group. An increase of FOHR is not significant related to a increase of RD for the body of the cingulate bundle for both hemispheres.

In the hippocampal part of the cingulate bundle there is an increase of $13.35 \times 10^{-5} \text{ mm}^2/\text{sec}$ in RD (95% CI $7.57 \times 10^{-5} - 19.13 \times 10^{-5} \text{ mm}^2/\text{sec}$, $p = .000$) for the left hemisphere and an increase of $10.73 \times 10^{-5} \text{ mm}^2/\text{sec}$ in RD (95% CI $3.52 \times 10^{-5} \text{ mm}^2/\text{sec} - 17.93 \times 10^{-5} \text{ mm}^2/\text{sec}$, $p = .004$) in the right hemisphere, for sCS compared with controls. A leftward asymmetry of RD in the cingulate hippocampal tracts is highlighted in FOHR: per 0.1 rise in FOHR, a significant increase of $7.34 \times 10^{-5} \text{ mm}^2/\text{sec}$ in RD (95% CI $3.93 \times 10^{-5} \text{ mm}^2/\text{sec} - 10.75 \times 10^{-5} \text{ mm}^2/\text{sec}$, $p = .000$) in the left hemisphere and an increase of $3.64 \times 10^{-5} \text{ mm}^2/\text{sec}$ in RD (95% CI $0.37 \times 10^{-5} \text{ mm}^2/\text{sec} - 6.92 \times 10^{-5} \text{ mm}^2/\text{sec}$, $p = .03$) in the right hemisphere is seen. No gender differences were observed.

Table 3. Linear regression on RD with independent variables sCS, gender, tractvolume and FOHR

Corpus Callosum body	Estimate*	SE*	2.5% CI	97.5% CI	P-Value
Intercept	57.68	15.13	27.43	87.93	<.001
Syndromic Craniosynostosis	22.8	5.39	12.03	33.57	<.001
Gender(female)	-0.85	3.92	-8.69	7	.83
Tractvolume in mm3	-0.01	0	-0.01	0	.002
FOHR per 0.10	17.22	3.24	10.74	23.69	<.001
Corpus Callosum Genu					
Intercept	36.52	14.39	7.7	65.34	.01
Syndromic Craniosynostosis	19.34	5.58	8.17	30.51	.001
Gender(female)	-3.28	3.5	-10.28	3.72	.35
Tractvolume in mm3	-0.01	0	-0.01	0	.003
FOHR per 0.10	17.91	2.83	12.23	23.58	<.001
Cingulate Bundle body left					
Intercept	73.91	7.85	58.18	89.63	<.001
Gender(female)	0.51	2.39	-4.28	5.29	.83
Syndromic Craniosynostosis	12.66	3.31	6.03	19.28	<.001
Tractvolume in mm3	-0.01	0	-0.02	0	.02
FOHR per 0.10	1.88	1.92	-1.96	5.72	.33
Cingulum Bundle body right					
Intercept	78.17	7.18	63.76	92.58	<.001
Gender(female)	-0.41	2.08	-4.58	3.77	0.87
Syndromic Craniosynostosis	10.71	2.75	5.19	16.24	<.001
Tractvolume in mm3	-0.02	0	-0.03	-0.01	<.001
FOHR per 0.10	2.22	1.76	-1.32	5.75	.21
Cingulate Bundle Hippocampal left					
Intercept	59.57	6.92	45.73	73.42	<.001
Gender(female)	0.85	2.17	-3.49	5.19	.70
Syndromic Craniosynostosis	13.35	2.89	7.57	19.13	<.001
Tractvolume in mm3	0	0	-0.01	0	.30
FOHR per 0.10	7.34	1.70	3.93	10.75	<.001
Cingulate Bundle Hippocampal right					
Intercept	73.5	6.19	61.1	85.91	<.001
Gender(female)	-0.69	2.48	-5.65	4.27	.78
Syndromic Craniosynostosis	10.73	3.6	3.52	17.93	.004
Tractvolume in mm3	0	0	-0.01	0.01	.42
FOHR per 0.10	3.64	1.64	0.37	6.92	.03

*all values are x 10⁻⁵

Abbreviations: RD: Radial Diffusivity, sCS: syndromic Craniosynostosis, FOHR: Frontal Occipital Horn Ratio

Type of syndrome

By linear regression analyses we observed correlations between an increase in RD and the type of syndrome for the 2 parts of the corpus callosum and the 4 parts of the cingulate bundle (**supplemental Table 1**). Identifying the association between having Apert, Crouzon, Muenke, Saethre-Chotzen or multisuture craniosynostosis and an increase in RD, Apert is the most affected syndrome for increase in RD, with the highest increase of $44.91 \times 10^{-5} \text{ mm}^2/\text{sec}$ in RD in the corpus callosum body (CI 95%, $31.15 \times 10^{-5} \text{ mm}^2/\text{sec} - 58.67 \times 10^{-5} \text{ mm}^2/\text{sec}$), relative to the increase of $17.91 \times 10^{-5} \text{ mm}^2/\text{sec}$ in complex patients and $19.17 \times 10^{-5} \text{ mm}^2/\text{sec}$ in Crouzon patients.

Discussion

In this report of white matter microstructure using DTI in under 4 year olds with non-operated sCS we have focused on significant differences in λ_2 and λ_3 between craniosynostosis and controls in the major white matter tracts. We found that sCS is associated with an increase in RD in parts of the corpus callosum and cingulate bundle. Consistent with previous studies of white matter asymmetry,²³ our results show lateralization in RD values. We failed to detect an effect of sex on RD.

During normal brain development and white matter maturation, FA increases and diffusivity (MD, AD and RD) decreases.^{24,25} Although differences in DTI can demonstrate differences in microstructure, the physics of the measurement is nonspecific and could reflect a variety of mechanisms.²³ As water movement is more restricted perpendicular to myelin membranes than it is parallel to these membranes, it is presumed that RD reflects myelin integrity. Furthermore, RD is determined by axon density and/or diameter of the white matter tract.^{26,27} Higher RD values in sCS patients, as found in the current study, in the corpus callosum and cingulate bundle, could therefore indicate less defined tissue organization, axonal pathology, reduced myelination or myelin damage.^{26, 27} This finding could be related to several mechanisms, including the biological effect of delayed maturation due to the genetic background of sCS, or the mechanical effect of ventriculomegaly.

Biological effect on increased RD

The corpus callosum is an early myelinated region of the brain, undergoing development in weeks 12 to 16 of pregnancy.²⁸ The finding that sCS is associated with increased RD in the corpus callosum could reflect delayed white matter maturation, compared to controls. Our previous study of 7 to 15 years olds with sCS, compared to aged matched controls, also found increased RD values in the corpus callosum and cingulate bundle,¹⁵ which suggests an intrinsic rather than acquired abnormality.

The fibroblast growth factor receptors have a role in myelination of the corpus callosum and cingulate gyrus. Wilke et al showed that in craniofacial development, *FGFR2* and *3* are involved in telencephalon development from which the cingulate bundle and corpus

callosum arises.²⁹ *FGFR-2* promotes oligodendrocyte generation in the developing and adult brain.^{7,8} (Oligodendrocytes are the myelin-forming cells that throughout life have their precursors arising from neural stem cells in the subventricular zone.) Taken together, the *FGFR* mutations could be an intrinsic factor resulting in increased RD values in sCS.

Mechanical effect on increased RD

We also used the current study to examine for any potential association between brain white matter microarchitecture changes and brain distortion^{30,31}. We used a measure of ventriculomegaly and found that in non-operated sCS patients, compared with controls, there was a significant interaction between RD and FOHR in sCS. In this study 0.1 increase in FOHR gives an increase of RD. Hence it remains unknown if this increase of RD is reversible, if this increase of RD has its effect on cognitive outcome and which corresponding FOHR cut-off point will improve the outcome.

Clinical relevance

To date there are no normal ranges of DTI measurements in children under the age of 4 years in literature. DTI is dependent on many technical variables, such as the type of MRI scanner used and the amount of diffusion encoding directions, which makes it extremely difficult to compare absolute DTI values with other DTI studies. With reference to DTI, studies in older children, autism or developmental delay have shown increased MD in the corpus callosum.^{32,33} Also increased diffusivity values within the cingulate bundle are associated with more severe internalizing and externalizing behaviour in children.³⁴ The findings in the current study are of value and relevance to future studies of cognitive development and diffusivity in sCS, particularly in the social and attention problems associated with Apert syndrome.¹

Limitations

This study is not without limitations. Our diffusion protocol may have been overly sensitive. Our use of a 0.1 threshold made it possible to track all structures in the control group and almost all structures in the craniosynostosis group. However, the 0.1 FA threshold meant that more aberrant tracts were generated and additional AND and NOT ROIs were required to exclude aberrant fibers. Though, equal measurements were made between two groups. Also, the sample size was small and, therefore, we may have failed to identify associations when in fact they do exist, and *vice versa*. That said, the current report is the largest DTI study, to date, in non-operated craniosynostosis patients.

CONCLUSION

Before any surgery, young sCS patients aged under 4 years have increased DTI RD values in the corpus callosum and cingulate bundle compared to age matched controls. This difference suggests both biologic causes and mechanical causes, in which there is an interaction between RD and FOHR in sCS.

ACKNOWLEDGEMENTS

We thank Eng. L.H. Boogaart for visualizing Figure 1.

ABBREVIATIONS

AD - Axial Diffusivity
FA - Fractional Anisotropy
FGFR - Fibroblast Growth Factor Receptors
FOHR - Frontal Occipital Horn Ratio
MD - Mean Diffusivity
RD - Radial Diffusivity
sCS - syndromic Craniosynostosis

REFERENCES

1. Maliepaard M, Mathijssen IM, Oosterlaan J, et al. Intellectual, behavioral, and emotional functioning in children with syndromic craniosynostosis. *Pediatrics* 2014;133:e1608-1615
2. Morriss-Kay GM, Wilkie AO. Growth of the normal skull vault and its alteration in craniosynostosis: insights from human genetics and experimental studies. *J Anat* 2005;207:637-653
3. Rijken BF, Lequin MH, Van Veelen ML, et al. The formation of the foramen magnum and its role in developing ventriculomegaly and Chiari I malformation in children with craniosynostosis syndromes. *J Craniomaxillofac Surg* 2015;43:1042-1048
4. Di Rocco C, Frassanito P, Massimi L, et al. Hydrocephalus and Chiari type I malformation. *Childs Nerv Syst* 2011;27:1653-1664
5. Britto JA, Evans RD, Hayward RD, et al. From genotype to phenotype: the differential expression of FGF, *FGFR*, and TGFbeta genes characterizes human cranioskeletal development and reflects clinical presentation in *FGFR* syndromes. *Plast Reconstr Surg* 2001;108:2026-2039; discussion 2040-2026
6. Raybaud C, Di Rocco C. Brain malformation in syndromic craniosynostoses, a primary disorder of white matter: a review. *Childs Nerv Syst* 2007;23:1379-1388
7. Furusho M, Dupree JL, Nave KA, et al. Fibroblast growth factor receptor signaling in oligodendrocytes regulates myelin sheath thickness. *J Neurosci* 2012;32:6631-6641
8. Azim K, Raineteau O, Butt AM. Intraventricular injection of FGF-2 promotes generation of oligodendrocyte-lineage cells in the postnatal and adult forebrain. *Glia* 2012;60:1977-1990
9. Cinalli G, Spennato P, Sainte-Rose C, et al. Chiari malformation in craniosynostosis. *Childs Nerv Syst* 2005;21:889-901
10. Collmann H, Sorensen N, Krauss J. Hydrocephalus in craniosynostosis: a review. *Childs Nerv Syst* 2005;21:902-912
11. Abu-Sittah GS, Jeelani O, Dunaway D, et al. Raised intracranial pressure in Crouzon syndrome: incidence, causes, and management. *J Neurosurg Pediatr* 2016;17:469-475
12. de Jong T, Bannink N, Bredero-Boelhouwer HH, et al. Long-term functional outcome in 167 patients with syndromic craniosynostosis; defining a syndrome-specific risk profile. *J Plast Reconstr Aesthet Surg* 2010;63:1635-1641
13. Tan K, Meiri A, Mowrey WB, et al. Diffusion tensor imaging and ventricle volume quantification in patients with chronic shunt-treated hydrocephalus: a matched case-control study. *J Neurosurg* 2018;129:1611-1622
14. Hattori T, Ito K, Aoki S, et al. White matter alteration in idiopathic normal pressure hydrocephalus: tract-based spatial statistics study. *AJNR Am J Neuroradiol* 2012;33:97-103
15. Rijken BF, Leemans A, Lucas Y, et al. Diffusion Tensor Imaging and Fiber Tractography in Children with Craniosynostosis Syndromes. *AJNR Am J Neuroradiol* 2015;36:1558-1564
16. Tax CM, Otte WM, Viergever MA, et al. REKINDLE: robust extraction of kurtosis INDices with linear estimation. *Magn Reson Med* 2015;73:794-808
17. Veraart J, Sijbers J, Sunaert S, et al. Weighted linear least squares estimation of diffusion MRI parameters: strengths, limitations, and pitfalls. *Neuroimage* 2013;81:335-346
18. Oishi K FA, van Zijl PC, et al. *MRI Atlas of Human White Matter*. Amsterdam: Elsevier; 2010

19. Qiu A, Mori S, Miller MI. Diffusion tensor imaging for understanding brain development in early life. *Annu Rev Psychol* 2015;66:853-876
20. O'Hayon BB, Drake JM, Ossip MG, et al. Frontal and occipital horn ratio: A linear estimate of ventricular size for multiple imaging modalities in pediatric hydrocephalus. *Pediatr Neurosurg* 1998;29:245-249
21. Feldman HM, Yeatman JD, Lee ES, et al. Diffusion tensor imaging: a review for pediatric researchers and clinicians. *J Dev Behav Pediatr* 2010;31:346-356
22. J C. *statistical power analysis for the behavioural sciences*. New York: Lawrence Erlbaum Associates; 1988
23. Dean DC, 3rd, Planalp EM, Wooten W, et al. Mapping White Matter Microstructure in the One Month Human Brain. *Sci Rep* 2017;7:9759
24. Lobel U, Sedlacik J, Gullmar D, et al. Diffusion tensor imaging: the normal evolution of ADC, RA, FA, and eigenvalues studied in multiple anatomical regions of the brain. *Neuroradiology* 2009;51:253-263
25. Yap QJ, Teh I, Fusar-Poli P, et al. Tracking cerebral white matter changes across the lifespan: insights from diffusion tensor imaging studies. *J Neural Transm (Vienna)* 2013;120:1369-1395
26. Song SK, Yoshino J, Le TQ, et al. Demyelination increases radial diffusivity in corpus callosum of mouse brain. *Neuroimage* 2005;26:132-140
27. Tasker RC, Westland AG, White DK, et al. Corpus callosum and inferior forebrain white matter microstructure are related to functional outcome from raised intracranial pressure in child traumatic brain injury. *Dev Neurosci* 2010;32:374-384
28. Dubois J, Dehaene-Lambertz G, Kulikova S, et al. The early development of brain white matter: a review of imaging studies in fetuses, newborns and infants. *Neuroscience* 2014;276:48-71
29. Wilke TA, Gubbels S, Schwartz J, et al. Expression of fibroblast growth factor receptors (*FGFR1*, *FGFR2*, *FGFR3*) in the developing head and face. *Dev Dyn* 1997;210:41-52
30. Mangano FT, Altaye M, McKinstry RC, et al. Diffusion tensor imaging study of pediatric patients with congenital hydrocephalus: 1-year postsurgical outcomes. *J Neurosurg Pediatr* 2016;18:306-319
31. Yuan W, McKinstry RC, Shimony JS, et al. Diffusion tensor imaging properties and neurobehavioral outcomes in children with hydrocephalus. *AJNR Am J Neuroradiol* 2013;34:439-445
32. Alexander AL, Lee JE, Lazar M, et al. Diffusion tensor imaging of the corpus callosum in Autism. *Neuroimage* 2007;34:61-73
33. Kumar A, Sundaram SK, Sivaswamy L, et al. Alterations in frontal lobe tracts and corpus callosum in young children with autism spectrum disorder. *Cereb Cortex* 2010;20:2103-2113
34. Bubb EJ, Metzler-Baddeley C, Aggleton JP. The cingulum bundle: Anatomy, function, and dysfunction. *Neurosci Biobehav Rev* 2018;92:104-127



CHAPTER 7

Sleep apnea in syndromic craniosynostosis occurs independent of hindbrain herniation

C. Driessen

K. F.M. Joosten

J.M.G. Florisson

M.H. Lequin

M.L.C. van Veelen

R. Dammers

H. Bredero-Boelhouwer

R.C. Tasker

I.M.J. Mathijssen

Child's nervous system : ChNS : official journal of the International Society for Pediatric Neurosurgery. 2013;29(2):289-96. Epub 2012/09/26.

ABSTRACT

Purpose: Hindbrain herniation (HH) is frequently found in syndromic craniosynostosis. It may cause impairment of the respiratory centres and manifest as sleep-disordered breathing. Our aim was to quantify sleep apnea caused by HH in children with syndromic craniosynostosis.

Methods: Seventy-one children with syndromic and complex craniosynostosis (aged 0 – 18 years) underwent prospective magnetic resonance imaging and a sleep study. The position of the cerebellar tonsils and respiratory parameters were evaluated and analysed. None of the included patients had undergone previous foramen magnum decompression.

Results: HH was present in 35% of the patients and was more frequent in children with Crouzon syndrome (63%) than in other types of craniosynostosis ($P = .018$). There was a positive association between the position of the cerebellar tonsils and papilledema ($p = .002$). Sleep studies of children with craniosynostosis and HH were not different from those without HH. Obstructive sleep apnea syndrome was not more prevalent in children with HH compared to those without HH ($p = .12$). A cluster analysis using indices of apnea revealed 3 new clusters between which age was significantly different ($p = .025$).

Conclusion: Sleep apnea in syndromic craniosynostosis is not caused by HH. Rather, our evidence suggests that sleep-disordered breathing in craniosynostosis may be caused by brain stem immaturity in young children or upper airway obstruction. Therefore, as long as the child remains asymptomatic, our preferred management of HH is to be conservative and provide regular neurosurgical follow-up.

INTRODUCTION

Hindbrain herniation (HH) is a frequent finding in syndromic and complex craniosynostosis(1, 2) (Figure 1). It is found in up to 72% of cases with Crouzon syndrome(3). In contrast, HH is identified in only a minority (3.6%) of children undergoing MR imaging for other indications(4).

Several theories have been proposed to explain the mechanism by which HH in craniosynostosis develops. Some authors suggest that HH is related to the small size of the posterior fossa, especially after premature closure of the lambdoid sutures. Others suggest that potential causes include anomalies in the cerebellum and brain stem, venous hypertension, increased intracranial pressure (ICP) and hydrocephalus(1, 5).

If hindbrain compression involves the brain stem, cranial nerves and upper spinal cord, then impaired respiratory homeostasis may be evident(6). For example, abnormalities in the rate and depth of breathing, presence of central and obstructive apneas and low arterial hemoglobin-oxygen saturation have all been observed in cases of HH(7-10). In theory, these problems occur during sleep because of the release from voluntary adjusting of autonomic action. However, to date, the limited evidence of sleep-disordered breathing and hypoventilation in children with HH is based on case reports(5, 10, 11) and only one case series(12). The aim of this study is to evaluate whether children with syndromic craniosynostosis and HH suffer from more sleep apnea than patients with syndromic craniosynostosis without HH. If HH induces sleep apnea, it could possibly be used as a physiologic function that matches the abnormal anatomy and clinical significance of HH.



Figure 1: Chiari I Malformation in a 16-year old patient with Crouzon syndrome.

MATERIALS AND METHODS

Study Subjects

This prospective study was undertaken at the Dutch Craniofacial Centre. We included patients with syndromic craniosynostosis; namely Apert, Crouzon, Pfeiffer, Muenke and Saethre Chotzen syndrome. The diagnoses in these children were based on genetic analysis. If none of the above conditions was identified, and at least 2 cranial sutures were involved, patients were considered to have complex craniosynostosis. It is our practice that patients undergo cranial vault surgery before the age of 12 months. We screen for increased ICP by using annual fundoscopy up to the age of 6 years. If papilledema is present or the clinical suspicion of increased ICP arises, we perform invasive ICP monitoring and secondary cranial vault remodelling. This makes persistent increased ICP uncommon.

The local research ethics committee (METC Erasmus MC MEC-2005-273) approved the study. In the period from 01/12/2009 to 01/03/2011, the parents of patients presenting at our outpatient department for routine clinical review were invited to participate in the study. One girl with Apert syndrome was excluded because of previous sub-occipital decompression which potentially influences the course and symptomatology of HH.

Study design

Magnetic Resonance Imaging (MRI)

All participants underwent cranial MRI on a General Electric (GE) 1.5 tesla scanner with Diffusion Tensor Imaging. Measurements on the images were made by hand by a pediatric neuroradiologist (ML) who was blinded to the results of the sleep study. HH was assessed on sagittal T1- and T2-weighted sequences for optimal assessment of the posterior fossa and cranio-cervical junction. We acknowledge the contradictive evidence on the definition of HH. A *Chiari I malformation (CM)* was defined as a descent of the cerebellar tonsils more than 5 mm below the basion-occiput line. If the position of the tonsils was in the grey area of 0 up to 5 mm below the foramen magnum it was referred to as *tonsillar herniation (TH)* (6). Syringomyelia was defined as any spinal cord cavity containing cerebrospinal fluid (CSF). Neurologic examination was performed by the pediatric neurosurgeon (MLvV) if HH was present.

Sleep studies

Overnight sleep respiratory recordings were captured using the Embletta Portable Diagnostic System, and analysed with Somnologica for Embletta software 3.3 ENU (Medcare Flaga, Reykjavik, Iceland). Thoracic and abdominal movements were followed using circumferential impedance elastic trace belts (X act). Nasal airflow was measured with a flow transducer attached to a nasal cannula (Salter Labs, Arvin, USA). Pulse oximetry hemoglobin-oxygen saturation (SpO₂) and heart rate (HR) were recorded using an infant or pediatric sensor (Nellcor, Pleasanton, USA). The overnight recordings were examined

Sleep apnoea in syndromic craniosynostosis occurs independent of hindbrain herniation

independently of the MRI findings. The following summary statistics, abnormalities and sleep data were analysed by visual inspection.

First, we quantified the duration of total sleep time. Total sleep time was calculated starting from the moment of regular respiratory movements during the night up to the change into an irregular signal in the morning. A successful study had a minimum of 360 minutes of traces free from artefact(13). Second, we assessed the nasal flow signals, the abdominal and thoracic impedance signals, and SpO₂ measurements for patterns indicative of various forms of abnormal breathing:

- Apneas were scored if $\geq 80\%$ of flow was reduced. To account for age-related variability in respiratory rate, the minimum length of an event in seconds was equivalent to two breaths(13, 14). Apneas associated with $\geq 4\%$ reduction in SpO₂ from baseline were all included regardless of length.
 - Isolated central apnea was defined as a respiratory pause during which the nasal, abdominal and thoracic airflow ceased.
 - Obstructive apnea was recognized on paradox respiratory trace excursions with absent or reduced nasal airflow.
 - Mixed apnea was identified as an apnea with both central and obstructive components.
- Hypopnea was identified when flow was reduced $\geq 50\%$ in the presence of thoracic and abdominal breathing movement. The minimum length in seconds was equivalent to $\frac{120}{(\text{baseline breathing rate per minute})}$ (15). Hypopneas were only included if a subsequent reduction in SpO₂ of $\geq 4\%$ from baseline occurred.

The summary statistics from the night sleep study included the apnea-hypopnea index (AHI); where the total number of obstructive, central and mixed apneas and pathologic hypopneas, were indexed to the duration of sleep (i.e., episodes per hour of sleep). This statistic is broken down into a central apnea index (CAI) and a combined obstructive apnea and pathologic hypopnea index (oAHI). Central events were also analysed according to periodicity. Periodic breathing was identified when there were consecutive cycles of central irregularity with apneas of at least 2 breaths separated by no more than 20 seconds of normal breathing(16). It was considered significant if it is present in at least 5% of the total sleep time(16). Obstructive sleep apnea syndrome (OSAS) was present when oAHI is greater than 1 per hour. A hemoglobin oxygenation-desaturation index (ODI) was calculated as the number of desaturations ($\geq 4\%$ from baseline) per hour of sleep time.

OSAS is treated if patient have complaints that interfere with growth or development. Treatments will be mentioned, although they do not influence the potential effects of HH on the sleep study outcome.

Statistical analysis

Our data do not conform to a normal distribution and so non-parametric statistics were used. Numerical summaries are presented with median (range). Descriptive statistics (i.e. Pearson chi-square (χ^2)) were used to analyse the distribution of HH for example in the diagnostic groups. Non-parametric tests for continuous variables were used: the Mann Whitney U test to compare the sleep study outcomes between two patients groups and the Kruskal-Wallis analysis of variance to compare sleep study outcomes between multiple patient groups..

The second part of this study includes a Ward's cluster analysis based on the AHI and CAI. Three newly identified clusters will be related to the anatomic level of the cerebellar tonsils, diagnosis and age.

The level of significance was set at a $P < .05$ (2-tailed) in all tests.

RESULTS

Eighty-one patients were invited to participate in the study. The parents of ten children did not consent to study (Figure 2). Seventy-one patients were therefore included in the analyses. Forty-six patients had a normal position of the cerebellar tonsils, 15 (21%) had CM and 10 (14%) had TH (Table 1), i.e. 35% of patients with syndromic or complex craniosynostosis exhibited some form of HH.

Nineteen patients experienced a period during which papilledema was found. In 1 child it was diagnosed before the initial cranial vault remodelling was performed. In 17 patients it developed after previous cranial vault surgery and a secondary cranial vault remodelling was required. Papilledema spontaneously disappeared in 1 child after two abnormal fundoscopies. There was an association between the position of the cerebellar tonsils and presence of papilledema (Pearson χ^2 12.5; 2df; $p = .002$).

Sleep apnoea in syndromic craniosynostosis occurs independent of hindbrain herniation

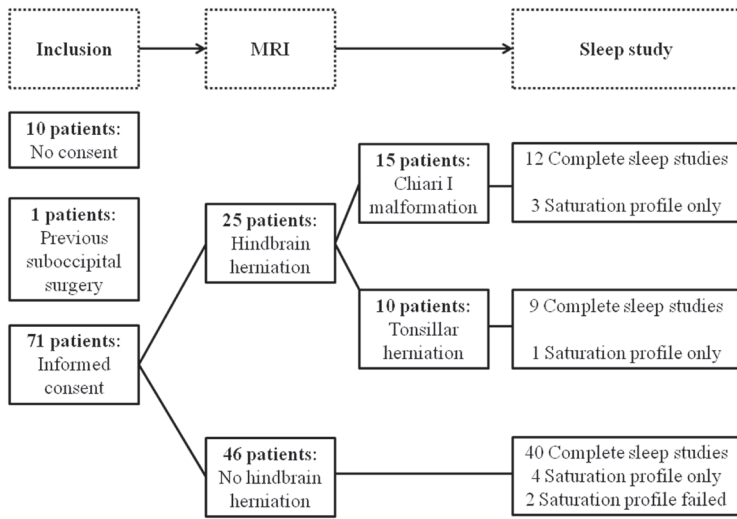


Figure 2: Inclusion chart. In 2 patients in whom no apneas were observed the saturation profile technically failed.

Table 1: Patient characteristics.

	Total	Tonsillar herniation	Chiari I malformation	Normal position of the tonsils
	71	10	15	46
Diagnosis (N)	13	2	2	9
- Apert	26	5	11	10
- Crouzon/ Pfeiffer	10	-	1	9
- Muenke	10	-	-	10
- Saethre-Chotzen	12	3	1	8
- Complex				
Male (N) : Female (N)	37 : 34	3 : 7	8 : 7	26 : 20
VP drain (N)	5	-	5	-
Age at MRI in yrs	9	9	9	9
	(0 - 19)	(3 - 18)	(2 - 19)	(0 - 14)
Age at sleep study in yrs	8	9	9	8
	(0 - 19)	(3 - 18)	(3 - 19)	(0 - 14)
Skull remodelling before MRI (N)	60	10	13	37
OSAS (N (%))	16 (25%)	3 (33%)	2 (17%)	11 (26%)
OSAS treatment (N)	1 CPAP 10 A(T)E 9 facial advancement	0 CPAP 3 A(T)E 3 facial advancement	1 CPAP 5 A(T)E 4 facial advancement	0 CPAP 2 A(T)E 2 facial Advancement

Data presented as median (range). Where: VP drain is ventriculoperitoneal drain; OSAS is obstructive sleep apnea syndrome ($\text{oAHI} > 1$); CPAP is continuous positive airway pressure; A(T)E is adenoidal-(tonsillar)-ectomy; and facial advancements include LeFort I, LeFort III, monobloc and median faciotomy.

Hindbrain herniation

Sixty of 71 (85%) cases underwent cranial vault surgery before MRI. Eleven did not: 3 because of late diagnosis of craniosynostosis; 2 because the syndrome was genetically confirmed without craniosynostosis or signs of increased ICP, 2 because they were first followed up elsewhere; and 4 were not yet operated on because they were too young at the time of study. Neurologic signs were absent in all but one patient with CM. This nineteen-year-old Apert girl presented with a slight asymmetric pharyngeal arch, some hypertonia in both legs, knee tendon reflex 2/2; biceps tendon reflex 0/-1; triceps tendon reflex 0/0 but no Babinski (although difficult to interpret in children with Apert because of deformity of the feet); her sleep study was normal.

HH was more prevalent in Crouzon than in the other diagnoses (χ^2 18.51; 8df; $p = .018$). Three patients with CM had a syrinx: in 1 case it was at the cervical vertebral level C4, in another case it was from C1 down to C7, and in the third case it started at C3 and continued up to the cone. Five patients with CM had a ventriculoperitoneal (VP) drain for the treatment of hydrocephalus.

Sleep apnea in hindbrain herniation

Sixty-one out of 71 sleep studies were complete. In the other 10 cases (3 CM, 1 TH, 6 without HH) only partial results could be used because of technical failure in the recording. The median sleep time was 9.5 hours (6 - 13.5) (Table 2).

There was no significant difference in the CAI ($U = 196.5$, $p = .25$) in children with Chiari I malformation and children without hindbrain herniation. The indices are plotted in Figure 3. Other sleep study parameters were comparable too (AHI $U = 224.5$, $p = .34$; oAHI $U = 236$, $p = .74$; ODI $U = 322$, $p = .89$; mean SpO₂ $U = 266.5$, $p = .27$) (Table 2 *). Similarly, there was no difference in the sleep study outcomes when comparing children with CM to children with TH (Table 2 **) nor when comparing the children with CM, TH and a normal cerebellar tonsils level.

Post-hoc analyses were performed in patients with Crouzon syndrome, who happened to have the highest prevalence of HH (63%). Children with Crouzon syndrome with HH did not exhibit different sleep study outcomes when compared with those without HH (AHI ($U = 53.5$, $p = .56$), CAI ($U = 50.5$, $p = .60$), oAHI ($U = 52.5$, $p = .70$), ODI ($U = 70$, $p = .62$), mean SpO₂ ($U = 70$, $p = .62$)).

The patient with the highest CAI in the group with HH (AHI 6.1; CAI 5.6; oAHI 0.5; ODI 4.7; mean SpO₂ 91.7%) had multiple non-periodic central apneas. This patient (complex craniosynostosis, 11 years old) with TH did not reveal additional signs of cerebellar or brain stem pathology during neurologic examination and is followed up annually by our paediatric neurosurgeon.

Table 2: Sleep study outcomes in patients with and without tonsillar herniation and Chiari I Malformation.

Diagnosis	N	AHI	CAI	oAHI	ODI ≥4%	Meansat	
Normal tonsillar position	46	2.0 (0.0-25.6)	1.2 (0.0-11.5)	0.4 (0.0-14.5)	0.3 (0.0-14.4)	97.9% (92.2-99.1)	} } * ** *** Ns
Chiari I	15	1.6 (0.0-5.6)	0.9 (0.0-3.9)	0.2 (0.0-5.0)	0.2 (0.0-30.6)	97.8% (91.3-99.1)	
Tonsillar herniation	10	1.2 (0.0-6.1)	0.8 (0.0-5.6)	0.4 (0.0-3.1)	1.0 (0.0-11.9)	97.3% (91.7-98.4)	

Presented as median (range). Ns = not significantly different

ODI ≥4% = oxygen desaturation index ≥4%

AHI = apnea hypopnea index

CAI = central apnea index

oAHI = obstructive apnea hypopnea index

Sat = saturation

* *CM vs Normal tonsillar position:* AHI U = 224.5, p = .34; CAI U = 196.5, p = .25; oAHI U = 236, p = .74; ODI U = 322, p = .89; mean SpO2 U = 266.5, p = .27

** *CM vs TH:* AHI U = 58, p >.99; CAI U = 49.5, p = .75; oAHI U = 53, p = .97; ODI U = 63, p = .53; mean SpO2 U = 67, p = .68

*** *CM vs TH vs Normal tonsillar position:* AHI χ^2 1.11, 2df; p = .58; CAI χ^2 1.74, 2df; p = .42; oAHI χ^2 0.11, 2df; p = .95; ODI χ^2 1.64, 2df; p = .44; mean SpO2 χ^2 1.66, 2df; p = .44

Periodic breathing was present in 2 patients. It was recorded in a newborn with complex craniosynostosis in 4% of the registered time (CAI 11.5) and in another newborn with Apert syndrome in 5% of the registered time (CAI 8.5), both without HH.

At the time of study, 17 patients (24%; 4 Apert patients, 9 Crouzon patients, 1 Muenke patient, 1 Saethre-Chotzen patient and 2 patients with complex craniosynostosis) had been treated for OSAS (Table 1). Nonetheless, 8/17 patients still had OSAS, and overall the incidence of obstructive sleep apnea was 27%. OSAS was not more common in patients with HH compared with patients without HH (χ^2 7.23; 4df; p = .12). In one multi-developmentally-impaired girl with Crouzon syndrome (ODI 30.6, Table 2), no treatment was started at the parents' request.

Cluster analysis

Ward's cluster analysis was carried out using the AHI and CAI outcomes. The three clusters that were found were composed of 64 cases (cluster 1), 5 cases (cluster 2) and the 2 outlying cases (cluster 3) (Figure 4). Neither of the 2 patients of cluster 3 had HH. In cluster 2, 1 patient had TH and 1 patient had CM. The median AHI was 1.5 (0.0 - 5.6) for cluster 1; 6.1 (3.8 - 7.6) for cluster 2 and 20.0 (14.4 - 15.6) for cluster 3. The median CAI was 1.0 (0.0 - 2.6) for cluster 1; 3.8 (3.2 - 5.6) for cluster 2 and 10.0 (8.5 - 11.5) for cluster 3. Syndromic diagnoses were equally distributed (χ^2 6.44; 8df; p = .60). The median age was 8 years (0 - 19) for cluster 1; 5 years (0 - 10) for cluster 2 and 4 months (3 - 5) for cluster 3, which was significantly different (χ^2 7.34; 2df; p = .025). Correlation of the CAI with age in the total cohort was significant (Spearman's rho -0.34; p = .006) (Figure 3).

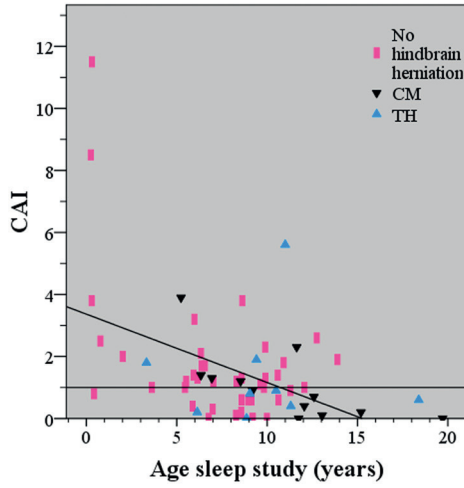


Figure 3: Scatterplot of CAI outcomes for patients with Chiari I Malformation, tonsillar herniation and a normal position of the cerebral tonsils. Black horizontal line at CAI = 1 shows the threshold for normality. Correlation of the CAI with age in the total cohort was significant (Spearman’s rho -0.34; p = .006).

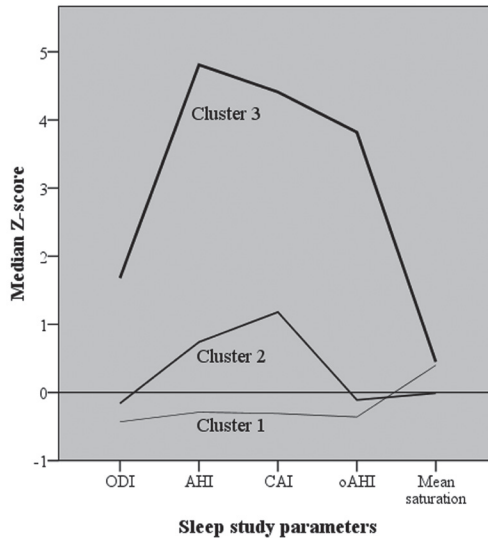


Figure 4: Clusters based on AHI and CAI within a cohort of craniosynostosis patients with and without hindbrain herniation. Ward’s analysis revealed three new clusters of 64 (cluster 1), 5 (cluster 2) and 2 (cluster 3) patients. All respiratory parameters except for mean saturation, were significantly different among these clusters (AHI χ^2 17.97; 2df; p < .001, CAI χ^2 18.49; 2df; p < .001, oAHI χ^2 8.13; 2df; p = .017, ODI χ^2 8.17; 2df; p = .017, mean saturation χ^2 0.52; 2df; p = .77). Median Z score for the CAI was -0.3 for cluster 1, 1.2 for cluster 2 and 4.4 for cluster 3, meaning that only cluster 3 lies above the 99 percentile of this cohort.

DISCUSSION

Chiari I malformation and tonsillar herniation is highly prevalent in children with syndromic and complex craniosynostosis. The overall prevalence is 35%, with a maximum of 63% in Crouzon and Pfeiffer patients. In our population, there were no differences in the sleep study parameters when comparing patients with syndromic craniosynostosis with and without hindbrain herniation. Since radiological criteria for diagnosing HH in MRI vary, as reported by Bejjani et al(17), it is important to emphasize that there were no differences in sleep apnea either if we excluded the cases with low grade TH (i.e. <5mm). Our observation is consistent with a case series by Gonzalez et al, that reported 13 patients with syndromic craniosynostosis and HH without any central apneas(12).

Our results are of great clinical relevance. At present, some craniofacial teams consider a decompression of the foramen magnum to be indicated as soon as HH is diagnosed. Our results show that sleep apnea is not more prevalent in patients with syndromic craniosynostosis and HH, meaning that sleep disordered breathing occurs independently of HH. Even other neurological symptoms were only present in one of the children. Routine surgical decompression appears to be overtreatment. However, few case reports have indeed demonstrated that hindbrain herniation may eventually result in neurological symptoms (e.g. cerebellar pathology) or sleep apnea, which emphasizes the importance of thorough clinical follow up.

Some specialists consider that in a child with symptomatic Chiari 0 malformation, a crowded posterior fossa may result in impaired CSF flow and syringomyelia even without descent of the tonsils(18). We computed three clusters by combining the AHI and CAI outcomes. In the two clusters in which the CAI was greater than 1, none of the patients had syringomyelia and only 2 had HH. The CAI was pathologically increased (>5) in the two very young patients in cluster 3, independent of HH. Given the significant decrease in CAI with increasing age we conclude that, in our population, age is the most important contributor to the CAI, as seen by others(14).

Systematic polysomnographic studies in pediatric neurosurgical patients without craniosynostosis show that CM leads to sleep fragmentation, a reduction in rapid eye movement sleep and a pathologic increase in both the CAI and oAHI. Typically, such patients have myelomeningocele, which is commonly associated with severe Chiari type II malformation. Twenty percent of a Canadian cohort of myelomeningocele patients suffered from moderate or severe sleep apnea (AHI >5), which predominantly consisted of central apneas in 71% and obstructive apneas in 29%.

Although HH most commonly leads to periodic breathing and central apneas(19), it may also be associated with obstructive apneas due to injury of the cranial nerves or syringomyelia. This might paralyse the vocal cords(20,21) or impair the afferent nerves

Chapter 7

of the tongue(22). It is hard to differentiate between obstructive apneas due to HH and those caused by the diversity of upper airway restrictions related to the craniofacial abnormality. We found that obstructive apneas and pathologic hypopneas were not more prevalent in children with HH. Since there was no increase in central apneas either, it is unlikely that the observed obstructive apneas were caused by HH-induced cranial or peripheral nerve neuropathology.

The big disparity in sleep study outcomes, also in our cohort without HH, illustrates that sleep disordered breathing in craniosynostosis is widely variable and probably multifactorial. Most notorious is the obstructive sleep apnea in patients with Crouzon and Pfeiffer syndrome(23) who also have the highest prevalence of HH. Although 16 patients in our series had undergone airway-treatment, the overall incidence of OSAS still was 27%. Long-lasting severe OSAS may increase ICP(24) and it is presumed that persistent increased ICP may result in HH(2). Our routine cranial vault remodelling in the first year of life, as well as secondary cranial vault expansion in case of increased ICP and OSAS-treatment if necessary may decrease the eventual prevalence of (symptomatic) HH. Future research should focus at the sequence of occurrence of increased ICP and HH. In our opinion, the question remains as to whether the deformity of HH is a primary causal abnormality or secondary finding. If it gradually occurs after birth, it is possible that secondary progression of HH might allow a certain degree of compression of the brain stem, cranial nerves and upper spinal cord without influencing physiology. An altered shape of the foramen magnum could be a second explanation.

CONCLUSIONS

Hindbrain herniation does not cause sleep apnea in patients with syndromic craniosynostosis of whom the majority underwent cranial vault remodelling and OSAS-treatment if necessary. Therefore, as long as the child remains asymptomatic, our preferred management of HH is to be conservative and provide regular neurosurgical follow-up. In keeping with other studies(12), we advocate the use of screening sleep studies to follow up on central irregularity and to diagnose obstructive sleep apnea.

REFERENCES

1. Cinalli G, Sainte-Rose C, Kollar EM, Zerah M, Brunelle F, Chumas P, et al. Hydrocephalus and craniosynostosis. *J Neurosurg.* 1998;88(2):209-14. Epub 1998/02/06.
2. Cinalli G, Spennato P, Sainte-Rose C, Arnaud E, Aliberti F, Brunelle F, et al. Chiari malformation in craniosynostosis. *Childs Nerv Syst.* 2005;21(10):889-901. Epub 2005/05/06.
3. Cinalli G, Renier D, Sebag G, Sainte-Rose C, Arnaud E, Pierre-Kahn A. Chronic tonsillar herniation in Crouzon's and Apert's syndromes: the role of premature synostosis of the lambdoid suture. *J Neurosurg.* 1995;83(4):575-82. Epub 1995/10/01.
4. Strahle J, Muraszko KM, Kapurch J, Bapuraj JR, Garton HJ, Maher CO. Chiari malformation Type I and syrinx in children undergoing magnetic resonance imaging. *J Neurosurg Pediatr.* 2011;8(2):205-13. Epub 2011/08/03.
5. Frim DM, Jones D, Goumnerova L. Development of symptomatic Chiari malformation in a child with craniofacial dysmorphism. *Pediatr Neurosurg.* 1990;16(4-5):228-31. Epub 1990/01/01.
6. Tubbs RS, Lyerly MJ, Loukas M, Shoja MM, Oakes WJ. The pediatric Chiari I malformation: a review. *Childs Nerv Syst.* 2007;23(11):1239-50. Epub 2007/07/20.
7. Botelho RV, Bittencourt LR, Rotta JM, Tufik S. A prospective controlled study of sleep respiratory events in patients with craniovertebral junction malformation. *J Neurosurg.* 2003;99(6):1004-9. Epub 2004/01/07.
8. Botelho RV, Bittencourt LR, Rotta JM, Tufik S. The effects of posterior fossa decompressive surgery in adult patients with Chiari malformation and sleep apnea. *J Neurosurg.* 2010;112(4):800-7. Epub 2009/08/12.
9. Henriques-Filho PS, Pratesi R. Sleep apnea and REM sleep behavior disorder in patients with Chiari malformations. *Arq Neuropsiquiatr.* 2008;66(2B):344-9. Epub 2008/07/22.
10. Venes JL. Arnold-Chiari malformation in an infant with Kleeblattschadel: an acquired malformation? *Neurosurgery.* 1988;23(3):360-2. Epub 1988/09/01.
11. Sandberg DI, Navarro R, Blanch J, Ragheb J. Anomalous venous drainage preventing safe posterior fossa decompression in patients with chiari malformation type I and multisutural craniosynostosis. Report of two cases and review of the literature. *J Neurosurg.* 2007;106(6 Suppl):490-4. Epub 2007/06/15.
12. Gonzalez SL, Thompson D, Hayward R, Lane R. Breathing patterns in children with craniofacial dysostosis and hindbrain herniation. *Eur Respir J.* 1998;11(4):866-72. Epub 1998/06/12.
13. Ward SL, Marcus CL. Obstructive sleep apnea in infants and young children. *J Clin Neurophysiol.* 1996;13(3):198-207. Epub 1996/05/01.
14. Guilleminault C. *Sleep and Its Disorders in Children.* New York: Raven Press; 1987.
15. Guilleminault C, Lee JH, Chan A. Pediatric obstructive sleep apnea syndrome. *Arch Pediatr Adolesc Med.* 2005;159(8):775-85. Epub 2005/08/03.
16. Iber C, Ancoli-Israel S, Chesson AL, Quan SF. *The AASM manual for the scoring of sleep and associated events: rules, terminology, and technical specifications.* Westchester, IL: 2007.
17. Bejjani GK. Definition of the adult Chiari malformation: a brief historical overview. *Neurosurg Focus.* 2001;11(1):E1. Epub 2006/05/27.

Chapter 7

18. Chern JJ, Gordon AJ, Mortazavi MM, Tubbs RS, Oakes WJ. Pediatric Chiari malformation Type 0: a 12-year institutional experience. *J Neurosurg Pediatr.* 2011;8(1):1-5. Epub 2011/07/05.
19. Petersen MC, Wolraich M, Sherbondy A, Wagener J. Abnormalities in control of ventilation in newborn infants with myelomeningocele. *J Pediatr.* 1995;126(6):1011-5. Epub 1995/06/01.
20. Kirsch WM, Duncan BR, Black FO, Stears JC. Laryngeal palsy in association with myelomeningocele, hydrocephalus, and the arnold-chiari malformation. *J Neurosurg.* 1968;28(3):207-14. Epub 1968/03/01.
21. Sieben RL, Hamida MB, Shulman K. Multiple cranial nerve deficits associated with the Arnold-Chiari malformation. *Neurology.* 1971;21(7):673-81. Epub 1971/07/01.
22. Bokinsky GE, Hudson LD, Weil JV. Impaired peripheral chemosensitivity and acute respiratory failure in Arnold-Chiari malformation and syringomyelia. *N Engl J Med.* 1973;288(18):947-8. Epub 1973/05/03.
23. Lowe LH, Booth TN, Joglar JM, Rollins NK. Midface anomalies in children. *Radiographics.* 2000;20(4):907-22; quiz 1106-7, 12. Epub 2000/07/21.
24. Hayward R, Gonzalez S. How low can you go? Intracranial pressure, cerebral perfusion pressure, and respiratory obstruction in children with complex craniosynostosis. *J Neurosurg.* 2005;102(1 Suppl):16-22. Epub 2005/10/07.

Sleep apnoea in syndromic craniosynostosis occurs independent of hindbrain herniation

7 



CHAPTER 8

Discussion

This thesis was primarily designed to study the pathophysiology of syndromic craniosynostosis. Patients with syndromic craniosynostosis suffer from skull and brain abnormalities. Intracranial hypertension is one of the main problems and the most important reason to operate. Nowadays the different causes of intracranial hypertension are still controversial.

This thesis provides an overview of craniosynostosis syndromes and describes the genetic background. The second autosomal dominant mutation in *MSX2* is described with the related phenotype. A new microdeletion syndrome is reported which is associated with complex craniosynostosis. Detection of both copynumber variations and Next generation sequencing based variant analysis will contribute to more accurate diagnostic classification of future craniosynostosis patients.

Concerning intracranial hypertension associated factors, this thesis has shown a significantly smaller diameter of the jugular foramen in syndromic craniosynostosis patients. Jugular foraminal narrowing and an abnormal venous system can be seen in syndromic craniosynostosis patients and may predispose to elevated intracranial pressure.

At the end of this thesis we show diffusion tensor imaging (DTI) of white matter tracts in our patient group. DTI tractography is challenging to perform in patient with craniosynostosis syndromes because of their abnormal shape of the head and different ventricular size and shape. We found differences in the diffusivity parameters which may suggest abnormal microstructural tissue properties of the different white matter tracts.

In summary, the pathophysiology of syndromic craniosynostosis is complex and still poorly understood. This thesis brings us further in unravelling the complexity of intracranial hypertension.

INTERPRETATION OF RESULTS

MSX2 is the first mutation described as a cause of craniosynostosis in 1993 (1). Moving forward at least 57 genes are indentified in syndromic craniosynostosis nowadays (2). In clinical practice, patients with syndromic craniosynostosis will be tested for mutations in *FGFR2*, *FGFR3* and *TWIST1* which are the genes with the most frequently occurring mutations. This thesis describes a Boston type craniosynostosis in a Dutch family who has a rare mutation with a very variable expression. Jabs et al. and Warman et al. describe the first family with a newly recognized form of autosomal dominant craniosynostosis. The family has a highly variable phenotype. Controversially this is the first craniosynostosis gene described but never found afterwards. The family that we present is the second family with a mutation in the *MSX2* gene and also shows variable clinical presentation. Still, we observe striking phenotypic similarities in these families. Frontal bossing and

Chapter 8

turricephaly are shown in the most severely affected patients. Gross limb abnormalities were not in these families. We have seen brachydactyly in three out of seven patients and may be part of the variable *MSX2* Boston type craniosynostosis.

The ancestral origin from these two families is different; the previous described family is from the United Kingdom, while our family is from Bosnian origin. Interestingly, the affected amino acid in *MSX2* in the Bosnian family (P148L) is at exact the same position as in the Boston family (P148H) and likely causing a similar and specific gain of function through increased or altered binding of the *MSX2* protein to DNA] (3). Given the rarity of this gain of function mutation it is likely that gain of function is only possible through a very limited mutations repertoire within the DNA-binding homeodomain. Most *MSX2* mutations described are loss of function mutations and the haploinsufficiency phenotype is different, causing parietal foramina [OMIM:168500] (4-8)

In our database of the Dutch craniofacial center we searched for patients with a complex form of craniosynostosis. These patients suspected to have a syndromic form of craniosynostosis, did not have any *FGFR1*, *FGFR2*, *FGFR3*, or *TWIST* mutations or deletions. SNP array analysis was used for these patients. We did find overlapping deletions in both patients in the 2p15p16.1 region. Deletions in the 2p15p16.1 region can lead to microcephaly, intellectual disability and additionally to craniosynostosis. This is an area which is recognized as a new microdeletion syndrome, and our patients had craniosynostosis as a clinical characteristic to this microdeletion syndrome.

MSX2 gene mutation occurs rarely and is clinically difficult to recognize in individual patients due to phenotypic variation.

Nowadays, genetic research is recommended to be done in craniosynostosis specialized centra to prevent unnecessary diagnostics. Genetic research is only done in patients with a confirmed diagnosis of craniosynostosis. In patients with an obvious phenotype targeted genetic testing should be performed to be more cost effective in healthcare. When there isn't a recognizable phenotype Next Generation Sequencing of the craniosynostosis panel genes is recommended, including genetic testing of the parents (trio-analysis) on indication. (9-18)

In the following years we focused at intracranial hypertension. Intracranial hypertension can be caused by craniocerebral disproportion, obstructive sleep apnea, tonsillar herniation, hydrocephalus and cerebral venous anomalies. These venous anomalies have been described in earlier research, and a reduced diameter of the jugular foramen is mentioned as one of the possible causes.(19, 20) In our study we show that in syndromic craniosynostosis having a narrow jugular foramen is common, irrespective of the presence of papilledema. (21) So this aberrant anatomy of the jugular foramen can be either the initial defect and thus impairing outflow which stimulated the development of venous collaterals, or it can

be the result of an hypoplastic or absent jugular vein; in both cases the underlying genetic change appears to be the causative. Our study shows presence of venous collaterals already in very young patients, independent of the development of high intracranial pressure. This suggests that the venous collaterals are persistent vessels from early embryonic development that remain patent because cerebral outflow partially depends on it.

De Goederen et al. measured the total cerebral venous volume in craniosynostosis patients. (22) They showed that intracranial hypertension is related to an increased straight sinus volume, but an unchanged total cerebral venous volume. We assume there is a venous blood volume redistribution in these patients. This additional outflow through occipital collaterals appear to contribute to the regulation of the intracranial pressure. Intracranial hypertension will not happen as long as this additional outflow is sufficient.

Additional imaging of the brain was done using diffusion tensor imaging (DTI) to study architectural alterations in the white matter of patients with syndromic craniosynostosis. DTI measurements of white matter tracts reveal significant white matter integrity differences between children with craniosynostosis and healthy controls. This could imply the presence of a primary disorder of the white matter micro-architecture causing the developmental delays seen in these patients. We generally found lower FA values in all white matter structures for patients compared to controls, decreased diffusion anisotropy, meaning lower FA value, is not unique for our study population but commonly observed concurrent with CNS pathology. (23-27) Also our FA value results suggest the presence of changes in white matter microstructural integrity in specific white matter regions in children diagnosed with syndromic or complex craniosynostosis. This seems to be in agreement with previously published data on white matter alterations, like thin corpus callosum, and septal anomalies, visible on conventional MRI scans.(28-33)

The correlation between primary disorder of the white matter micro-architecture and developmental delays seen in these patients still needs to be proven.

In a DTI study in the unoperated craniosynostosis patients lower FA and higher diffusivity parameters were found in syndromic craniosynostosis patients compared to control subjects, indicating deficits in the white matter axonal organization and disturbances in the myelination. Since this is true for young unoperated patients, it is likely that secondary factors, such as intracranial hypertension and surgery have less influence. It is more likely that these disturbances are caused by an intrinsic factor, such as altered brain perfusion or the genetic mutation itself. Future studies are already started to investigate the relation between local brain perfusion and white matter organization in the same region. Doerga et al published arterial spin labeling research which shows that young untreated craniosynostosis patients have a lower cerebral blood flow compared to control patients. (34) When patients get older and have had their vault expansion cerebral blood flow normalizes, but what the main driver of this improvement is, remains unclear.

Up to 63% of the syndromic craniosynostosis patients may suffer from hindbrain herniation. We show that sleep apnea is not more prevalent in patients with syndromic craniosynostosis and hindbrain herniation, meaning that sleep disordered breathing occurs independently of hindbrain herniation. We show a significant decrease in central apnea index with increasing age. Age is the most important contributor in central apnea index. We can agree with others that a young age is the most important contributor to central sleep apnea in syndromic craniosynostosis patients. (35)

Long lasting severe OSAS may increase intracranial pressure and it is presumed that persistent increased intracranial pressure may result in hindbrain herniation. We advocate screening with sleep studies to follow up on central irregularity and to diagnose obstructive sleep apnea. In syndromic craniosynostosis patients who develop central apnea, a cervical MRI and neurological physical follow up should evaluate tonsillar herniation or a syrinx. (36, 37). Doerga presents that neurological symptoms provides no diagnostic certainty in ruling in or ruling out normal cerebellar tonsillar position. This is confirming the theory that the often encountered neurological symptoms occur independent of tonsillar herniation or syrinx and appear to reflect abnormalities of the central nervous system in syndromic craniosynostosis. A neurological follow up is recommended and should last until adulthood, as a deterioration of neurological symptoms can be a warning sign of progression of tonsillar herniation or syrinx.

FUTURE PERSPECTIVES

There are still many syndromic craniosynostosis patients without a confirmed genetic diagnose. Whole Exome Sequencing of the patients and the parents could display more genetic mutations in these patients. This genetic mutations could give us more insight in the details of the syndrome and help us to understand the consequences of having syndromic craniosynostosis and guide screening and treatment. Because of the small patient numbers available, craniosynostosis teams worldwide should invest in a multicentre prospective study to unravel genetics.

Further research should focus on dynamic studies of regional cerebral blood flow and venous flow in order to explore venous blood volume distribution. Transcranial Doppler sonography in pre and post operative craniosynostosis patients should learn us more of venous hypertension. Tasker opens a possibility for rational, point of care treatment decisions in pediatric patients with suspected raised ICP undergoing intensive care (38). The first non-invasive intracranial pressure estimation is done by an algorithm, based on arterial blood pressure and bedside trans cranial doppler and cerebral blood flow velocity waveform measurements.

We reported the largest DTI study in craniosynostosis patients. A new large multicentre study in craniosynostosis patients could verify the impact of genetic disorder in the brain

of these patients. Auto generated analysis could make it more time efficient and more reproducible for other study groups. Ultimately, in new innovative research, we need the neuropsychological data of all children to reliably associate it with the DTI results and establish a predictive value of neuropsychological development.

REFERENCES

1. Jabs EW, Muller U, Li X, Ma L, Luo W, Haworth IS, et al. A mutation in the homeodomain of the human *MSX2* gene in a family affected with autosomal dominant craniosynostosis. *Cell*. 1993;75(3):443-50. Epub 1993/11/05.
2. Twigg SR, Wilkie AO. A Genetic-Pathophysiological Framework for Craniosynostosis. *Am J Hum Genet*. 2015;97(3):359-77. Epub 2015/09/05.
3. Ma L, Golden S, Wu L, Maxson R. The molecular basis of Boston-type craniosynostosis: the Pro148-->His mutation in the N-terminal arm of the *MSX2* homeodomain stabilizes DNA binding without altering nucleotide sequence preferences. *Hum Mol Genet*. 1996;5(12):1915-20.
4. Wilkie AO. Epidemiology and genetics of craniosynostosis. *Am J Med Genet*. 2000;90(1):82-4. Epub 1999/12/22.
5. Wuyts W, Reardon W, Preis S, Homfray T, Rasore-Quartino A, Christians H, et al. Identification of mutations in the *MSX2* homeobox gene in families affected with foramina parietalia permagna. *Hum Mol Genet*. 2000;9(8):1251-5. Epub 2000/04/18.
6. Garcia-Minaur S, Mavrogiannis LA, Rannan-Eliya SV, Hendry MA, Liston WA, Porteous ME, et al. Parietal foramina with cleidocranial dysplasia is caused by mutation in *MSX2*. *Eur J Hum Genet*. 2003;11(11):892-5. Epub 2003/10/23.
7. Spruijt B, Rijken BF, Joosten KF, Bredero-Boelhouwer HH, Pullens B, Lequin MH, et al. Atypical presentation of a newborn with Apert syndrome. *Childs Nerv Syst*. 2015;31(3):481-6. Epub 2014/12/01.
8. Mavrogiannis LA, Taylor IB, Davies SJ, Ramos FJ, Olivares JL, Wilkie AO. Enlarged parietal foramina caused by mutations in the homeobox genes *ALX4* and *MSX2*: from genotype to phenotype. *Eur J Hum Genet*. 2006;14(2):151-8. Epub 2005/12/02.
9. Agochukwu NB, Solomon BD, Muenke M. Impact of genetics on the diagnosis and clinical management of syndromic craniosynostoses. *Childs Nerv Syst*. 2012;28(9):1447-63. Epub 2012/08/09.
10. Mathijssen IM. Guideline for Care of Patients With the Diagnoses of Craniosynostosis: Working Group on Craniosynostosis. *J Craniofac Surg*. 2015;26(6):1735-807. Epub 2015/09/12.
11. Azimi C, Kennedy SJ, Chitayat D, Chakraborty P, Clarke JT, Forrest C, et al. Clinical and genetic aspects of trigonocephaly: a study of 25 cases. *Am J Med Genet A*. 2003;117A(2):127-35. Epub 2003/02/05.
12. Clarke CM, Fok VT, Gustafson JA, Smyth MD, Timms AE, Frazar CD, et al. Single suture craniosynostosis: Identification of rare variants in genes associated with syndromic forms. *Am J Med Genet A*. 2018 Feb;176(2):290-300. *Am J Med Genet A*. 2018;176(11):2522. Epub 2018/12/12.
13. Ittleman BR, McKissick J, Bosanko KA, Ocal E, Golinko M, Zarate YA. Less common underlying genetic diagnoses found in a cohort of 139 individuals surgically corrected for craniosynostosis. *Am J Med Genet A*. 2018;176(2):487-91. Epub 2017/11/22.
14. Johnson D, Wilkie AO. Craniosynostosis. *Eur J Hum Genet*. 2011;19(4):369-76. Epub 2011/01/21.
15. Miller KA, Twigg SR, McGowan SJ, Phipps JM, Fenwick AL, Johnson D, et al. Diagnostic value of exome and whole genome sequencing in craniosynostosis. *J Med Genet*. 2017;54(4):260-8. Epub 2016/11/26.

16. Timberlake AT, Choi J, Zaidi S, Lu Q, Nelson-Williams C, Brooks ED, et al. Two locus inheritance of non-syndromic midline craniosynostosis via rare SMAD6 and common BMP2 alleles. *eLife*. 2016;5. Epub 2016/11/01.
17. Ye X, Guilmatre A, Reva B, Peter I, Heuze Y, Richtsmeier JT, et al. Mutation Screening of Candidate Genes in Patients with Nonsyndromic Sagittal Craniosynostosis. *Plast Reconstr Surg*. 2016;137(3):952-61. Epub 2016/02/26.
18. Wilkie AOM, Johnson D, Wall SA. Clinical genetics of craniosynostosis. *Current opinion in pediatrics*. 2017;29(6):622-8. Epub 2017/09/16.
19. Martinez-Perez D, Vander Woude DL, Barnes PD, Scott RM, Mulliken JB. Jugular foraminal stenosis in Crouzon syndrome. *Pediatr Neurosurg*. 1996;25(5):252-5.
20. Rich PM, Cox TC, Hayward RD. The jugular foramen in complex and syndromic craniosynostosis and its relationship to raised intracranial pressure. *AJNR Am J Neuroradiol*. 2003;24(1):45-51.
21. Florisson JM, Barmpalios G, Lequin M, van Veelen ML, Bannink N, Hayward RD, et al. Venous hypertension in syndromic and complex craniosynostosis: the abnormal anatomy of the jugular foramen and collaterals. *J Craniomaxillofac Surg*. 2015;43(3):312-8. Epub 2015/01/22.
22. de Goederen R, Cuperus IE, Tasker RC, den Ottelander BK, Dremmen MHG, van Veelen MC, et al. Dural sinus volume in children with syndromic craniosynostosis and intracranial hypertension. *J Neurosurg Pediatr*. 2020:1-8. Epub 2020/02/01.
23. Castriota Scanderbeg A, Tomaiuolo F, Sabatini U, Nocentini U, Grasso MG, Caltagirone C. Demyelinating plaques in relapsing-remitting and secondary-progressive multiple sclerosis: assessment with diffusion MR imaging. *AJNR Am J Neuroradiol*. 2000;21(5):862-8. Epub 2000/05/18.
24. Filippi M, Cercignani M, Inglese M, Horsfield MA, Comi G. Diffusion tensor magnetic resonance imaging in multiple sclerosis. *Neurology*. 2001;56(3):304-11. Epub 2001/02/15.
25. Neil JJ, Shiran SI, McKinstry RC, Schefft GL, Snyder AZ, Almlí CR, et al. Normal brain in human newborns: apparent diffusion coefficient and diffusion anisotropy measured by using diffusion tensor MR imaging. *Radiology*. 1998;209(1):57-66. Epub 1998/10/14.
26. Werring DJ, Clark CA, Barker GJ, Thompson AJ, Miller DH. Diffusion tensor imaging of lesions and normal-appearing white matter in multiple sclerosis. *Neurology*. 1999;52(8):1626-32. Epub 1999/05/20.
27. Werring DJ, Toosy AT, Clark CA, Parker GJ, Barker GJ, Miller DH, et al. Diffusion tensor imaging can detect and quantify corticospinal tract degeneration after stroke. *Journal of neurology, neurosurgery, and psychiatry*. 2000;69(2):269-72. Epub 2000/07/15.
28. Cohen MM, Jr. Pfeiffer syndrome update, clinical subtypes, and guidelines for differential diagnosis. *Am J Med Genet*. 1993;45(3):300-7. Epub 1993/02/01.
29. Proudman TW, Clark BE, Moore MH, Abbott AH, David DJ. Central nervous system imaging in Crouzon's syndrome. *J Craniofac Surg*. 1995;6(5):401-5. Epub 1995/09/01.
30. Quintero-Rivera F, Robson CD, Reiss RE, Levine D, Benson CB, Mulliken JB, et al. Intracranial anomalies detected by imaging studies in 30 patients with Apert syndrome. *Am J Med Genet A*. 2006;140(12):1337-8. Epub 2006/05/13.

Chapter 8

31. Tokumaru AM, Barkovich AJ, Ciricillo SF, Edwards MS. Skull base and calvarial deformities: association with intracranial changes in craniofacial syndromes. *AJNR Am J Neuroradiol.* 1996;17(4):619-30.
32. Yacubian-Fernandes A, Palhares A, Giglio A, Gabarra RC, Zanini S, Portela L, et al. Apert syndrome: analysis of associated brain malformations and conformational changes determined by surgical treatment. *J Neuroradiol.* 2004;31(2):116-22.
33. Raybaud C, Di Rocco C. Brain malformation in syndromic craniosynostoses, a primary disorder of white matter: a review. *Childs Nerv Syst.* 2007;23(12):1379-88.
34. Doerga PN, Lequin MH, Dremmen MHG, den Ottelander BK, Mauff KAL, Wagner MW, et al. Cerebral blood flow in children with syndromic craniosynostosis: cohort arterial spin labeling studies. *J Neurosurg Pediatr.* 2019:1-11. Epub 2019/12/28.
35. Guilleminault C, Stoohs R, Quera-Salva MA. Sleep-related obstructive and nonobstructive apneas and neurologic disorders. *Neurology.* 1992;42(7 Suppl 6):53-60. Epub 1992/07/01.
36. Noudel R, Jovenin N, Eap C, Scherpereel B, Pierot L, Rousseaux P. Incidence of basioccipital hypoplasia in Chiari malformation type I: comparative morphometric study of the posterior cranial fossa. Clinical article. *J Neurosurg.* 2009;111(5):1046-52. Epub 2009/05/26.
37. Sandberg DI, Navarro R, Blanch J, Ragheb J. Anomalous venous drainage preventing safe posterior fossa decompression in patients with chiari malformation type I and multisutural craniosynostosis. Report of two cases and review of the literature. *J Neurosurg.* 2007;106(6 Suppl):490-4.
38. Fanelli A, Vonberg FW, LaRovere KL, Walsh BK, Smith ER, Robinson S, et al. Fully automated, real-time, calibration-free, continuous noninvasive estimation of intracranial pressure in children. *J Neurosurg Pediatr.* 2019:1-11. Epub 2019/08/24.



CHAPTER 9

Summary

Samenvatting

SUMMARY

Craniosynostosis most commonly occurs sporadically as an isolated defect and commonly involves one suture. Syndromic craniosynostosis typically involves multiple sutures synostosis as part of a larger constellation of associated anomalies. This thesis focuses on several aspects of craniosynostosis syndromes. This chapter will summarize the most important findings and the clinical implications following from this thesis.

In **chapter 2** a family with a craniosynostosis and limited extra cranial features is described. With linkage analysis we found an autosomal dominant underlying genetic mutation. We found a missense mutation in all affected family members in *MSX2*. This is the second family where a second mutation in *MSX2* is found.

In **chapter 3** we further explore genetics and we performed a screening project by using a 250K SNP arrays. Of all complex craniosynostosis patients we identified two patients with craniosynostosis and a microcephaly with a deletion in the 2p15p16.1 chromosomal region. FISH (fluorescence in situ hybridization) and qPCR were used to further analyze the deletions.

In **chapter 4** we focused at elevated intracranial hypertension. Elevated ICP is an actual and still unknown problem in syndromic craniosynostosis patients. Potential causes which are mentioned are cranio-cerebral disproportion, obstructive sleep apnea, tonsillar herniation of the cerebellum and venous hypertension. We focused at the relation between the diameter of the jugular foramen and the presence of papilledema. We showed a smaller diameter of the jugular foramen in syndromic craniosynostosis patients and also abnormal venous collaterals were most often observed in patients with Apert, Crouzon-Pfeiffer and Saethre Chotzen syndrome. These findings confirm an abnormal venous system which may predispose to an elevated ICP.

Not only genetics and elevated intracranial pressure may contribute to the known developmental and psychological problems in craniosynostosis patients, but also intrinsic brain abnormalities may contribute. Therefore, we also investigated whether architectural alterations exist in the white matter of the brain.

In **chapter 5** we performed the first step and set up the first prospective diffusion tensor imaging study. Diffusion tensor imaging measurements of white matter tracts reveal significant white matter integrity differences between children with craniosynostosis and healthy control subjects. Subsequently the next step is explained in **chapter 6** where we performed a prospective MRI study in young craniosynostosis patients. This study shows that craniosynostosis patients who have had cranial vault surgery, have similar abnormal microstructural tissue properties compared to unoperated patients. Additionally, these patients have an abnormal white matter fiber organization. Because there is no effect

of surgery and impact of intracranial hypertension is minimized in these young patients, our results strongly suggest an intrinsic factor, most likely as the genetic mutation itself as its cause.

Chapter 7 a magnetic resonance imaging and sleep study is performed. In this prospective study syndromic craniosynostosis patients obtained a MRI which showed the position of the cerebellar tonsils. The respiratory parameters were evaluated with a sleep study. We could not confirm that sleep apnoea in syndromic craniosynostosis is caused by hindbrain herniation. Rather, our evidence suggest that sleep disordered breathing in craniosynostosis may be caused by brain stem immaturity in young children. Our advice according to hindbrain herniation is to be conservative and provide regular neurosurgical follow-up as long as the child remains asymptomatic.

In conclusion this thesis has travelled along the different parts of syndromic craniosynostosis. This thesis dissolves a small piece of the overall craniosynostosis puzzle. Further research is necessary to optimize treatment and to predict the clinical outcome of all individual craniosynostosis patients.

SAMENVATTING

Syndromale craniosynostose treedt zelden op als een geïsoleerd probleem. Bij deze kinderen zijn meestal meerdere schedelnaden te vroeg gesloten en hebben vaak ook nog andere bijbehorende problemen. Dit proefschrift richt zich op verschillende aspecten van syndromale craniosynostose. De Nederlandse samenvatting geeft een overzicht van de belangrijkste bevindingen en de klinische implicaties van dit proefschrift.

Hoofdstuk 2 beschrijft een familie met craniosynostose en enkele extra craniale afwijkingen. Met linkage analyse is er een autosomaal dominante onderliggende genetische mutatie gevonden. Een missense mutatie in het *MSX2* gen is in alle aangedane familieleden gevonden. Dit is de tweede familie ter wereld waar een mutatie in het *MSX2* gen is gevonden.

In **hoofdstuk 3** wordt er verder ingegaan op de genetica en is er een screenings project gedaan met behulp van een 250K SNP array. Van alle complexe craniosynostosis patiënten hebben we twee patiënten met een craniosynostose en een microcephalie beschreven waar we een deletie in het 2p15p16.1 hebben gevonden. FISH (fluorescence in situ hybridization) en qPCR is gebruikt om de deletie verder te analyseren.

Hoofdstuk 4 is gericht op verhoogde intracraniele hersendruk. Verhoogde intracraniele druk is een actueel en onopgelost probleem in kinderen met een syndromale craniosynostose. Mogelijke oorzaken zijn cranio-cerebrale-disproportie, obstructief slaap apneu, tonsillaire herniatie van het cerebellum en veneuze hypertensie. We hebben ons met name gericht op de relatie tussen de diameter van het foramen jugulare en de aanwezigheid van papiloedeem. Een kleinere diameter van het foramen jugulare in syndromale craniosynostose patiënten en abnormale veneuze collateralen worden het vaakst gezien in patiënten met het syndroom van Apert, Crouzon-Pfeiffer en Saethre – Chotzen. Dit onderzoek bevestigt dat een abnormale veneuze afvoer, invloed kan hebben op een verhoogde intracraniele druk.

Niet alleen genetica en verhoogde intracraniele druk draagt bij aan de ontwikkeling en psychologische problemen in craniosynostose patiënten, maar ook de intrinsieke hersenafwijkingen dragen hieraan bij. Dit hebben we verder onderzocht om te kijken of er afwijkingen te vinden zijn in de witte stof in de hersenen van craniosynostose patiënten.

Hoofdstuk 5 toont de eerste prospectieve DTI (diffusion tensor imaging) studie. DTI parameters van de witte stof meten hoe makkelijk watermoleculen kunnen bewegen in en tussen de wittestof banen. Met deze parameters zien we verschillen tussen kinderen met craniosynostose en gezonde controles. De volgende stap wordt uitgelegd in **hoofdstuk 6** waar we een prospectieve MRI Studie hebben gedaan in jonge craniosynostose patiënten.

Deze studie laat zien dat geopereerde craniosynostose patiënten dezelfde afwijkingen hebben als ongeopereerde craniosynostose patiënten, een abnormaal witte stof organisatie. Aangezien er dus geen effect is van de schedeloperatie en de invloed van intracraniële hypertensie heel beperkt is op jonge leeftijd wijzen onze resultaten op een intrinsieke factor. De meest waarschijnlijke intrinsieke factor is de genetische mutatie zelve.

Hoofdstuk 7 is een MRI studie gecombineerd met een slaap studie. In deze prospectieve studie hebben syndromale craniosynostose patiënten een MRI ondergaan en hiermee is de positie van de cerebellaire tonsillen bepaald. Tevens is er een slaap studie gedaan waar respiratoire parameters zijn gemeten. In deze studie konden we niet aantonen dat slaap apneu in syndromale craniosynostose veroorzaakt wordt door cerebellaire hernatie. Onze studie wijst in de richting dat slaap apneu veroorzaakt wordt door hersenstam immaturiteit. Wij adviseren bij een cerebellaire hernatie zonder symptomen een conservatief beleid te voeren en de patiënt geregeld te monitoren door een neurochirurg.

Dit proefschrift neemt je mee langs te verschillende onderdelen van syndromale craniosynostose. Het proefschrift lost een klein stukje van de puzzel op. Er is meer onderzoek nodig om de behandeling voor syndromale craniosynostose patiënten te optimaliseren en de klinische uitkomst beter te kunnen voorspellen.



APPENDICES

PhD Portfolio
List of Publications
Dankwoord
Curriculum Vitae

PHD PORTFOLIO

Name PhD student: J.M.G Florisson

Erasmus MC Departments: Plastic and Reconstructive Surgery

Promotor: Prof Dr. I.M.J. Mathijssen

Co-promotor: Dr. M.H. Lequin

PhD training	Year	Workload (hours)
Introduction to Clinical Research	2008	40 hrs
Biostatistics for clinicians	2008	20hrs
Genetic Research in Medicine and Public Health	2008	40 hrs
Course Molecular Diagnostics III	2008	40 hrs
Biomedical English Writing and Communication	2009	20hrs
Teach the Teacher	2019	20 hrs
Periorbital surgery , Wenen	2019	20 hrs

Specific courses	Year	Workload (hours)
Microsurgery; Mw. JM Hekking Skillslab Plastic and reconstructive Surgery	2007-2010	180 hrs

Teaching	Year	Workload (hours)
Coach Microsurgery course	2008-2010	80 hrs
Anatomy of the arm and hand course (2-4rd year medical students)	2008-2009	60 hrs

Oral presentations	Year	Workload (hours)
NVPC. Den bosch Papilledema in single-suture craniosynostosis.	2008	20 hrs
NVSCA. Nijmegen Papilloedeem bij kinderen met geïsoleerde craniosynostose.	2008	20 hrs
Refereeravond Plastische Chirurgie Erasmus MC Radiologische bevindingen bij kinderen met een syndromale craniosynostose.	2009	20 hrs

Oral presentations	Year	Workload (hours)
NVPC, Maastricht Hersenafwijkingen bij kinderen met een syndromale Craniosynostose.	2009	20 hrs
International Society of Craniofacial Surgery, Oxford Analysis of brain malformations in syndromic craniosynostosis and psychological development.	2009	40 hrs
European Society of Radiology, Wenen A DTI Study in syndromic craniosynostosis.	2010	20 hrs
European Society of Paediatric Radiology, Bordeaux Brain malformations in children with syndromic craniosynostosis.	2010	20 hrs
International Society of craniofacial surgery, Jackson Hole. Craniosynostosis: Abnormal anatomy of the jugular foramen and collaterals.	2013	40 hrs
International Society of craniofacial surgery, Tokyo Intelligence and behavior versus neuroimaging in patients with syndromic craniosynostosis: A DTI Study.	2015	40 hrs

LIST OF PUBLICATIONS

(1-10)

1. Coolen JC, **Florisson JM**, Bissett IP, Parry BR. Evaluation of knowledge and anxiety level of patients visiting the colorectal pelvic floor clinic. *Colorectal disease : the official journal of the Association of Coloproctology of Great Britain and Ireland*. 2006;8(3):208-11. Epub 2006/02/10.
2. **Florisson JM**, Coolen JC, Bissett IP, Plank LD, Parry BR, Menzi E, et al. A novel model used to compare water-perfused and solid-state anorectal manometry. *Techniques in coloproctology*. 2006;10(1):17-20. Epub 2006/03/11.
3. **Florisson JM**, van Veelen ML, Bannink N, van Adrichem LN, van der Meulen JJ, Bartels MC, et al. Papilledema in isolated single-suture craniosynostosis: prevalence and predictive factors. *The Journal of craniofacial surgery*. 2010;21(1):20-4. Epub 2010/01/15.
4. **Florisson JM**, Dudink J, Koning IV, Hop WC, van Veelen ML, Mathijssen IM, et al. Assessment of white matter microstructural integrity in children with syndromic craniosynostosis: a diffusion-tensor imaging study. *Radiology*. 2011;261(2):534-41. Epub 2011/08/20.
5. Driessen C, Joosten KF, **Florisson JM**, Lequin M, van Veelen ML, Dammers R, et al. Sleep apnoea in syndromic craniosynostosis occurs independent of hindbrain herniation. *Child's nervous system : ChNS : official journal of the International Society for Pediatric Neurosurgery*. 2013;29(2):289-96. Epub 2012/09/26.
6. **Florisson JM**, Mathijssen IM, Dumee B, Hoogeboom JA, Poddighe PJ, Oostra BA, et al. Complex craniosynostosis is associated with the 2p15p16.1 microdeletion syndrome. *American journal of medical genetics Part A*. 2013;161A(2):244-53. Epub 2013/01/11.
7. **Florisson JM**, Verkerk AJ, Huigh D, Hoogeboom AJ, Swagemakers S, Kremer A, et al. Boston type craniosynostosis: report of a second mutation in *MSX2*. *American journal of medical genetics Part A*. 2013;161A(10):2626-33. Epub 2013/08/21.
8. **Florisson JM**, Barmpalios G, Lequin M, van Veelen ML, Bannink N, Hayward RD, et al. Venous hypertension in syndromic and complex craniosynostosis: the abnormal anatomy of the jugular foramen and collaterals. *Journal of cranio-maxillo-facial surgery : official publication of the European Association for Cranio-Maxillo-Facial Surgery*. 2015;43(3):312-8. Epub 2015/01/22.
9. de Vries CEE, Kalff MC, van Praag EM, **Florisson JMG**, Ritt M, van Veen RN, et al. The Influence of Body Contouring Surgery on Weight Control and Comorbidities in Patients After Bariatric Surgery. *Obesity surgery*. 2020;30(3):924-30. Epub 2019/12/04.
10. de Planque CA, **Florisson JMG**, Tasker RC, Rijken B, van Veelen MLC, Mathijssen IMJ, et al. Corpus callosum and cingulate bundle white matter abnormalities in non-operated craniosynostosis patients – a Diffusion Tensor Imaging study. Submitted.

DANKWOORD

Vele lieve mensen hebben in al die jaren bijgedragen aan dit proefschrift. Veel dank. Enkele mensen bedank ik graag in het bijzonder.

Cranio kinderen en ouders, hartelijk dank voor jullie medewerking aan dit proefschrift. Zonder jullie was het niet gelukt.

Prof. Dr. I.M.J. Mathijssen, Beste Irene, je gedrevenheid en talent zijn niet te evenaren. Ik kan me geen betere promotor voorstellen. Het was een voorrecht je promovendus te mogen zijn. Dankjewel.

Dr. M.H. Lequin, Beste Maarten, je begeleiding als copromotor was pragmatisch en helder. Mede door jouw kritische blik is dit proefschrift tot een goed einde gekomen. Bedankt.

Prof. Dr. P.J. van der Spek, Beste Peter, je tomeloze energie en bevoegenheid voor je vak zijn ongekend. Veel dank voor de samenwerking, je nimmer aflatende vertouwen, geduld en kritische noot.

Prof. Dr. R.R.J.W. Van der Hulst, **Prof. Dr. C.M.F. Dirven**, **Prof. Dr. K.F.M. Joosten** en **Prof. Dr. M.A.M Mureau**. Hartelijk dank voor het kritisch beoordelen van mijn proefschrift en voor de bereidwilligheid mij het vuur aan de schenen te leggen.

Plastisch chirurgen uit het Erasmus MC. Jullie hebben een prachtige afdeling en een fantastisch team. Ik ben trots dat ik bij jullie de grondslag van mijn specialistische opleiding heb kunnen leggen. Met veel plezier kijk ik terug op mijn opleidingstijd. Ik heb veel van jullie geleerd, waarvoor veel dank.

Lieve collega 's. Esther Moerman, Annekatrien van de Kar, Paula Roossink, Anouk Tan, Edin Hajder, Josien van der Meer en Jesse van Lieshout. Wat een heerlijkheid om elke dag met dit fijne team te mogen werken. Ik ben blij dat ik bij jullie terecht ben gekomen.

Lieve vrienden en vriendinnen. Jullie vriendschap is me veel waard. Wat fijn dat jullie er zijn!

Lieve familie en schoonfamilie. Bedankt voor de immer aanwezige interesse in mijn proefschrift. Ik besef me dat ik nooit antwoord heb gegeven maar jullie oprechte interesse is goud waard.

Paranimfen, Paula en Annekatrien, every brownie needs a blondie, and I need two. Lieve Paula, je bent een gouden collega, staat altijd klaar om te helpen en bent immer enthousiast voor een nieuwe uitdaging. Lieve Annekatrien, met jou is elk congres gezellig, je bent een

Appendices

fantastisch chirurg en overziet altijd het grotere plaatje. Lieve paranimfen, ik ben blij dat jullie mijn steun en toeverlaat willen zijn op deze spannende dag.

Papa en mama, bedankt voor jullie onvoorwaardelijke steun, liefde en vertrouwen. Jullie staan altijd klaar voor mij maar zeker ook voor Roy, Jort, Clio en Fender. Jullie zijn fantastisch! Ik kan niet zonder jullie.

Roy, het leven is een feestje met jou. Dankjewel dat je er bent!

Jort, Clio en Fender, jullie maken me gelukkig!

CURRICULUM VITAE

Joyce Florisson (18-06-1980) was born and raised in Maastricht, the Netherlands.

She finished high school at the Jeanne D'Arc College Maastricht in 1999. Immediately after high school she started medical school at the University of Diepenbeek (Belgium). After one year she returned to the Netherlands to continue medical school at Maastricht University. She graduated from Medical school in 2006. To perform research she went to Auckland, New-Zealand during her internships. There she did a research project at the department of General Surgery.



Immediately after her internships she started at the Erasmus Medical Center Rotterdam as a resident. After one year of residency she was accepted for the plastic surgery training program. An almost three year period as a PhD student, which commenced in 2007, preceded the start of her surgical training. The research was focused on brain malformations, genetics and psychological development of craniosynostosis. (Prof I.M.J Mathijssen, Dr. M.H. Lequin).

In October 2012 she finished her two years of basic general surgery training at the department of General Surgery, Ikazia Rotterdam (Dr. T. den Hoed). She continues her training at the department of Plastic and Reconstructive Surgery, Erasmus MC Rotterdam (Prof. dr. I.M.J. Mathijssen) which she finished in May 2017. At the Catharina Hospital, Eindhoven, she further developed her surgical skills and specialized in facial surgery, breast surgery and body contouring in 2017-2018. In 2018 she started as a plastic surgeon at the Onze Lieve Vrouwe Gasthuis Amsterdam and at the Jan van Goyen Esthetic Center Amsterdam.

She is married with Roy Hoevenaars, together they are having three beautiful children.